TECHNISCHE UNIVERSITÄT MÜNCHEN
FAKULTÄT FÜR MEDIZIN

The bone morphogenetic protein 7 (BMP7) plays a pro-tumorigenic role in pheochromocytoma

Ines Leinhäuser

Vollständiger Abdruck der von der Fakultät für Medizin der

Technischen Universität München zur Erlangung des akademischen Grades eines

Doktors der Naturwissenschaften

genehmigten Dissertation.

Vorsitzende: Univ.- Prof. Dr. Stefanie E. Combs

Prüfer der Dissertation:

1. Univ.- Prof. Dr. Michael John Atkinson

2. Univ.- Prof. Dr. Gabriele Multhoff

Die Dissertation wurde am 14.07.2015 bei der Technischen Universität München eingereicht und durch die Fakultät für Medizin am 16.09.2015 angenommen.

Statutory Declaration:

I declare that I have authored this thesis independently, that I have not used other than the declared sources/resources, and that I have explicitly marked all material which has been quoted either literally or by content from the used sources.

Munich, ……

Ines Leinhäuser

Eidesstattliche Erklärung

Ich erkläre an Eides statt, dass ich die vorliegende Arbeit selbstständig verfasst, keine anderen als die angegebenen Quellen/Hilfsmittel benutzt, und die den benutzten Quellen wörtlich und inhaltlich entnommene Stellen als solche kenntlich gemacht habe.

München, ……

Ines Leinhäuser

ZUSAMMENFASSUNG

Während in erblichen Phäochromozytomen, einem Tumor des Nebennierenmarks, bereits einige Gene, die zur Tumorentstehung und Progression führen, identifiziert wurden, bleibt der genetische Hintergrund in den sporadisch auftretenden Phäochromozytomen noch häufig ungeklärt. Neue Behandlungsmethoden und Strategien basieren auf der Klärung der zugrundeliegenden molekularen Signalwege. Als möglicher Ansatzpunkt wurde in dieser Arbeit das bone morphogenic protein 7 gene untersucht. Es ist in Phäochomozytomen von Patienten, und dem hier verwendeten Rattenmodel MENX, überexprimiert. BMP7 ist ein Wachstumsfaktor aus der TGF-Familie, der eine pro-oder anti-onkogene Wirkung, je nach Zell-und Tumortyp aufweist. In dieser Arbeit wurde in 72% einer großen Patientenkohorte mit Nebennieren- und extraadrenalen Phäochromozytomen erhöhte BMP7- Werte gefunden. Diese korrelieren positiv mit prognostischen Markern, die für eine erhöhte Malignität der Tumore sprechen. Um die Rolle des BMP7 in den Tumorzellen zu entschlüsseln, wurde die Expressionsrate im zellulären Tumormodell an PC12, MPC, MTT-Zellen variiert und funktionelle Test durchgeführt. In diesen Modellen aktivierte BMP7 Signalwege, die Zellteilung, Migration und Invasivität fördern. Zusätzlich zeigte eine Runterregulation des endogenen BMP7 in primären Phäochromazytomazellen der MENX-Ratte eine reduzierte Viabilität der Tumorzellen.

BMP7 aktiviert den PI3K/AKT/mTOR-Signalweg in Phäochromozytom-Zellen, welcher wiederum die Expression von Integrin β1 hochreguliert. Die Expressionsrate von Integrin β1 beeinflusste direkt Zellmigration und – invasion im PC12-Zellmodell.

Durch die Behandlung von MENX Ratten mit dem zweifachen PI3K/mTOR Inhibitor (NVP-BEZ235) in vivo, sollte geklärt werden, ob sich der BMP7-Signalweg für die Therapie von Phäochromozytomen eignet. Der aktuell in klinischen Studien getestete Wirkstoff, NVP-BEZ235, reduzierte die Zellteilungsrate von Tumorzellen und erhöhte deren Apoptoserate in vivo. Dies korrelierte mit einer verringerten Integrin β1 Expression. Als direkten Angriff auf den aktiven BMP-Signalweg der Phäochromozytome wurde zudem der neue BMP-Antagonist DMH1 eingesetzt. Auch hier wiesen die Zellen nach der Behandlung mit DMH1 eine geringere Zellteilung und erhöhten Zelltod auf.

In dieser Studie konnte also eine pro-onkogene Wirkung der Aktivierung des BMP7-Signalwegs in Phäochromozytomen gezeigt werden. Dadurch erscheint eine Therapie von progressiven und inoperablen Phäochromozytomen durch die Blockade des BMP7- Signalweges vielversprechend.

ABSTRACT

Although several genes involved in pheochromocytoma predisposition have been identified, the sporadic cases remain mostly genetically unexplained. Elucidation of the molecular pathways driving pheochromocytoma development could identify novel targets leading to improved treatment of the aggressive forms. We previously reported that the bone morphogenetic protein 7 (*BMP7*) gene is overexpressed in pheochromocytomas developing in MENX-affected rats and human patients. The BMP7 is a secreted growth factor belonging to the TGFβ superfamily, which plays pro- or anti-oncogenic roles in cancer in a cell type-dependent manner. Here we analyzed a large cohort of patients with adrenal and extra-adrenal pheochromocytomas and found that 72% of cases showed elevated levels of the BMP7 protein. High BMP7 expression positively correlated with features suggestive of higher malignant potential such as location of the tumor (extra-adrenal) and tumor size. As the role of BMP7 in pheochromocytoma was unknown, we conducted functional assays following the modulation of endogenous BMP7 levels in pheochromocytoma cell lines (PC12, MPC, MTT). We could demonstrate that active BMP signaling promotes proliferation, migration, and invasion of pheochromocytoma cells. Specifically, we observed that upregulation of the BMP7 protein enhances proliferation, migration and invasion in the PC12 cell line, while downregulation of *Bmp7* impairs these properties in MPC and MTT cells. Moreover, knockdown of the high endogenous *Bmp7* gene levels in primary cultures of MENX- associated pheochromocytoma cells reduced cell viability. We determined that BMP7 signals through the PI3K/AKT/mTOR pathway in pheochromocytoma cells and causes the upregulation of integrin β1 expression. Integrin β1 (*Itgb1*) gene knockdown suppressed BMP7-dependent increase in PC12 cell migration and invasion. To verify that targeting BMP7 signaling holds potential for pheochromocytoma treatment, we evaluated a dual PI3K/mTOR inhibitor currently in clinical trials (NVP-BEZ235) in the context of active BMP signaling (MENX-affected rats) *in vivo*. Tumors treated with NVP-BEZ235 had lower proliferation and integrin β1 levels and higher apoptosis compared with tissues of placebo treated rats. In pheochromocytoma cells having active BMP signaling, treatment with a recently developed BMP antagonist, DMH1, decreased cell proliferation and survival. In conclusion, our study shows that BMP7 activates pro-oncogenic pathways in pheochromocytoma. Downstream effectors of

BMP7-mediated signaling should be exploited as therapeutic targets for treating progressive or inoperable pheochromocytomas, tumors with poor outcome and still orphan of effective therapy.

ABBREVIATIONS

∅	average/diameter
°C	degree Celsius
%	percent
α	anti
µ	micro- (10^{-6})
AB	**A**nti**b**ody
AcVr	**Ac**ti**v**in **r**eceptor
APS	**a**mmonium **p**er**s**ulfate
AKT	serine/threonine-specific protein **k**inase
BCA	**Bic**inchoninic **a**cid
bp	**b**ase **p**air
bidest.	**bidest**illatus
Bmp	**b**one **m**orphogenetic **p**rotein
BMPR	**b**one **m**orphogenetic **p**rotein **r**eceptor
BSA	**b**ovine **s**erum **a**lbumin
B2m	β_2 microglobulin
c	**c**enti- (10^{-2})
CDK	**c**ycline-**d**ependent **k**inase
cDNA	**c**omplemetary **d**eoxyribo**n**ucleic **a**cid
Cited1	Cbp/p300-interacting transactivator 1
DAPI	4',6-**dia**midino-2-**p**heny**l**indole
DNA	**d**eoxyribo**n**ucleic **a**cid
DMEM	**D**ulbecco's **M**odified **E**agle's **M**edium
DMH1	selective BMP receptor inhibitor
DMSO	**d**i**m**ethyl **s**ulf**o**xide
dNTP	**d**eoxyribonucleotide
DTT	**d**i**t**hio**t**hreitol
E. coli	***E**scherichia **coli***
ECL	**e**nzymatic **c**hemi**l**uminescence
ECM	**e**xtra **c**ellular **m**atrix
EDTA	**e**thylene**d**iamine**t**etra**a**cetic acid
ELISA	**e**nzyme-**l**inked **i**mmuno**s**orbent **a**ssay
ENS@T	European Network for the Study of Adrenal Tumors
EtBr	**et**hidium **br**omide
ER	**e**ndoplasmatisches **r**eticulum
ERK	**e**xtracellular-signal **r**egulated **k**inase
E2F5	**E2F** transcription factor **5**
FACS	**f**luorescence **a**ctivated **c**ell **s**orting
FBS	**f**etal **b**ovine **s**erum
FFPE	**f**ormalin-**f**ixed**, p**araffin-**e**mbedded
FH	**f**umarate **h**ydratase
FITC	**f**luorescein **i**so**t**hio**c**yanate

GFP	**g**reen **f**luorescent **p**rotein
h	**h**ours
HBSS	**H**anks' **B**alanced **S**alt **S**olution
HE	**h**ematoxylin and **e**osin
HIF	**h**ypoxia-**i**nducible **f**actors
HRP	**h**orse**r**adish **p**eroxidase
HS	**h**orse **s**erum
IHC	**I**mmuno**h**isto**c**hemistry
i.e.	**i**d **e**st
IgG	**I**mmuno**g**lobulin **G**
itgb1	**i**d **e**st
JNK	c-**J**un **N**-terminal **k**inases
k	**k**ilo- (10^3)
kbp	**k**ilo-**b**ase **p**air
Ki67	Antigen KI-67
KIF1B	**Ki**nesin **F**amily Member **1B**
l	**l**itre
LB	Luria-Bertani medium)
m	**m**etre/**m**illi- (10^{-3})/**m**ouse
M	**m**olar concentration
MAPK	**m**itogen**-a**ctivated **p**rotein **k**inase
MAX	**M**YC **a**ssociated factor **X**
MCC	**m**utant **c**olorectal **c**ancer protein
mTOR	**m**echanistic **t**arget **o**f **r**apamycin
MEF	**m**ouse **e**mbryonic **f**ibroblast
MEN	**m**ultiple **e**ndocrine **n**eoplasia
MENX	**m**ultiple **e**ndocrine **n**eoplasia-like syndrome
min	**min**ute
$MgCl_2$	**m**a**g**nesium **cl**orid
mo	**mo**nths
mut	**mut**ant
MTT	3-(4,5-Dimethylthiazol-2-yl)-2,5-diphenyltetrazoliumbromid
n	**n**ano- (10^{-9})
NaCL	**na**trium clorid
NaOH	**na**trium hydroxid
NF-H	**N**euro**f**ilament-**H**
NGF	nerve growth factor
NP-40	**n**onyl **p**henoxypolyethoxyl- ethanol
NSCLC	**n**on-**s**mall **c**ell **l**ung **c**ancer
OD	**o**ptical **d**ensity
OptiMEM	reduced serum media modification of Eagle's Minimum Essential Media
P	**p**robability
p	**p**ico- (10^{-12})/**p**lasmid
p-AKT	phosphorylated serine/threonine-specific protein **k**inase
p27Kip1	cycline-dependent kinase inhibitor (p27)
PGL	**p**ara**g**ang**l**ioma

PBS	**p**hosphate **b**uffered **s**aline
PCR	**p**olymerase **c**hain **r**eaction
Pen	**pen**icillin
PFA	**p**ara**f**orm**a**ldehyde
pH	minus the decimal logarithm of the **h**ydrogen ion activity in a solution
PHEO	**pheo**chromocytoma
PI3K	**P**hospho**i**nositide **3**-**k**inase
Plaur	**Pl**asminogen **a**ctivator**, u**rokinase **r**eceptor
PNMT	penylethanolamine-**N**-**m**ethyl**t**ransferase
qRT-PCR	**q**uantitative **r**evers **t**ranskriptase **p**olymerase **c**hain **r**eaction
r	**r**at
RAC	Rho family of GTPases
RAS	**Ra**t **s**arcoma
RASSF1	**RAS-**a**s**sociated domain **f**amily **1**
RB	**R**etino**b**lastoma
rBMP	**r**ecombinant **b**one **m**orphogenetic **p**rotein
REF	**r**at **e**mbryonic **f**ybroblast
RET	**Ret** Proto-Oncogene
rhBMP	**r**ecombinant human **b**one **m**orphogenetic **p**rotein
RIPA	**r**adio**i**mmuno**p**recipitation **a**ssay
RNA	**r**ibo**n**ucleic **a**cid
RNAi	**r**ibo**n**ucleic **a**cid **i**nterference
rpm	**r**evolutions **p**er **m**inute
RPMI	**R**oswell **P**ark **M**emorial **I**nstitute
R-SMAD	receptor associated transcrption factor SMAD
RT	**r**oom **t**emperature
RT-PCR	**r**everse **t**ranscriptase-**p**olymerase **c**hain **r**eaction
scr	**scr**ambled
sec	**sec**ond
shRNA	**s**mall **h**airpin **r**ibo**n**ucleic **a**cid
SD	**s**tandard **d**eviation
SDH	succinate dehydrogenase subunit
SDS	**s**odium **d**odecyl **s**ulfate
SDS-PAGE	**s**odium **d**odecyl **s**ulfate **p**oly-**a**crylamide **g**el **e**lectrophoresis
SMAD	Mothers Against Decapentaplegic, Drosophila, Homolog
siRNA	**s**mall **i**nterfering **r**ibo**n**ucleic **a**cid
Strep	**strep**tomycin
TAK	**T**GFβ-**a**ktivated **k**inase
TBE	**T**ris/**b**oric acid/**E**DTA
TBS-T	**T**ris **b**uffered **s**aline with **T**ween 20
TMA	**t**issue **m**icro **a**rray
TEMED	*N,N,N',N'*-**te**tra**m**ethyl**e**thane-1,2-iamine
TGFβ	**t**ransforming **g**rowth **f**actor beta

Tm	**m**elting **t**emperature	v	**v**olt
TMEM	**t**rans**mem**brane protein	*VHL*	**V**on **H**ippel–**L**indau tumor suppressor gene
Tris	2-amino-2-hydroxymethyl-propane-1,3-diol	W	**w**att
tx	transfected	wt	**w**ild**t**ype
UV	**u**ltra**v**iolet	w/v	**w**eight per **v**olume utx untransfected
v/v	**v**olume per **v**olume		

All gene names and corresponding RNAs are indicated in italics, human genes in capital letters, e.g. *BMP7*, genes from other species in lowercase with capital first letters, e.g. *Bmp7*. All proteins, regardless of species, are written in regular font. Chemical elements and compounds are abbreviated according to common chemical nomenclature. Amino acids are abbreviated according to the established three letter system.

TABLE OF CONTENT

1. INTRODUCTION

1.1. The Adrenal Gland

The adrenal glands are endocrine organs situated above both the right and left kidneys. Each gland is comprised of two parts, the cortex and the medulla, and is surrounded by an adipose capsule and by the renal fascia (Figure 1). The cortex, the outer structure of the adrenal glands, produces several steroid hormones (cortisol, corticosterone, androgens such as testosterone, and aldosterone) that affect growth (Cacciari, Mazzanti et al. 1990), blood pressure (Dodic, Wintour et al. 1999) and blood sugar levels (Even, Crosby et al. 2012), as well as sexual behavior (Kreuz, Rose et al. 1972, Nussey and Whitehead 2001).

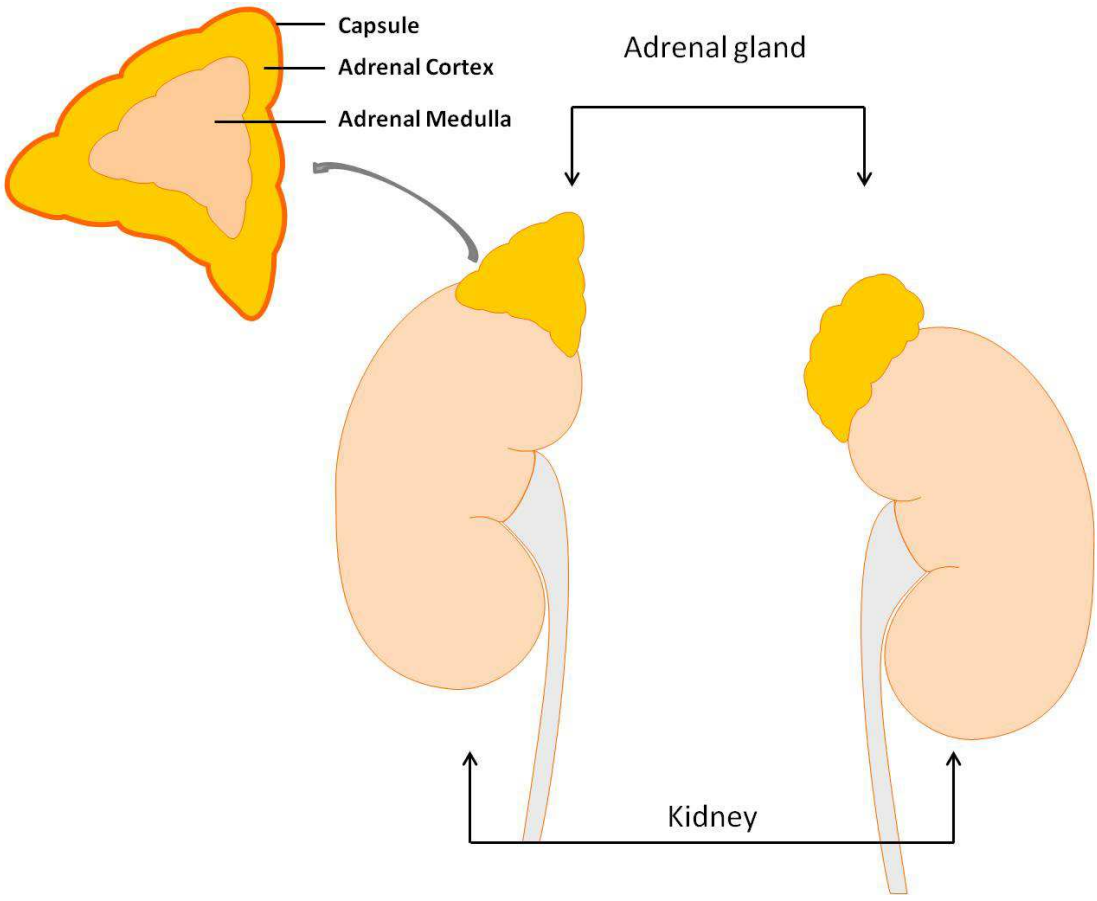

Figure 1. Scheme of the human kidney and adrenal medulla in human. The figure shows a scheme of both adrenal glands situated above the kidneys and a scheme of the cross section of the adrenal gland representing the capsule, the adrenal cortex and the adrenal medulla. Modified from motifolio.com

The adrenal medulla is composed of chromaffin cells, which are neuroendocrine cells of neural crest origin deriving from the sympathoadrenal progenitor cells that populate the adrenal gland and sympathetic paraganglia, including the carotid body and ‘‘organ of Zuckerkandl” during early embryogenesis (Huber 2006). Along their migratory route toward their final location, sympathoadrenal progenitor cells acquire the specific characteristics of mature catecholamine-producing cells (Cochard, Goldstein et al. 1978) and synthesize the circulating catecholamines adrenaline (epinephrine) and noradrenaline (norepinephrine) (Cochard, Goldstein et al. 1978, Ernsberger, Patzke et al. 1995, Ernsberger, Reissmann et al. 2000) both derived from the amino acid tyrosine (Spector, Sjoerdsma et al. 1965).

Innervation of preganglionic nerve fibers from the sympathetic nervous system regulates the hormonal release by the chromaffin cells (Perlman and Chalfie 1977). Catecholamine synthesis can also be stimulated by adrenocortical cortisol secretion (Perlman and Chalfie 1977, Kantorovich and Pacak 2010), which promotes the upregulation of the enzyme phenylethanolamine-N-methyltransferase (PNMT) in chromaffin cells. PNMT catalyzes the transformation of noradrenalin in adrenalin.

Similar to endocrine cells, chromaffin cells are characterized by their very large storage vesicles, the “chromaffin granules” (Coupland 1965), whose soluble content is released in the extracellular space by exocytosis upon stimulation (De Robertis and Vaz Ferreira, 1957). There are two types of chromaffin granules containing adrenaline or noradrenaline, which segregate to distinct chromaffin cell populations (Coupland 1965). Due to their secretory products chromaffin cells play crucial roles in various homeostatic mechanisms such as liver metabolism (Sherwin and Sacca 1984) and vascular perfusion (Cripps and Dearnaley 1972). Specifically, the catecholamines adrenalin and noradrenaline have multiple roles including those as a hormone and a neurotransmitter (Clutter and Cryer 1980). Secreted in the bloodstream, they affect the autonomous nervous system, which controls functions such as heart rate (Breuer, Skyschally et al. 1993), blood pressure (Gombos, Hulet et al. 1962) and sweating (Allen and Roddie 1972).

1.2. Pheochromocytoma in Human

Tumors that develop from chromaffin cells in the adrenal medulla are called pheochromocytomas (Karagiannis, Mikhailidis et al. 2007). They are characterized by a black or dark brown color (phaios=dark, brown) (Pick 1912). These tumors can also

develop in sympathetic and parasympathetic ganglia and are termed extra-adrenal pheochromocytoma or paraganglioma (PGL). While 80% of normal adrenal medullary cells produce adrenalin and 20% noradrenaline, pheochromocytoma cells ordinarily express both catecholamines but usually more noradrenaline than adrenaline (noradrenergic pheochromocytoma) (Guyton et al. 1996). Pheochromocytomas that produce more adrenaline than noradrenaline are referred to as adrenergic pheochromocytoma (Lehnert 1998). According to the World Health Organization (WHO) 2004 classification, similar to adrenal pheochromocytomas extra-adrenal paragangliomas produce significant amounts of catecholamines demonstrating the classical clinical picture of pheochromocytomas. In contrast, parasympathetic PGLs, tumors of the paraganglia (Thompson 2006), do not derive from chromaffin cells and are mainly situated in the head and neck, and rarely produce significant amounts of catecholamines (Thompson 2006, van Duinen, Steenvoorden et al. 2010).

The prevalence of pheochromocytomas is not precisely known since there are no recent epidemiological studies available. The most recent study from 1980 until 1992 showed that the average annual incidence rate in the Spanish population in South Galicia was 2.06 per million. The incidence rate of the female population was significantly higher compared with the males (2.26 vs. 1.84) and the mean age at diagnosis was at 21–65 years (Fernandez-Calvet and Garcia-Mayor 1994).

One of the clinical manifestations of pheochromocytomas is hypertension which is caused by sustained catecholamine secretion (Zuber, Kantorovich et al. 2011). Additional symptoms associated with pheochromocytomas are: headache, palpitations, and diaphoresis (Bravo and Tagle 2003, Manger 2006). Most pheochromocytomas are benign and curable by surgical resection, but about 5-26% depending on the underlying studies are clinically malignant (Goldstein, O'Neill et al. 1999, Edstrom Elder, Hjelm Skog et al. 2003, Gimenez-Roqueplo, Favier et al. 2003, Eisenhofer, Bornstein et al. 2004). Pheochromocytomas can metastasize by both lymphatic and haematogenous pathways and can infiltrate into the liver, lymph nodes, lung and bone (Cascon, Ruiz-Llorente et al. 2004). For patients with these malignant tumors the 5 year survival rate is below 50% (Eisenhofer, Bornstein et al. 2004, Nomura, Kimura et al. 2009). A more recent study in Korea has reported the overall 5-year survival rate of patients with malignant pheochromocytoma to be below 12% (Park, Song et al. 2011).

About 60% of the pheochromocytomas are sporadic, but a significant percentage (~40%) are hereditary (Neumann, Bausch et al. 2002, Gimenez-Roqueplo, Dahia et al. 2012) and can be found in patients with germline mutations in one of the following genes: *RET* (Machens, Brauckhoff et al. 2005), *VHL* (Zbar, Kishida et al. 1996), succinate dehydrogenase subunit A (*SDHA*) (Burnichon, Briere et al. 2010), B (*SDHB*) (Astuti, Latif et al. 2001), C (*SDHC*) (Niemann and Muller 2000), D (*SDHD*) (Baysal, Ferrell et al. 2000) and *SDHAF2* (Hao, Khalimonchuk et al. 2009), *NF1* (Wallace, Marchuk et al. 1990), *TMEM127* (Qin, Yao et al. 2010), *Max* (Comino-Mendez, Gracia-Aznarez et al. 2011) and *FH* (Castro-Vega, Buffet et al. 2014). In addition to the hereditary forms, approximately a total of 7.5% of the sporadic pheochromocytoma harbor somatic mutations in one of the pheochromocytoma susceptibility genes (0% *RET*, 4.4% *VHL*, 1.6% *SDHD*, and 1.5% *SDHB*) mentioned before (Korpershoek, Van Nederveen et al. 2006). Moreover, candidate gene approaches studying sporadic pheochromocytoma have identified some tumor suppressor genes inactivated in the tumors, such as the RAS-association domain family 1, isoform A (*RASSF1A*) (Astuti, Agathanggelou et al. 2001) and the p16 (*CDKN2A)* (Muscarella, Bloomston et al. 2008) tumor suppressor gene (Astuti, Agathanggelou et al. 2001). *RASSF1A* and *CDKN2A* were both found to be downregulated through promoter region hyper-methylation in 22-48% (Astuti, Agathanggelou et al. 2001) and in 24-35% (Muscarella, Bloomston et al. 2008) of pheochromocytomas, respectively. We have identified a decrease/loss (56% of cases) of the tumor suppressor gene p27 in sporadic pheochromocytomas (Pellegata, Quintanilla-Martinez et al. 2007) .

Besides the stratification in “hereditary and sporadic” pheochromocytoma/paraganglioma genome-wide expression studies which were performed on these tumors have suggested that they can be divided into two groups based on its transcription profile. The first group (cluster 1) encloses tumors carrying *VHL, SDHx* (*SDHA*, *SDHB*, *SDHC*, *SDHD*, *SDHAF2*), *HIF2α* and *FH* mutations and also about 30% of the sporadic tumors (Castro-Vega, Letouze et al. 2015). This cluster is characterized by the high expression of genes involved in the hypoxic pathway (Eisenhofer, Huynh et al. 2004, Lopez-Jimenez, Gomez-Lopez et al. 2010). The second group (cluster 2) includes 70% of sporadic tumors and hereditary tumors bearing mutations in the susceptibility genes *NF1*, *RET*, *KIF1Bβ*, and *TMEM127* (Gimenez-Roqueplo, Dahia et al. 2012, Vicha, Musil et al. 2013). This

cluster is characterized by activation of kinase signaling and protein translation (Burnichon, Vescovo et al. 2011, Dahia 2014).

1.3. Multiple Endocrine Neoplasias Type 1&2 Syndromes (MEN1 and MEN2)

Multiple endocrine neoplasias (MENs) are a group of hereditary disorders characterized by tumors occurring in more than one neuroendocrine-derived tissue. Two major forms of MEN syndromes can occur in humans, MEN type 1 (MEN1) and MEN type 2 (MEN2), are both inherited as autosomal dominant traits with high penetrance. Germline mutations in the *Menin* tumor suppressor gene cause MEN1 (Chandrasekharappa, Guru et al. 1997, Zarnegar, Brunaud et al. 2002), while MEN2 is related to germline mutations in the *RET* proto-oncogene (Mulligan, Kwok et al. 1993). Patients affected by MEN1 develop multiple parathyroid adenomas, pancreatic islet cell neoplasia and pituitary adenomas (Carty, Helm et al. 1998, Brandi, Gagel et al. 2001). Depending on the tumor pattern, MEN2 can be divided into two subtypes (Mise, Drosten et al. 2006): MEN2A is defined by pheochromocytomas and medullary thyroid carcinoma or of medullary thyroid carcinoma and parathyroid adenoma (Hansford and Mulligan 2000); MEN2B (also known as MEN3) is characterized by pheochromocytomas, medullary thyroid carcinoma as well as mucosal and digestive ganglioneuromatosis (Koch 2005) (Table 1). Pheochromocytomas which occur in the context of the multiple endocrine neoplasia type 2 syndromes have a penetrance of 50% (Thosani, Ayala-Ramirez et al. 2013).

Table 1. Genotype and phenotype of MEN syndromes are shown. The predisposing mutations of the genes leading to the different MEN syndromes and to the different phenotypes are shown. Men = multiple endocrine neoplasia; RET = Ret Proto-Oncogene; CDKN1B = Cyclin-Dependent Kinase Inhibitor 1B; Menin = Multiple Endocrine Neoplasia

Syndrome	**MEN1**	**MEN2A**	**MEN2B**	**MEN4**	**MENX**
Gene mutation	*MEN1*	*RET*	*RET*	*CDKN1B*	*Cdkn1b*
Phenotype	parathyroid adenomas, pancreatic islet cell neoplasia and pituitary adenomas	pheochromocytomas and medullary thyroid carcinoma or medullary thyroid carcinoma and parathyroid adenoma	pheochromocytomas, medullary thyroid carcinoma, mucosal and digestive ganglioneuromatosis	not clearly defined	bilateral pheochromocytomas, paragangliomas, multifocal pituitary adenoma, multifocal thyroid C-cell hyperplasia and endocrine pancreas hyperplasia

1.4. New MEN Syndromes: MENX and MEN4

In 2002, a novel variant of MEN that spontaneously developed in a Sprague-Dawley rat colony was detected. This cancer syndrome in the rat is referred to as multiple endocrine neoplasia-like syndrome (MENX). Affected animals show overlapping phenotypes with the human MEN syndromes as they develop bilateral pheochromocytomas, paragangliomas, multifocal pituitary adenoma, multifocal thyroid C-cell hyperplasia and endocrine pancreas hyperplasia (Figure 2). Additionally, affected animals present bilateral cataract in the first few weeks of life (Fritz, Walch et al. 2002).

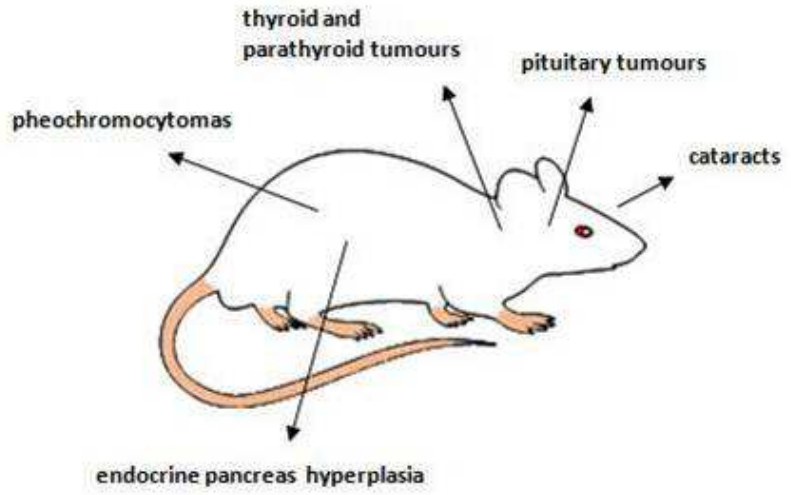

Figure 2. Tumor spectrum in MENX. Rats affected by the multiple endocrine neoplasia-like syndrome (MENX) show bilateral cataracts, bilateral pheochromocytomas, paragangliomas (extra-adrenal pheochromocytomas), pituitary tumors, bilateral thyroid and parathyroid tumors, as well as endocrine pancreas hyperplasia.

It was determined that MENX in these animals is caused by a homozygous tandem duplication of 8 nucleotides in exon 2 of the *Cdkn1b* gene causing a frameshift. The *Cdkn1b* gene encodes the cyclin-dependent kinase (Cdk) inhibitor p27Kip1 (p27) (Pellegata, Quintanilla-Martinez et al. 2006). p27 is a key player in the regulation of the cell cycle transition from G1 to S phase and belongs to the Cip/Kip family of cyclin-dependent kinase inhibitors (CDKIs) (Sheaff, Groudine et al. 1997). p27 binds to the CyclinE/Cdk2 complex which in turn leads to the inhibition of the kinase activity (Sheaff, Groudine et al. 1997). Binding by p27 prevents Cdk2 from phosphorylating the Retinoblastoma protein (Rb) which usually represses the transcription factors of the E2F family (Sheaff, Groudine et al. 1997). The E2F transcription factor is required to induce the expression of genes necessary for cell cycle progression (Dyson 1998).

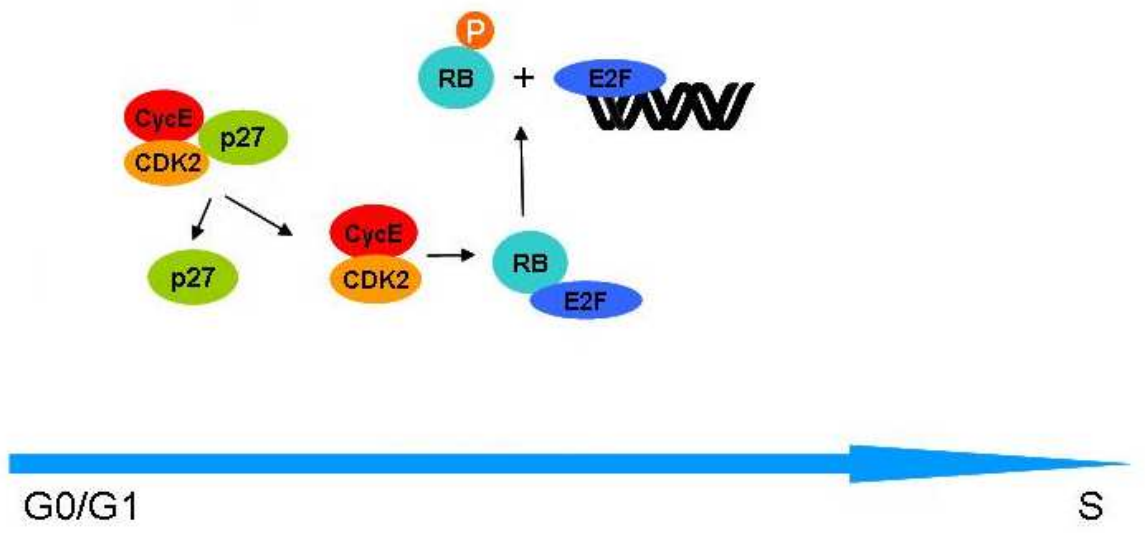

Figure 3. Cell cycle regulatory function of p27. Based on mitogenic signals, p27 dissociates from the Cyclin E/Cdk2 complex, thereby activating Cdk2 that in turn phosphorylates Rb. Phosphorylated Rb relieve bound E2F transcription factors that induce transcription of genes needed for G to S phase transition. Modified from (Marinoni and Pellegata 2011)

In the absence of p27, Rb is phosphorylated by the Cyclin E/CDK2 complex. Phosphorylated Rb releases E2F transcription factors which in turn allow the transcription of genes required for the progression to the S phase, thereby promoting cell proliferation (Fero, Randel et al. 1998, Sherr and Roberts 1999, Slingerland and Pagano 2000, Philipp-Staheli, Payne et al. 2001, Besson, Hwang et al. 2007, Neganova and Lako 2008, Lee, Marinoni et al. 2013) (Figure 3). Beside its function in cell-cycle progression, emerging evidence suggests that p27 can regulate other cellular functions, including cell differentiation, migration and apoptosis (Philipp-Staheli, Payne et al. 2001, Blagosklonny 2002, Besson, Gurian-West et al. 2004, Collard 2004).

The mutation in *Cdkn1b* identified in MENX-affected rats leads to the generation of an unstable mutant protein, which is only present at a low level or is completely absent in the rat tissues *in vivo* (Pellegata, Quintanilla-Martinez et al. 2006). In humans, *CDKN1B* germline mutations were also found to predispose to multiple endocrine tumors (Pellegata, Quintanilla-Martinez et al. 2006). These mutations cause a MEN1-like syndrome recently termed as MEN4 [OMIM #610755]. The *CDKN1B* mutations associated with MEN4 affect localisation, stability and protein

binding abilities of p27(Marinoni and Pellegata 2011). At the moment the tumor spectrum of MEN4 is not clearly defined because of the limited number of patients so far identified (Lee and Pellegata 2013).

1.5. MENX-related Pheochromocytomas

Rats affected by the MENX syndrome develop bilateral tumors of the adrenal medulla with complete penetrance: adrenomedullary hyperplasia is evident at 2 months of age and progresses to pheochromocytomas by 6 to 8 months of age. The cells expanding in these tumors do not express the enzyme *PNMT* which catalyzes the methylation of noradrenaline to form adrenaline in the last step of the catecholamine biosynthesis pathway(Kirshner and Goodall 1957). This suggests these tumors to be noradrenergic (Molatore, Liyanarachchi et al. 2010). Gene expression array analysis performed on adrenomedullary hyperplasia and pheochromocytoma tumors from homozygous mutant rats identified 183 genes that were overexpressed at least two fold in the lesions compared to normal adrenomedullary tissue (Molatore, Liyanarachchi et al. 2010). *Bmp7* was one of the most highly expressed genes in the rat pheochromocytomas when compared to normal adrenal tissue. Subsequently, we identified the upregulation of several genes downstream of the Bmp-Smad pathway including *Sox9*, *Gata2* and *Hoxc4*, suggesting that Bmp signaling is activated in rat pheochromocytoma cells. Interestingly, the high expression of *Bmp7* is already evident in the adrenal medulla of young mutant rats (1 month old) before they show any pathological phenotype in this tissue (Molatore, Liyanarachchi et al. 2010).

Human pheochromocytomas also show overexpression of several genes that were upregulated in the rat tumors, including *BMP7* (Molatore, Liyanarachchi et al. 2010). Indeed, we found that the overexpression of *BMP7* occurred in 88% of sporadic and 69% of familial pheochromocytoma cases, and that the level of mRNA expression was on average 42 times that of normal adrenal medulla. There is no evidence that these high levels of the *BMP7* gene translate into increased protein levels of BMP7, yet.

It has been shown that MENX-related pheochromocytomas share at least some molecular mechanisms with the corresponding human tumors independent of the p27 status.

1.6. The role of BMP7 in development

Bone morphogenetic proteins (BMPs) are multi-functional growth factors that belong to the transforming growth factor beta (TGFβ) superfamily of cytokines (Wozney, Rosen et al. 1988, Celeste, Iannazzi et al. 1990) that regulate a wide array of fundamental cellular processes, including proliferation (Ille, Atanasoski et al. 2007, Yuan, Pan et al. 2013), differentiation (Ille, Atanasoski et al. 2007, Yuan, Pan et al. 2013) and cell death (Pajni-Underwood, Wilson et al. 2007). They were found to be widely expressed in vertebrate embryonic structures (Liu and Niswander 2005) and shown to be involved in a variety of key embryonic processes such as dorsal-ventral axis specification (Ramel and Hill 2013), epithelial-mesenchymal interactions (Vainio, Karavanova et al. 1993), heart development (van Wijk, Moorman et al. 2007), cartilage development and postnatal bone formation (Zhao, Harris et al. 2002). Furthermore, BMPs have been described to act as autocrine (Sakai, Furihata et al. 2012) or paracrine (Shaw, Gipp et al. 2010) modulators of tumor progression and to play a functional role in a number of cancer entities (Langenfeld, Calvano et al. 2003, Hsu, Rovinsky et al. 2005, Johnsen and Beuschlein 2010).

BMP7, a member of the BMP family (Celeste, Iannazzi et al. 1990), has biological functions both in embryonic development (Solloway and Robertson 1999) and in regeneration of injured tissues in the adult (Marumo, Hishikawa et al. 2008). BMP7 accelerates bone differentiation and fracture healing, a feature that is therapeutically used (Reddi and Cunningham 1993, Tsiridis, Morgan et al. 2007). The expression of the *BMP7* gene is tightly controlled both during embryonic development and adult life through numerous signaling pathways (Lagna, Hata et al. 1996, Pouponnot, Jayaraman et al. 1998, Frontelo, Leader et al. 2004). In adult organisms, BMP7 is especially highly expressed in kidney, specifically in podocytes, distal tubules and collecting ducts (Mitu and Hirschberg 2008, Oxburgh 2009). Originating from the wall of the dorsal aorta, BMP7 has been shown to play an important role in the development of adrenal medulla as it drives the sympathetic neuron development (Schneider, Wicht et al. 1999).

1.7. BMP7 signaling pathways

At the molecular level, BMP7 is synthesized as a large precursor protein and includes both a native signal sequence targeting it to the endoplasmic reticulum (ER) for secretion, and a N-terminal prodomain (Cui, Jean et al. 1998, Constam and Robertson 1999). In the ER, the protein folds into a homodimeric complex, then traffics to the Golgi where it is proteolytically cleaved by subtilisin-like proprotein convertases (SPCs) (Cui, Jean et al. 1998, Constam and Robertson 1999). The primary cleavage event results in the removal of the prodomain that may remain associated in a latent complex that is secreted from the cell (Annes, Munger et al. 2003, Brown, Zhao et al. 2005, Ge, Hopkins et al. 2005). Cell signaling can be initiated by the binding of the BMP7 dimer to one of the two types of serin-threonin-kinase BMP receptors (BMPRs), i.e. type I (A*lk2* (Liu, Ventura et al. 1995), *Alk3* (Xu, Qi et al. 2010) and *Alk 6* (Xu, Qi et al. 2010)) and type II receptors (BMPR II (Perron and Dodd 2009), *AcVR*2a (Liu, Ventura et al. 1995) and *AcVR2b* (Liu, Ventura et al. 1995), located in the cytoplasmic membrane (Massague 1992), to that BMP7 reverently binds to. BMP7 binding initiates the dimerization of type 1 and type 2 receptors (Laiho, Weis et al. 1990). The constitutively activated BMPRII phosphorylates BMPRI (Rosenzweig, Imamura et al. 1995, Lane, Machado et al. 2000), which in turn leads to the phosphorylation of the receptor-associated transcriptions factors SMAD 1,5 and 8 (R-SMADs) (Heldin, Miyazono et al. 1997) (Figure 4). Phosphorylated R-SMADs can form oligomeric complexes with SMAD4 (Co-SMAD) and be translocated into the nucleus where they act as transcription factors by binding to the DNA in association with other cofactors i.e. repressors or activators (Lagna, Hata et al. 1996). The transcriptional outcome is influenced by interaction with these general transcriptional activators such as p300 and CBP, or by association with the specific repressors such as Suv39h or CtBP (Pouponnot, Jayaraman et al. 1998, Postigo 2003, Frontelo, Leader et al. 2004, Oxburgh 2009). The R-SMAD/SMAD4 complex can be inhibited by the SMAD-inhibitor SMAD6 (Hata, Seoane et al. 2000). Further, the BMP–SMAD signaling pathway is subject to autofeedback, suggesting that this may modulate the duration and/or intensity of BMP signaling (Cho and Blitz 1998, von Bubnoff and Cho 2001).

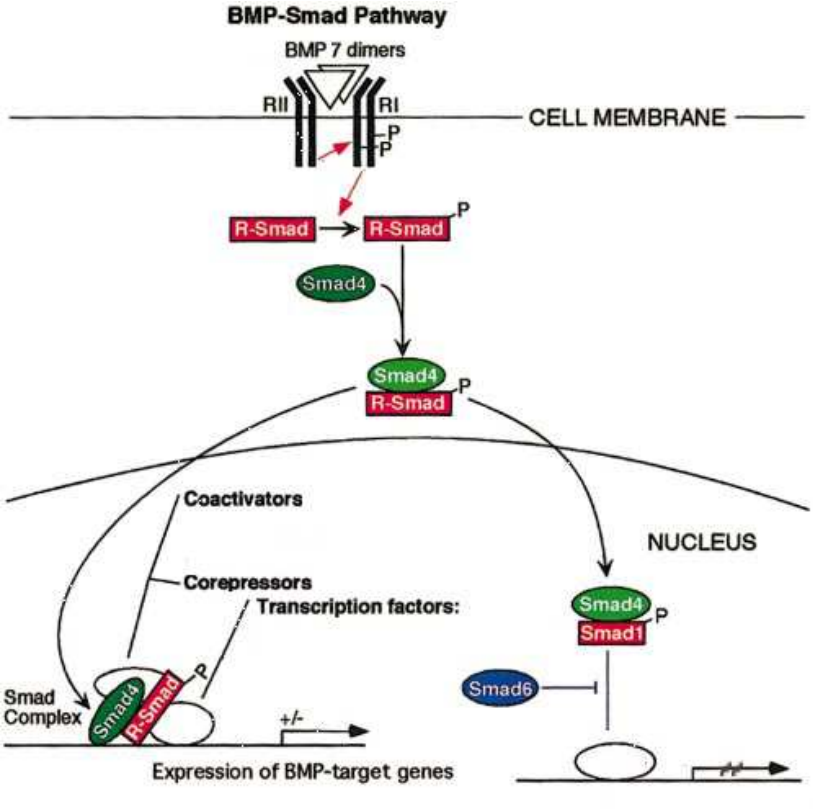

Figure 4. The BMP–Smad pathway. BMP7 binds to one of its receptor (RII and RI) which leads to the dimerization of RII and RI. The constitutively activated BMPRII phosphorylates BMPRI, which in turn leads to the phosphorylation of the receptor-associated transcriptions factors SMAD (R-SMADs). Phosphorylated R-SMADs can form oligomeric complexes with SMAD4 (Co-SMAD) and be translocated into the nucleus. After entering the nucleus, the complex of Smad4 and the activated R-Smad can bind DNA to activate or repress target genes depending on which nuclear cofactors are present. The R-SMAD/SMAD4 complex can be inhibited by SMAD6. Red indicates activation, while blue indicates inhibition and green shows Smad4. RI and RII indicate type I and type II receptors. modified (von Bubnoff and Cho 2001)

Besides the canonical pathway, which has been described earlier in the text, BMPs can activate SMAD-independent pathways such p38 MAPK (Moriguchi, Kuroyanagi et al. 1996, Kimura, Matsuo et al. 2000), JNK (Blank, Brown et al. 2009) or PI3K/P-AKT (He, Zhang et al. 2004). Specifically it has been shown that BMP7-evoked chemotaxis of monocytes is due to PI3K/P-AKT-dependent signaling (Perron and Dodd 2009).

The regulation of the balance between activation of these different intracellular mechanisms is not well understood. Furthermore, the mode of physical interaction between BMPRI and BMPRII receptors regulates the signaling outcome (Perron and Dodd 2009). Activation of preformed BMPRI/RII complexes at the cell surface preferentially initiates SMAD activation, whereas ligand-induced assembly of

BMPRI/RII complexes results in the activation of MAPK (Nohe, Hassel et al. 2002). Factors that differentially influence the mode of receptor complex formation have not been identified, yet (Oxburgh 2009).

Regarding adrenal chromaffin cells, which derive from the embryonic neural crest, BMPs released from the dorsal aorta during embryogenesis (mainly BMP4/7) are important positional signals for the induction of a sympathoadrenal catecholaminergic differentiation cell fate. It has been shown that the neural crest generates a population of multipotent progenitor cells, which have the capacity to give rise to both sympathetic neurons and chromaffin cells located in the adrenal medulla; BMPs including BMP7 are known to drive this chromaffin cell fate (Figure 5) (Huber, Franke et al. 2008).

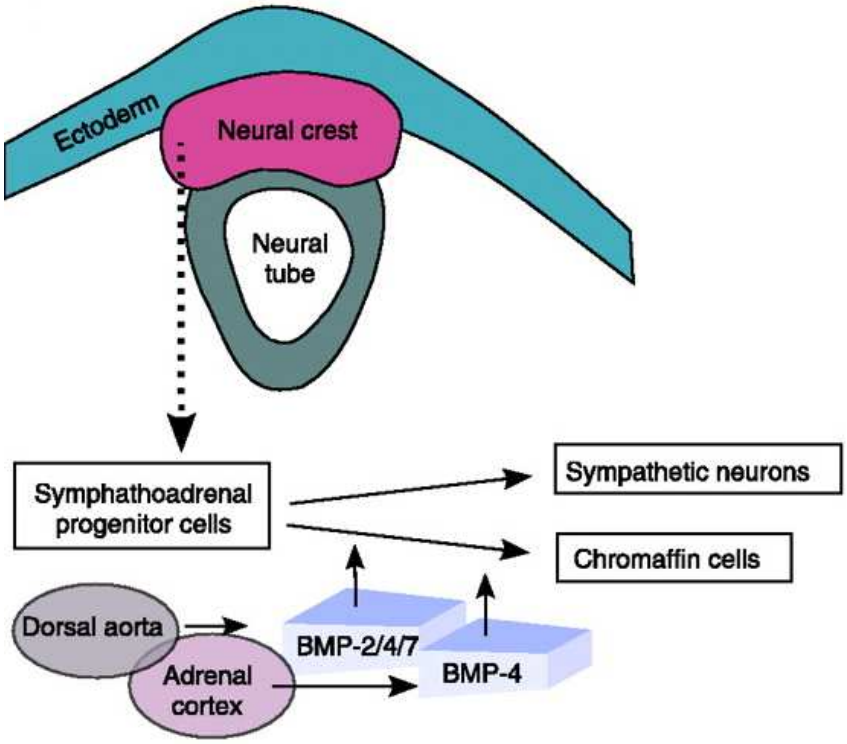

Figure 5. Roles of BMPs during adrenal development. Sympathoadrenal progenitor cells undergo differentiation to adrenomedullary chromaffin cells caused by the effect of BMP2/BMP4/BMP7 (secreted by dorsal aorta and adrenal cortex). (⟶, stimulation). Modified (Johnsen and Beuschlein 2010)

In addition to their developmental functions, BMPs which are secreted locally by the adrenal cortex could also determine the cellular fate of tissue progenitor cells in the adrenal medulla of the adult (Kano, Otsuka et al. 2005, Huber, Franke et al. 2008,

Goto, Otsuka et al. 2009). Indeed, a direct functional role of BMPs (BMP2, BMP4, BMP6 and BMP7) on adrenomedullary hormone secretion has been proposed (Kano, Otsuka et al. 2005, Goto, Otsuka et al. 2009). Interestingly, BMPs (BMP2, BMP4, BMP6 and BMP7) are thought to induce catecholamine production from adrenomedullary cells by interfering with steroid hormone-dependent signaling (Kano, Otsuka et al. 2005, Goto, Otsuka et al. 2009).

1.8. BMPs and Tumorigenesis

In addition to the role of BMPs in development, there is an increasing body of evidence that the perturbation of BMP pathways can affect tumorigenesis. Mutations of genes acting in the BMP7 pathway are responsible for some familial cancer syndromes. Germline mutations in BMP receptor IA (*BMPR-IA)* have been identified in a subset of families with Cowden syndrome, an inherited breast cancer syndrome. The same applies for mutations of *SMAD4* and *BMPR-IA* which were detected as being genetically responsible for some cases of familial juvenile polyposis (Howe, Roth et al. 1998). Furthermore, it has been reported that various sporadic human cancers also exhibit aberrations in BMP signaling pathways (Johnsen and Beuschlein 2010) and BMPs can affect tumorigenesis themselves by the modulation of various cancer- and cell-type specific signaling pathways. It was shown by *in vitro* experiments that BMP7 has a growth suppressive effect on the colon cancer via SMAD-independent pathways (Beck, Jung et al. 2006, Carethers, Beck et al. 2006).
Moreover, BMP7 has been shown to have anti- or pro-carcinogenic effects in various tumor types (Blanco Calvo, Bolos Fernandez et al. 2009). It was observed that BMP7 has an anti-apoptotic, anti-metastatic and anti-invasive role in prostate cancer cells (Buijs, Rentsch et al. 2007). BMP7 also shows a growth inhibitory effect on melanomas (Na, Seok et al. 2009) cervical cancer (Cassar, Li et al. 2008) and thyroid carcinoma cells. For instance, in thyroid cancer cells BMP7 induces a G1-phase arrest by upregulation of the cyclin dependent kinase inhibitors (CDKIs) p21 and p27 (Franzen and Heldin 2001).
In contrast, it has been reported that BMP7 may promote metastatic behavior in other tumor types. Indeed, BMP7 induces the scattering of colon cancer cells by activating ERK, JNK and RAC signaling cascades (Gespach, Grijelmo et al. 2007). The formation of bone metastasis is another potential characteristic of the BMP7 protein which is under investigation (Buijs, Henriquez et al. 2007, Alarmo, Korhonen et al.

2008). Moreover, BMP7 expression was correlated with tumor size, invasion and patient postoperative outcome in gastric cancer (Aoki, Ishigami et al. 2011).

There is an increasing body of evidence that BMP7 stimulation can promote different phenotypes in different cell types as it has been described for breast cancer cells (Alarmo, Parssinen et al. 2009), where BMP7 may either inhibit or promote the growth, metastasis and invasion of breast cancer cells (Kallioniemi, Alarmo et al. 2006, Yan and Chen 2007, Alarmo, Korhonen et al. 2008). Also in prostate cancer, a dual role of BMP7 as anti-tumorigenic or anti-apoptotic factor has been reported (Yang, Lim et al. 2006).

While the functional significance of BMP7 has already been studied in some tumor types, its role in adrenomedullary tumorigenesis has not been explored so far. The mechanisms mediating the pro-metastatic effect of BMP7 in cancers are still not well understood. Elucidation of BMP7 dependent molecules and pathways will be helpful to better understand mechanism mediating an aggressive and metastasizing phenotype and will help to identify novel therapeutic targets.

1.9. Integrins involved in migratory processes

As already described most pheochromocytomas are benign and curable by surgical resection, but approximately 10% are clinically malignant and the 5 year survival rate for these patients is below 50% (Eisenhofer, Bornstein et al. 2004, Nomura, Kimura et al. 2009). Therefore, it is very important to understand the mechanisms mediating the development of metastases. In order to block the migratory and invasive potential of tumor cells it is essential to develop a new approach for treat patients with malignant disease (Hood and Cheresh 2002).

The phenotypic change during migration and invasion is initially caused by alterations in the expression of cell-surface molecules, such as integrins, and by the release of proteases that remodel the extracellular matrix (ECM) (Duffy 1992, Stamenkovic 2000, Mierke, Frey et al. 2011). These molecules can induce signaling cascades which regulate processes such as gene expression (Missan, Chittur et al. 2014), cytoskeletal organization (Hood and Cheresh 2002), cell adhesion (Akiyama 1996) and cell survival (Stupack and Cheresh 2002).

Integrins are a family of glycoproteins that build heterodimeric (α,β) receptors that bind to ECM molecules (Knudsen, Horwitz et al. 1985, Hynes 1987, Burke 1999,

Hynes 2002). Each subunit has a large extracellular domain, a single membrane-spanning domain, and a short, non-catalytic cytoplasmic tail (Hynes, Marcantonio et al. 1989, Hynes 2002).

The integrin family can generate at least 25 distinct receptors from the pairing of 18 different alpha-subunits with the 8 beta-subunits (Hynes, Marcantonio et al. 1989, Hynes 2002). Each pair is specific for a unique set of ECM components. For example, integrin alphav/beta3 binds a wide range of ECM molecules, whereas integrin alpha5/beta1 selectively binds fibronectin-5 (van der Flier and Sonnenberg 2001). Following extracellular ligand binding, integrins build intracellular contacts to link physically with many different actin-associated proteins, such as alpha-actinin, vinculin, tensin and paxillin (Bellis, Miller et al. 1995, Ziegler, Gingras et al. 2008, Roca-Cusachs, del Rio et al. 2013, Haynie 2014). These particles build a link between the integrins and the cytoskeleton (Sastry and Burridge 2000). Integrins also activate intracellular kinases that phosphorylate cytoskeletal proteins, mediating cell shape and migration, or recruit signaling proteins that regulate integrin adhesiveness to the ECM (Chen, Kinch et al. 1994).

It has been reported that integrin signaling activates phosphatidylinositol 3-kinase (PI3K), which in turn regulates cell motility by phosphorylating the protein kinase B (AKT) (Figure 6) (Qian, Zhong et al. 2005, Xue and Hemmings 2013). Activated Akt phosphorylates downstream substrates that trigger different functions in a variety of cellular conditions.There substrates include several cytoskeleton-regulating proteins and EMT–activating proteins that specifically modulate cell motility (Montero, Kilian et al. 2003, Xue and Hemmings 2013). PI3K is activated following integrin ligation, in kidney epithelial cells, in breast carcinomas and mammary epithelial cells (Keely, Westwick et al. 1997, Khwaja, Rodriguez-Viciana et al. 1997, Shaw, Rabinovitz et al. 1997).

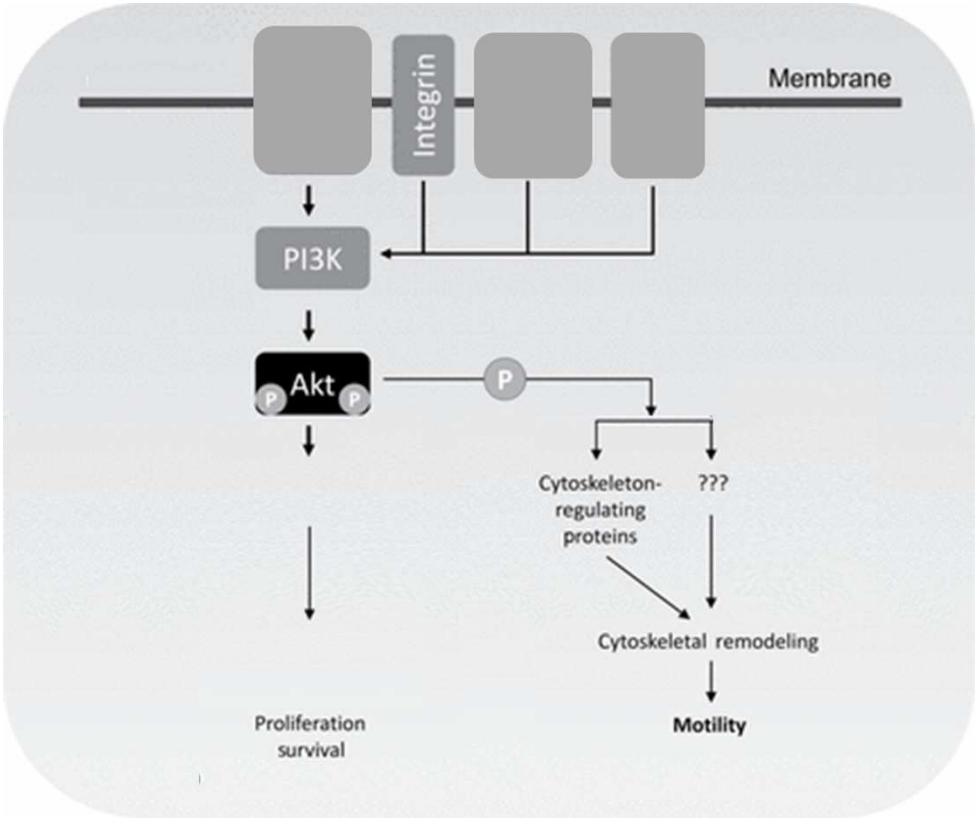

Figure 6. Classical phosphoinositide 3 kinase (PI3K)/AKT signaling pathway. Upon activation by integrin, PI3K is activated and provokes AKT membrane targeting. AKT can be maximal phosphorylated at serin (473) and threonine 308 (T308). Activated Akt phosphorylates various substrates, including several cytoskeleton-regulating proteins and proteins that specifically regulate cell motility. Modified (Xue and Hemmings 2013)

In addition to the stimulating effect of integrins on PI3K/AKT pathway, it was shown that PI3K/AKT itself enhances integrin-mediated migration. For example, activated PI3K affects the epidermal growth factor (EGF) and its family member, heregulin (both expressed by metastatic breast cancer cells), which in turn enhances beta1-integrin-mediated adhesion and migration in breast carcinomas (Adelsman, McCarthy et al. 1999). Similarly, has been shown that BMP2, another BMP family member, acts through the PI3K/AKT pathway, to activate integrin β1 thereby contributing to the migration of human chondrosarcoma cells (Fong, Li et al. 2008).

1.10. Hypothesis

MENX-affected rats develop bilateral pheochromocytomas with complete penetrance during their first year of life. The MENX syndrome is caused by a frameshift mutation in *Cdkn1b*, the gene encoding the cell cycle inhibitor p27. This mutation leads to a massive reduction of the p27 protein in adrenal chromaffin cells *in vivo*. MENX-associated pheochromocytomas were found to express at high level the mRNA encoding the bone morphogenetic protein *Bmp7*, a molecule that is usually involved in development and regeneration of injured tissues. Sporadic and hereditary human pheochromocytomas (without p27 mutation) also show overexpression of *BMP7* (Molatore, Liyanarachchi et al. 2010). Studies by other groups on rodent and human cancer models have produced conflicting results concerning the effects of BMP7 on tumor cell proliferation, invasive and metastasis potential.

Given that pheochromocytomas in both rats and human patients overexpress BMP7, we hypothesized that this molecule must play a role in pheochromocytoma tumorigenesis. As currently no information is available about the possible function of active BMP7 signaling in pheochromocytomas, we decided to address this issue. Thus, the aim of our project was to investigate the role of BMP7 in both rat and human pheochromocytoma tumorigenesis.

To accomplish this aim, we assessed the effect of modulating BMP7 levels (up- and down- regulation) on tumor cell characteristics such as cell proliferation and migration. Furthermore, we wanted to identify downstream targets in adrenomedullary cells which are activated by BMP7 signaling.

The results of these studies are expected to elucidate the molecular mechanisms underlying the formation of pheochromocytomas and eventually to help to identify novel therapeutic targets or to develop new treatment strategies for this tumor entity.

2. MATERIALS AND METHODS

2.1. Materials

2.1.1. EQUIPMENT

Adhesive seal applicator	**3M Deutschland, Neuss (Germany)**
Automated immunostainer, Discovery XT	**Ventana Medical System, Inc., Tucson (AZ, USA)**
Centrifuge Biofuge fresco	**Heraeus Instruments, Osterode (Germany)**
Rotor: 3325B 1.5 ml	**Thermo Fisher Sci., Waltham (MA, USA)**
Centrifuge Biofuge pico	**Heraeus Instruments, Osterode (Germany)**
Rotor: 3325B 1.5 ml	**Thermo Fisher Sci., Waltham (MA, USA)**
Centrifuge eppendorf 5415D	**eppendorf, Hamburg (Germany)**
Rotor: F45-24-11 1.5 ml	**eppendorf, Hamburg (Germany)**
Centrifuge Fisherbrand Mini	**Fisher Scientific, Schwerte (Germany)**
Rotors 0.2 ml, 1.5 ml	**Fisher Scientific, Schwerte (Germany)**
Centrifuge Rotanta 460R	**Andreas Hettich, Tuttlingen (Germany)**

Rotor: 5624 15 ml, 50 ml	**Andreas Hettich, Tuttlingen (Germany)**
Centrifuge Rotina 420R	**Andreas Hettich, Tuttlingen (Germany)**
Rotor: 4790 1.5 ml	**Andreas Hettich, Tuttlingen (Germany)**
Centrifuge Variofuge 3.0R	**Heraeus Sepatech, Osterode (Germany)**
Rotor: #8074, inserts #8078 15 ml, 50 ml	**Heraeus Sepatech, Osterode (Germany)**
Counting chamber Improved Double Neubauer Ruling	**Brand, Wertheim (Germany)**
Dispenser Multipette® plus	**eppendorf, Hamburg (Germany)**
Electrophoresis Cell GT MINI-SUB®	**Bio-Rad Laboratories, Munich (Germany)**
Electrophoresis Mini-Cell XCell *SureLock™* Novex	**Invitrogen, Darmstadt (Germany)**
Electrophoresis Transfer Cell Mini Trans-Blot®	**Bio-Rad Laboratories, Munich (Germany)**
Freezer -20°C Liebherr Comfort	**Liebherr, Biberach an der Riss (Germany)**
Freezer -80 °C HFC86-360	**Heraeus Instruments, Osterode (Germany)**
Freezing container NALGENE™ Cryo 1 °C	**Thermo Fisher Sci., Roskilde (Denmark)**
Fridge +4 °C Liebherr Premium	**Liebherr, Biberach an der Riss (Germany)**

Gas burner Fuego SCS basic	WLD-TEC, Goettingen (Germany)
Gel documentation system	Vilber Lourmat, Eberhardzell (Germany)
Heating block Thermomixer® comfort 1.5 ml	eppendorf, Hamburg (Germany)
Heating block Thermomixer® compact 1.5 ml	eppendorf, Hamburg (Germany)
Heating block ThermoStat plus 1.5 ml	eppendorf, Hamburg (Germany)
Hood Uniflow UVUB 1800	UniEquip, Planegg (Germany)
Ice machine	Ziegra, Isernhagen (Germany)
Incubator shaker Model G25	New Brunswick Sci., Edison (NJ, USA)
Incubator innova CO-170	New Brunswick Sci., Edison (NJ, USA)
Infinite M200 plate reader	Tecan, Crailsheim (Germany)
Magnetic stir bars, various sizes	neoLab, Heidelberg (Germany)
Magnetic stirrer MR2000	Heidolph Instr., Schwabach (Germany)
Maxwell® 16	Promega (Madison WI, USA)
Microplate Reader Model 680	Bio-Rad Laboratories, Munich (Germany)
Microscope Apotome	Carl Zeiss, Jena (Germany)
Microscope Axiovert 135	Carl Zeiss, Jena (Germany)
Microscope BX 43	Olympus, Hamburg (Germany)

Microscope EVOS xl	AMG, Bothell (WA, USA)
Microwave Privileg 1034HGD	Otto, Hamburg (Germany)
Microwave Whirlpool ProMicro 825	Bauknecht Hausg., Stuttgart (Germany)
Multichannel pipette Finnpipette® 50-300 µl	Thermo LabSys., Waltham (MA, USA)
4D-Nucleofector™ System (Core and X unit)	Lonza, Basel (Switzerland)
PCR cycler GeneAmp® PCR system 9700	Applied Biosystems, Carlsbad (CA, USA)
PCR cycler Real-Time 7300	Applied Biosystems, Carlsbad (CA, USA)
PCR cycler SensoQuest labcycler	SensoQuest, Goettingen (Germany)
PCR cycler TPersonal Thermocycler	Biometra, Goettingen (Germany)
pH meter inoLab® Level 1	WTW, Weilheim (Germany)
Pipette Discovery 100-1000 µl	Abimed, Langenfeld (Germany)
Pipette Discovery 20-200 µl	Abimed, Langenfeld (Germany)
Pipette Discovery 10-100 µl	Abimed, Langenfeld (Germany)
Pipette Discovery 2-20 µl	Abimed, Langenfeld (Germany)
Pipette Discovery 0.5-10 µl	Abimed, Langenfeld (Germany)
Pipette P1000	Gilson, Middleton (WI, USA)
Pipette P200	Gilson, Middleton (WI, USA)
Pipette P100	Gilson, Middleton (WI, USA)

Pipette P20	**Gilson, Middleton (WI, USA)**
Pipette P10	**Gilson, Middleton (WI, USA)**
Pipettor accu-jet®	**Brand, Wertheim (Germany)**
Pipettor PIPETBOY acu	**Integra Biosciences, Fernwald (Germany)**
Pipettor pipetus®-akku	**Hirschmann Laborg., Eberstadt (Germany)**
Power supply Model 200/2.0	**Bio-Rad Laboratories, Munich (Germany)**
Power supply PowerPac 300	**Bio-Rad Laboratories, Munich (Germany)**
Pressure cooking pot Tender Cooker	**Nordic Ware, Minneapolis (MN, USA)**
Reaction tube rotator L29	**A. Hartenstein, Wuerzburg (Germany)**
Rocker table Rocky®	**Fröbel Labortechnik, Lindau (Germany)**
Scales Sartorius basic	**Sartorius, Göttingen (Germany)**
Scales Sartorius universal	**Sartorius, Göttingen (Germany)**
Scanner 3000 7G with autoloader	**Affimetrix (USA)**
Spectrophotometer NanoDrop® ND-1000	**Thermo Fisher Sci., Waltham (MA, USA)**
Spectrophotometer UV/VIS Novaspec II	**Pharmacia LKB, Uppsala (Sweden)**
Tweezers No.5	**A.Dumont&Fils, Montignez (Switzerland)**

Vacuum Concentrator plus	**eppendorf, Hamburg (Germany)**
Vortexer Reax top	**Heidolph Instr., Schwabach (Germany)**
Vortexer Vortex-Genie 2	**Scientific Industries, Bohemia (NY, USA)**
Water bath shaker #1083	**G. f. Labortechnik, Burgwedel (Germany)**
Water bath shaker SW21	**Julabo Labortechnik, Seelbach (Germany)**

2.1.2. CONSUMABLE MATERIALS

Adhesive seal films MicroAMP™	**Applied Biosys., Foster City (CA, USA)**
Blotting paper grade 3m/N 65 g/m²	**Munktell & Filtrak, Bärenstein (Germany)**
Cell strainer Falcon™ 70 µm, nylon	**BD Biosciences, Bedford (MA, USA)**
Combitips® for Multipette® 12.5 ml	**eppendorf, Hamburg (Germany)**
Cover slips 12 mm round	**Carl Roth, Karlsruhe (Germany)**
Cryogenic vials sterile 2 ml freestanding Falcon®	**BD Biosciences, Franklin Lakes (NJ, USA)**
Cuvettes PLASTIBRAND® 1.5 ml semi-micro	**Brand, Wertheim (Germany)**
Gel cassettes 1.5 mm	**Invitrogen, Grand Island (NY, USA)**

Glass slides SuperFrost® 76 x 26 mm	Carl Roth, Karlsruhe (Germany)
Cell Culture Inserts for 24-well plates. 8.0 µm pores, Transparent PET Membrane. BD BioCoat™ BD	Biosciences, Franklin Lakes (NJ, USA)
Membrane for Western Amersham™ Hybond™-ECL	GE Healthcare, Munich (Germany)
Microplates, TC 96 well, clear bottomed, white walled	Lonza, Basel (Switzerland)
Needles Sterican® Ø 0.60 x 60 mm 23G x 2 $^{3}/_{8}$”	B. Braun, Melsungen (Germany)
Needles Sterican® Ø 0.80 x 50 mm 21G x 2”	B. Braun, Melsungen (Germany)
Parafilm®	Carl Roth, Karlsruhe (Germany)
PCR plate (0.2 ml) Thermo-Fast® 96-well, non-skirted	Abgene/Thermo Sci., Rockford (IL, USA)
PCR tube strips 0.2 ml	eppendorf, Hamburg (Germany)
Petri dishes 100 x 15 56.7 cm^2 Nunclon™ Δ	nunc, Roskilde (Denmark)
Petri dishes glass bottom poly-D-lysine coated no. 1.5	MatTek, Ashland (MA, USA)
pH indicator strips	Merck, Darmstadt (Germany)
Photographic film Amersham Hyperfilm™ ECL	GE Healthcare, Little Chalfont (England)
Pipettes, Pasteur glass 3.2 ml	Carl Roth, Karlsruhe (Germany)
Pipettes, serological CELLSTAR® 5 ml	Greiner BioOne, Frickenhausen (Germany)

Pipettes, serological CELLSTAR® 10 ml	Greiner BioOne, Frickenhausen (Germany)
Pipettes, serological CELLSTAR® 25 ml	Greiner BioOne, Frickenhausen (Germany)
Pipette tips Graduated Filter Tips TipOne® 0.1-10 µl	Starlab, Ahrensburg (Germany)
Pipette tips Graduated Filter Tips TipOne® 1-20 µl	Starlab, Ahrensburg (Germany)
Pipette tips Graduated Filter Tips TipOne® 1-100 µl	Starlab, Ahrensburg (Germany)
Pipette tips Graduated Filter Tips TipOne® 1-200 µl	Starlab, Ahrensburg (Germany)
Pipette tips Graduated Filter Tips TipOne® 101-1000 µl	Starlab, Ahrensburg (Germany)
Pipette tips, DIAMOND® Standard Tips DL10	Gilson S.A.S, Villiers le Bel (France)
Pipette tips, DIAMOND® Standard Tips D200	Gilson S.A.S, Villiers le Bel (France)
Pipette tips, DIAMOND® Standard Tips D1000	Gilson S.A.S, Villiers le Bel (France)
Reaction tubes 1.5 ml	eppendorf, Hamburg (Germany)
Reaction tubes 2 ml	eppendorf, Hamburg (Germany)
Reaction tubes Falcon™ Blue Max 15 ml	BD Biosciences, Franklin Lakes (NJ, USA)
Reaction tubes Falcon™ Blue Max 50 ml	BD Biosciences, Franklin Lakes (NJ, USA)

Reaction tubes, RNase-free 1.5 ml	**Zymo Research, Orange (CA, USA)**
Scalpel, sterile, disposable	**Aesculap, Tuttlingen (Germany)**
Syringe, single-use 50 ml (60 ml)	**Henke-Sass-Wolf, Tuttlingen (Germany)**
Tissue culture flasks 25 cm^2, filter cap Nunclon™ Δ	**nunc, Roskilde (Denmark)**
Tissue culture flasks 75 cm^2, filter cap	**Greiner BioOne, Frickenhausen (Germany)**
Tissue culture plates 6 well Nunclon™ Δ	**nunc, Roskilde (Denmark)**
Tissue culture plates 24 well MULTIWELL™ flat	**BD, Franklin Lakes (NJ, USA)**
Tissue culture plates 48 well MULTIWELL™ flat	**BD, Franklin Lakes (NJ, USA)**
Tubes, plastic 5 ml 75x12 mm	**Sarstedt, Nuembrecht (Germany)**

2.1.3. CHEMICALS AND REAGENTS

β-mercaptoethanol	Sigma-Aldrich, Steinheim (Germany)
Agarose LE for gel electrophoresis	Biozym, Hessisch Oldendorf (Germany)
Ampicillin sodium salt	Sigma-Aldrich, Steinheim (Germany)
Ampuwa® water	Fresenius KABI, Bad Homburg (Germany)
APS	Sigma-Aldrich, Steinheim (Germany)
Bis-acrylamide ProtoGel 30 % (w/v)	national diagnostics, Atlanta (GA, USA)
Bovine Serum Albumin (BSA)	Sigma-Aldrich, Steinheim (Germany)
Butane Campingaz® CV360	CampingGaz, Hungen-Inheiden (Germany)
Chemiluminescent substrate SuperSignal® West Femto	Pierce/Thermo Sci., Rockford (IL, USA)
Chemiluminescent substrate SuperSignal® West Pico	Pierce/Thermo Sci., Rockford (IL, USA)
Chloroform	Merck, Darmstadt (Germany)
Cresol red	AppliChem, Darmstadt (Germany)
DMEM + GlutaMAXTM-I, 4.5 g/l D-glucose, pyruvate	Gibco/Invitrogen, Grand Island (NY, USA)
DMSO	Sigma-Aldrich, Steinheim

	(Germany)
dNTP Mix 10 mM each	Fermentas, St. Leon-Rot (Germany)
DTT 0.1 M	Invitrogen, Grand Island (NY, USA)
DMH1	MCE MedChem Express, Stockholm (Sweden)
Ethanol	Merck, Darmstadt (Germany)
Ethidium bromide	Sigma-Aldrich, Steinheim (Germany)
F-12K Nutrient Mixture, Kaighn's Modification (1X), liquid	Gibco/Invitrogen, Grand Island (NY, USA)
Fetal bovine serum (FBS)	Gibco/Invitrogen, Grand Island (NY, USA)
First strand buffer 5x	Invitrogen, Grand Island (NY, USA)
Fungizone™	Gibco/Invitrogen, Grand Island (NY, USA)
Gel loading dye, blue 6x	New England Biolabs, Ipswich (MA, USA)
Geneticin® (G418)	Gibco/Invitrogen, Grand Island (NY, USA)
Glyerol	Sigma-Aldrich, Steinheim (Germany)
GnRH agonist Sigma L4513	Sigma-Aldrich, Steinheim (Germany)

GSK690693	**Sigma-Aldrich, Steinheim (Germany)**
HBSS 1x without $CaCl_2$/$MgCl_2$	**Gibco/Invitrogen, Grand Island (NY, USA)**
HCl 5 M	**neoLab, Heidelberg (Germany)**
Hoechst 33258 bisBenzimide	**Sigma-Aldrich, Steinheim (Germany)**
Isopropanol	**Merck, Darmstadt (Germany)**
Kanamycin A monosulfate	**Sigma-Aldrich, St. Louis (MO, USA)**
Laemmli sample buffer 1x	**Bio-Rad Lab., Hercules (CA, USA)**
LB broth base	**Invitrogen, Grand Island (NY, USA)**
Methanol	**Merck, Darmstadt (Germany)**
Mounting medium VECTASHIELD®	**Vector Lab., Burlingame (CA, USA)**
Thiazolyl Blue Tetrazolium Bromide (MTT)	**Sigma-Aldrich, St. Louis (MO, USA)**
NP-40 Tergitol®	**Sigma-Aldrich, St. Louis (MO, USA)**
NVP-BEZ235	**Novartis Pharma, Nürnberg (Germany)**
Opti-MEM® Reduced Serum Medium, no phenol red	**Gibco/Invitrogen, Grand Island (NY, USA)**
Paraformaldehyde	**Merck, Darmstadt (Germany)**
PBS powder pH 7.4	**Sigma-Aldrich, St. Louis (MO,**

	USA)
Penicillin-Streptomycin, liquid	Gibco/Invitrogen, Grand Island (NY, USA)
Phenol Red	Sigma-Aldrich, Steinheim (Germany)
Photographic developer G153 A and B	Agfa Healthcare, Mortsel (Belgium)
Photographic fixer G354	Agfa Healthcare, Mortsel (Belgium)
Polybrene	Sigma-Aldrich, Steinheim (Germany)
Ponceau S practical grade	Sigma-Aldrich, Steinheim (Germany)
Protease inhibitor cocktail tablets complete mini	Roche Diagnostics, Mannheim (Germany)
Red blood cell Lysing Buffer	Sigma-Aldrich, Steinheim (Germany)
Recombinant Human BMP-7	R&D Systems (USA, Canada)
Recombinant Human Noggin	Bio Vision Inc. (USA)
RNase inhibitor RNaseOUT™	Invitrogen, Grand Island (NY, USA)
RNaseZAP®	Sigma-Aldrich, St. Louis (MO, USA)
RNase*Zap*®	Ambion, Austin (TX, USA)
RPMI 1640	Gibco/Invitrogen, Grand Island (NY, USA)

SDS 10 % (w/v) solution	Bio-Rad Laboratories, Munich (Germany)
SDS-PAGE running buffer Rotiphorese®, 10x	Carl Roth, Karlsruhe (Germany)
Skimmed milk powder	Saliter, Oberguenzburg (Germany)
Sodium chloride	Merck, Darmstadt (Germany)
Sodium deoxycholate	Sigma-Aldrich, St. Louis (MO, USA)
Sodium hydroxide tablets	Merck, Darmstadt (Germany)
Stripping buffer for Western Blots Restore™ PLUS	Pierce/Thermo Sci., Rockford (IL, USA)
TaqMan® universal PCR master mix 2x	PE Applied Biosys, Weiterstadt (Germany)
TBE Tris/Boric Acid/EDTA, 10x	Bio-Rad Lab., Hercules (CA, USA)
TBS-T, 10x	Bio-optica (Italy)
TEMED	Amresco, Solon (OH, USA)
Toluidine blue O (C.I. 52040) Certistain®	Merck, Darmstadt (Germany)
Transfection Reagent FuGENE HD	Roche Diagnostics, Mannheim (Germany)
Transfection Reagent LipofectaminTM 2000	Invitrogen, Darmstadt (Germany)
Transfection XtremeGENE HP	Roche Diagnostics, Mannheim (Germany)
Triton X-100	Sigma-Aldrich, Steinheim (Germany)

Trizma® base	**Sigma-Aldrich, Steinheim (Germany)**
TRIzol® reagent	**Invitrogen, Grand Island (NY, USA)**
Trypan blue solution 0.4 %	**Sigma-Aldrich, St. Luis (MO, USA)**
Trypsin, 0.05% with EDTA	**Gibco/Invitrogen, Grand Island (NY, USA)**
Tween 20	**Carl Roth, Karlsruhe (Germany)**
W-CAP Citratpuffer PH6	**Bio-optica (Italy)**
Xylol	**Merck, Darmstadt (Germany)**

2.1.4. BUFFERS AND SOLUTIONS

If not stated otherwise, all solutions listed were prepared in bidest. water.

Agarose gel

1 % (w/v) agarose in 1x TBE
boil until dissolved, cool to approximately 60 °C
add 0.005 % (v/v) ethidium bromide

PCR master mix

6 % (w/v) sucrose
200 µM dATP
200 µM dCTP
200 µM dTTP
200 µM dGTP
10 % (v/v) 10x buffer (biotherm, no $MgCl_2$)
3 % (v/v) $MgCl_2$
40 ng/ml Cresol red

Paraformaldehyde (2 %, pH 7.4)

2 % (w/v) paraformaldehyde in PBS
15 µl phenol red
add 10 M NaOH until dissolved (colour change from pink to colourless)
adjust pH to 7.4 with HCl using pH indicator strips

Ponceau dye

0.1 % (w/v) Ponceau S
5 % (v/v) acetic acid

RIPA buffer (pH 8.0)

50 mM Trizma® base
150 mM NaCl
0.1 % (w/v) SDS
0.5 % (w/v) sodium deoxycholate
1 % (w/v) NP-40

Separating gel (12 %) for SDS-PAGE (10 ml)

4 ml 30 % (w/v) acrylamide/bis
3.35 ml H_2O bidest.
2.5 ml 1.5 M Tris (pH 8.8)
100 µl 10% (w/v) SDS
50 µl 10 % (w/v) APS
5 µl TEMED

Stacking gel (4 %) for SDS-PAGE (5ml)

670 µl 30 % (w/v) acrylamide/bis
3 ml H_2O bidest.
1.26 ml 0.5 M Tris (pH 6.8)
50 µl 10% (w/v) SDS
25 µl 10 % (w/v) APS
5 µl TEMED

TBS-T 10x (pH 7.6)

0.2 M Trizma® base

1.5 M NaCl

1 % (v/v) Tween 20

for 1x, dilute 1:10 in H_2O bidest

2.1.5. COMMERCIALLY AVAILABLE KITS

BCA Protein Assay Pierce®	23225; Thermo Sci., Rockford (IL, USA)
Caspase-Glo® 3/7 Assay	G8091, Promega (Madison WI, USA)
Cell Proliferation Reagent WST-1	05015944001 Roche Diagnostics, Mannheim (Germany)
Histo mark Biotin Streptavidin HRR-system Goat anti Rabbit IgG (H+L)	71-00-19, Kirkegaard & Perry Laboratories (MD, USA)
Histo mark Biotin Streptavidin HRR-system Goat anti Mouse IgG (H+L)	71-00-18, Kirkegaard & Perry Laboratories (MD, USA)
Human BMP7 ELISA Kit	RAB0033-1KT; Sigma-Aldrich, (Germany)
Miniprep Kit QIAprep® Spin (50)	27104; Qiagen, Hilde (Germany)
Mycoplasma detection kit	PK-CA20-700-20; PromoKine, (Germany)
Maxwell® 16 simply RNA Tissue Kit	AS1280; Promega (Madison WI, USA)
Rat ELISA Kit Bone Morphogenetic Protein 7 (rat)	SEA799Ra; USCN Life Science Inc. (China)
SF Cell Line 4D-Nucleofector™ X Kit	V4XC-1024; Lonza, Basel (Switzerland)

2.1.6. STANDARDS

DNA Molecular Weight Marker VIII (19-1114 bp)	Roche Diagnostics, Mannheim (Germany)
PageRuler™ prestained protein ladder	Fermentas, St. Leon-Rot (Germany)

2.1.7. CONSTRUCTS

The **pCMV6**-Entry vector containing BMP7 (Myc/DDK tagged) (Figure 7) was commercially acquired by ORIGENE Technologies, Rockville (MD, USA).

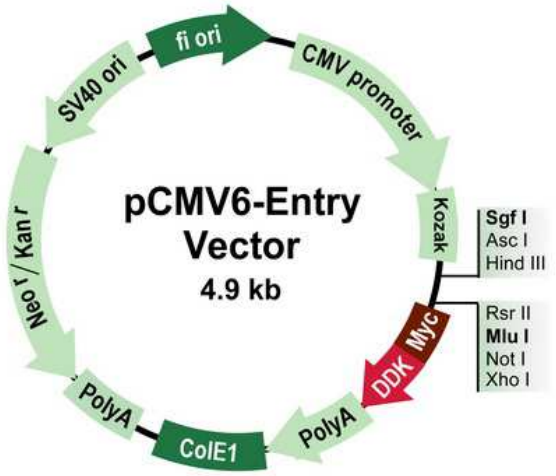

Figure 7. BMP7 vector (pCMV6-Entry Vector).

The **pCMV-Myc** vector (BD Biosciences, Erembodegem, Belgium) (Figure 8) was used as a mock-vector.

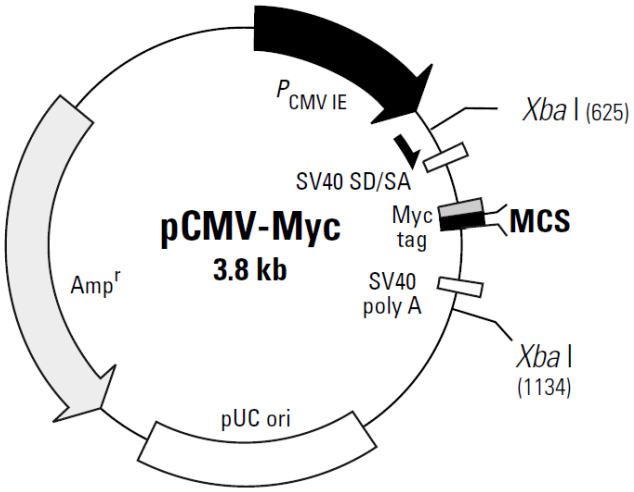

Figure 8. Mock vector (pCMV-Myc).

The **pGP** transfer vector (Figure 9) was a kind gift of Dr. Anastasov (Anastasov, Hofig et al. 2012).

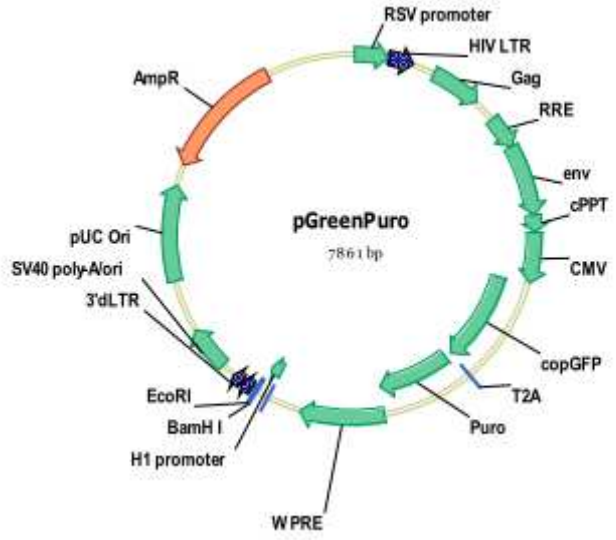

Figure 9. Map and Features for pGreenPuro™ Vector.

2.1.8. PRIMERS

For reverse transcription, random primers purchased from Promega (Madison WI, USA) were used. The following primers for RT-PCR were designed using Primer4 software (http://frodo.wi.mit.edu/primer4/) and ordered from metabion (Martinsried, Germany).

Table 2. Sequences of random primers used for RT-PCR

rat		mouse	
rAcvr2b-F:	5'-CATCACGTGGAACGAACTGTGC -3	*mAcvr2a*-F:	5'-AAACGGCGACATTGTTTTGC-3
rAcvr2b-R:	5'-AGCATGTACTCATCGACAGGCC-3	*mAcvr2a*-R:	5'-GTGTGACTTCCATCTCCGGA-3
rAcvr2a-F:	5'-TCAGACTGGTGTTGAGCCTT-3	*mAcvr2b*-F:	5'-CATCACGTGGAACGAACTGTGC-3
rAcvr2a-R:	5'-GTGTGACTTCCATCTCCGGA-3	*mAcvr2b*-R:	5'-AGCATGTACTCATCGACAGGCC-3
rAlk2-F:	5'-TGCTAATGATGATGGCTCTCC-3	mALK2-F:	5'-TCGATGGAGTAATGATCCTTCC-3
rAlk2-R:	5'-CGATCCAGGGAAGGATTTC-3	mALK2-R:	5'-CCGTGATGTTCCTGTTACACC-3
rAlk3-F:	5'-GGAGGAATCGTGGAGGAATAT-3	mALK3-F:	5'-CAGACTTGGACCAGAAGAAGCC-3
rAlk3-R:	ATACGCAAAGAACAGCATGTC-3	mALK3-R:	5'-ACATTCTATTGTCTGCGTAGC-3
rAlk6-F:	5'-AGACTGAGATATATCAGACGGTCC-3	*mAlk6-F:*	5'-AGACTGAGATATATCAGACGGTCC-3
rAlk6-R:	5'-CGTGTGTAGATGGCACAGG-3	*mAlk6-R:*	5'-CGTGTGTAGATGGCACAGG-3
rBmpr2-F:	5'-GGAGAAATCAAAAGGGGAC-3	*mBmpr2-F:*	5'-GGAGAAATCAAAAGGGGAC-3
rBmpR2-R:	5'-CTCCTGTCAACATTCTGTATCC-3	*mBmpR2-R:*	5'-CTCCTGTCAACATTCTGTATCC-3

2.1.9. siRNAs

siRNA p27 rat (sip27)
L-RAT-XX-0005; Thermo scientific Dharmacon Lafayette (CO,USA)

ON TARGETplus Non-targeting siRNA
D-001810-01-05; Thermo scientific Dharmacon Lafayette (CO,USA)

ON TARGETplus SMARTpool, rat BMP7
L-093793-02-0005; Thermo scientific Dharmacon Lafayette (CO,USA)

ON-TARGETplus Set of 4 Upgrade rat Bmp7 siRNA
LU-093793-02-0002; Thermo scientific Dharmacon Lafayette (CO,USA)

2.1.10. Enzymes

Bgl2	Roche Diagnostics, Mannheim (Germany)
Collagenase type	Biochrome, Berlin (Germany)
EcoR1	Roche Diagnostics, Mannheim (Germany)
Hind3	Roche Diagnostics, Mannheim (Germany)
Reverse transcriptase SuperScript® II	Invitrogen, Grand Island (NY, USA)
Taq DNA polymerase	Fermentas, St. Leon-Rot (Germany)

2.1.11. Antibodies

Primary antibodies for Western blotting

All primary antibodies used for Western blotting, were diluted in 3 % (w/v) BSA plus 0.1 % sodium azide. Dilutions were stored at 4 °C and re-used several times.

Table 3. Primary antibodies used for Western blotting.

Antibody	Company	ID	Host	Dilution	band size
anti-myc (monoclonal)	Clontech, Saint-Germain-en-Laye France)	#631206	mouse	1:400	-
anti- P-SMAD1/5/8 (polyclonal)	Cell Signalling Technology, Danvers (MA, USA)	# 9511	rabbit	1:1000	~ 60 kDa
anti-α-tubulin (monoclonal)	Sigma-Aldrich, Steinheim(Germany)	#T5168	mouse	1:1000	~50 kDa
Human anti- BMP7 (monoclonal)	R&D Systems (USA, Canada)	#164311	mouse	1:500	~50kDa
Mouse & rat anti-Bmp7 (polyclonal)	Cell Signalling, Technology,Danvers (MA,USA)	#4693	rabbit	1:500	~50kDa
anit-Integrinβ1 (monoclonal)	abcam	#EP1041Y	rabbit	1:500	~140kDa
Anti-P-Akt (S473) (monoclonal)	Cell Signalling, Technology,Danvers (MA,USA)	#4060	rabbit	1:500	~60 kDa
Anti-Akt (polyclonal)	Cell Signalling, Technology,Danvers	#9272	rabbit	1:500	~60 kDa
anti-Neurophilament-H (monoclonal)	Cell Signalling, Technology,Danvers (MA,USA)	#2836	rabbit	1:400	200 kDa

Secondary antibodies for Western blotting

Secondary antibodies were diluted freshly for each use in 5 % (w/v) skimmed milk in TBS-T.

Table 4. Secondary antibodies used for Western blotting.

Antibody	Company	ID	Host	Dilution
anti-rabbit IgG HRB-linked	GE Healthcare, Little Chalfont (UK)	NA934-1ML	donkey	1:4000
anti-mouse IgG HRB-linked	GE Healthcare, Little Chalfont (UK)	NA931-1ML	Sheep	1:2000

Antibodies for immunohistochemistry on paraffin fixed tissue sections

Table 5. Antibodies for immunohistochemistry on paraffin fixed tissue sections.

Antibody type	Antibody	Company	ID	Host	dilutions
First AB	Human anti-BMP7 (monoclonal)	R&D Systems (USA, Canada)	#164311	mouse	1:500
First AB	Bmp7 (polyclonal)	Cell Signalling Technology, Danvers (MA, USA)	#4693	rabbit	1:100
First AB	P-S6 (polyclonal)	Cell signaling Technology, Danvers (MA, USA)	#2211	rabbit	1:500
Second AB	Histomark Biotin Streptavidin HRP- system Goat anti rabbit IgG	Kirkegaard & Perry Laboratories inc. (MA,USA)	#710019	rabbit	undiluted
Second AB	Histomark Biotin Streptavidin HRP- system Goat anti mouse IgG	Kirkegaard & Perry Laboratories inc. (MA,USA)	#710018	mouse	undiluted

Antibodies for immunofluorescence on paraffin fixed tissue sections

Table 6. Antibodies for immunofluorescence on paraffin fixed tissue sections.

Antibody type	Antibody	Company	ID	host	dilutions
First AB	Activated-Caspase 3 (polyclonal)	Cell Signalling Technology, Danvers (MA, USA)	#9661	rabbit	1:100
First AB	Annexin5 (polyclonal)	Abcam	ab14196	rabbit	1:150
First AB	Bmp7 (polyclonal)	Cell Signalling Technology, Danvers (MA, USA)	#4693	rabbit	1:100
First AB	Integrin β1 (monoclonal)	Abcam	#EP10041Y	rabbit	1:500
First AB	Ki67 (clone: B56) (monoclonal)	BD Biosciences, Bedford (MA, USA)	550609	mouse	1:100

Second AB	Alexa fluor 555	Cell Signalling Technology, Danvers (MA, USA)	#4413	rabbit	1:100
Second AB	Alexa fluor 555	Cell Signalling Technology, (MA, USA)	#4409	mouse	1:100
Second AB	Alexa fluor FITC	Cell Signalling Technology, (MA, USA)	#4412	rabbit	1:100
Second AB	Alexa fluor FITC	Cell Signalling Technology, (MA, USA)	#4408	mouse	1:100

Antibodies for immunofluorescence on cells

Table 7. Antibodies for immunofluorescence on cells.

Antibody type	Antibody	Company	ID	host	dilutions
First AB	Annexin5	Abcam	ab14196	rabbit	1:100
First AB	Bmp7 (polyclonal)	Cell Signalling Technology, Danvers (MA, USA)	#4693	rabbit	1:100
First AB	Neurofilament H (NF-H) (monoclonal)	Cell Signalling Technology, Danvers (MA, USA)	#2836	rabbit	1:400
Second AB	Alexa fluor 555	Cell Signalling Technology, Danvers (MA, USA)	#4413	rabbit	1:100
Second AB	Alexa fluor 555	Cell Signalling Technology, Danvers (MA, USA)	#4409	mouse	1:100
Second AB	Alexa fluor FITC	Cell Signalling Technology, Danvers (MA, USA)	#4412	rabbit	1:100
Second AB	Alexa fluor FITC	Cell Signalling Technology, Danvers (MA, USA)	#4408	mouse	1:100

2.1.12. BACTERIA AND CELLS

Bacteria

One Shot® TOP10 *E. coli* competent cells Invitrogen, Grand Island (NY, USA)

Cell lines

Primary mouse embryonic fibroblasts (MEFs); from p27-/-, p27+/- and p27+/+ mouse embryos established in our laboratory.

primary rat embryonic fibroblasts (REFs); from rat embryos established in our laboratory.

HEK293T cells: CRL-11268™ courtesy of Dr Anastasov

PC12; CRL 1721™ purchased from LGC Standards

MPC 4/30 PRR; courtesy of Dr Pacak

MTT; courtesy of Dr Pacak

2.1.13. TISSUES AND BLOOD

Human Pheochromocytoma Samples.
Tissue microarrays (TMA) containing a total of 166 pheochromocytoma and 38 paragangliomas were obtained from the ENS@T (European Network for the Study of Adrenal Tumors).
Human plasma samples of pre-operative pheochromocytoma patients were kindly provided by Prof. Mannelli and control plasma samples were kindly provided by Prof. Eisenhofer

2.1.14. DESINFECTION

Antifect® FD10	Schülke & Mayr, Norderstedt (Germany)
Pursept®-A Classic Fresh	Merz, Frankfurt a.M. (Germany)
Ethanol 70 % (v/v) in water for bacteriology	
Ethanol 80 % (v/v) in water for cell culture	

2.1.15. SOFTWARE

7300 System SDS v1.4	Applied Biosystems, Carlsbad (CA, USA)
AimImageBrowser	Carl Zeiss, Jena (Germany)
AxioVision 4.6	Carl Zeiss, Jena (Germany)
Microplate Manager 5.2.1	Bio-Rad Laboratories, Munich (Germany)
MS Office 2010	Microsoft, Unterschleißheim (Germany)
Primer4	Whitehead Institute, Cambridge (MA, USA)

2.2. Methods

2.2.1. WORK WITH BACTERIA

TOP10 *E. coli* competent cells were used for amplification of plasmids.

Transformation

50 µl of One Shot® TOP10 *E. coli* competent cells were thawed on ice. 1 µg of plasmid DNA was added and gently mixed. After 30 min incubation on ice, bacteria were heat shocked for 30 sec at 42 °C in a water bath and then put in ice. Bacteria were then allowed to recover in 250 µl pre-warmed LB medium for 1 h at 37 °C and 300 rpm. Bacteria were plated on agar plates (100 µl/plate) containing the appropriate selection antibiotic and incubated at 37 °C over night. The next day, clones were picked to be inoculated in 4-20 ml LB medium. After overnight incubation at 37 °C, bacteria were harvested for either plasmid isolation or preparation of glycerol stocks.

Plasmid isolation

Plasmids were isolated from 10 ml bacteria culture using a miniprep kit from Qiagen and following the manual instructions.

2.2.2. CULTIVATION OF ESTABLISHED CELL LINES

All cells were only handled in a sterile hood with controlled airflow and incubated at 37 °C in an atmosphere of 8% CO_2. Cells were handled under sterile conditions. Cell lines were handled separately to minimize risk of cross-contamination. Media and trypsin were pre-warmed to 37 °C before use. When cells had reached a confluence of approximately 90% they were split in a ratio between 1:2 and 1:10 depending on their growth kinetics and intended use. Cells were cultured in special cell culture flasks that are available in different shapes and sizes.

MEFs and REFs were cultured under sterile conditions as monolayers in Dulbecco's Minimal Essential Medium (DMEM), supplemented with 10% fetal bovine serum (FBS), 100 units/ml of penicillin G sodium, 100 µg/ml streptomycin and 2.5 µg/ml

Fungizone. Rat PC12 pheocromocytoma cells. The cell line was cultured in FK12 (DMEM), Medium with 15% (v/v) horse serum, 10% (v/v) FBS and 1% (v/v) penicillin-streptomycin. Mouse pheochromocytoma cells, MPC and its more aggressive derivative MTT cells, were cultured in RPMI medium (Sigma, Hamburg, Germany) containing 5% FBS, 10% (v/v) horse serum and 1% (v/v) penicillin/streptomycin at 37 °C in a 5% CO_2 atmosphere.

Thawing of cells

Vials of cryoconserved cells were taken from the liquid nitrogen storage tank and transported on dry ice. Cell suspensions were rapidly thawed in a 37 °C water bath for 1-2 min and quickly transferred to 5 ml pre-warmed cell-specific medium. Rapid dilution of the freezing medium is essential due to the toxicity of the cryoprotectant DMSO at RT. To remove as much of the DMSO as possible, cells were centrifuged at 300 x g at 4 °C for 5 min, resuspended in fresh medium and transferred to 25 cm^2 tissue culture flasks.

Passage of adherent cell lines

In order to avoid effects of space limitation such as growth inhibition and cell death, the cell density was reduced by either expanding the size of the culture flask or by reducing the cell number before complete confluency was reached. For this purpose, cells were washed with PBS to remove calcium and trypsin inhibitors from the serum-containing medium and treated with 0.05% trypsin/EDTA for approximately 5 min at 37 °C to break cell-cell and cell-matrix contacts. The effect of trypsin was inhibited by adding an at least equivalent volume of medium-containing serum. By carefully pipetting up and down, cell aggregates were dissolved. Cells were split in a ratio between 1:3 and 1:8 every two to four days. Medium was routinely changed every two to three days for all cell lines. So as to forestall changes in phenotype and functional differentiation, cells were passaged for a limited number of times (30 passages at most). Older cells were discarded and a fresh cryoconserved vial was thawed.

Cryoconservation of cells

For cryoconservation, cells with low passage numbers were expanded in 75 cm^2 flasks to approximately 80% confluency within two to three passages after thawing a

cell line. Cells were detached as described above and pelleted in 15 ml tubes at 300 x g and 4 °C for 6 min. The cell pellet was resuspended in 4 ml FBS containing 10 % (v/v) DMSO per 75 cm^2 flask. As DMSO is cytotoxic, all subsequent steps were carried out as quickly as possible. The cell suspension was divided into two cryogenic vials (2 ml/vial) and quickly transferred to a freezing container filled with isopropanol, which was in turn placed at -80 °C. The circumfluent isopropanol layer ensured a continuous temperature reduction of 1 °C per minute. After approximately 72 h, the vials containing frozen cells were transferred to liquid nitrogen tanks (-196 °C) for long time storage.

Mycoplasma test

While fungal or other bacterial infections are usually easily detectable, mycoplasma contaminations often elude detection. Therefore, every new cell line was routinely tested for mycoplasma contamination by the mycoplasma test kit (PromoKine). For the preparation of the test sample, 0.5–1.0 ml cell culture supernatant was transferred into a 2 ml centrifuge tube. The supernatant was briefly centrifuged at 250 x g to pellet cellular debris. The supernatant was then transferred into a fresh sterile tube and centrifuged at 15000-20000 x g for 10 min to sediment mycoplasma. The supernatant was carefully discarded and the pellet resuspended in 50 µl of the buffer solution. The mixture was heated to 95 °C for 3 min. For PCR amplification, following reagents (Table 7) were prepared in a PCR tube:

Table 8. PCR amplification for mycoplasma test

Reagents	**Volume**
H2O	35 µl
Reaction Mix	10 µl
Test sample	5 µl

The tubes were placed in a PCR thermal cycler and the program set to following conditions (Table 8); steps 2-4 were repeated for 35 cycles. Only mycoplasma free cells were used for experimental setups.

Table 9. PCR Setup

Step	Temperature [°C]	Time
1	94	30 sec
2	94	30 sec
3	60	120 sec
4	72	60 sec
5	94	30 sec
6	60	120 sec
7	72	5 min

2.2.3. ISOLATION AND CULTIVATION OF RAT PRIMARY CELLS

After dissection, adrenal glands from rats with homozygous p27 mutations were transferred to a glas slide with a drop of sterile HBSS. The fat tissue and blood vessels were removed from the organ before transferring it into a Petri dish containing 10 ml HBSS for washing. After the washing step the adrenal gland was transferred to a fresh Petri dish containing a drop of sterile collagenase, further injected with collagenase using a needle and incubated at RT for 3 min. After the incubation, the organ was chopped with razor blade into pieces smaller than 0.5 mm. These pieces were collected and transferred to a 15 ml conical tube, then incubated at 37 °C for 15 min. Every 5 min the suspension was mixed by pipetting to ensure proper digestion of connective tissues. To inactivate the collagenase 1 ml of FBS and 10 ml medium were added. The cell suspension was then passed through a 70 µm cell strainer and centrifuged at 1000 rpm for 5 min. After removing the supernatant, the cell pellet was resuspended in 1 ml erythrocyte lyses buffer, incubated at RT for 3 min and centrifuged (same condition as before). Cells were finally resuspended in 1 ml medium and counted using a Neubauer counting chamber.

For cultivation of rat primary cells, the following medium was used: RPMI 1640 (high-glucose) with 10% (v/v) FBS, 1% (v/v) penicillin-streptomycin and 1% (v/v) Fungizone. All media, serum and antibiotics/antimycotics were purchased from Gibco/Invitrogen, Grand Island (NY, USA).

2.2.4. MANUAL CELL COUNTING

10 µl of cell suspension were mixed 1:1 with trypan blue to selectively color and distinguish dead cells. Four large corner squares of a Neubauer counting chamber were counted to achieve a statistically significant count.

2.2.5. CELL HARVEST

To harvest cells for protein or RNA extraction, cells were detached as described above and pelleted at 8000 x g and 4 °C for 5 min. Pellets for RNA extraction were dissolved in 500 µl TRIzol and stored at -20 °C until further use, while pellets for protein extraction were directly stored at -20 °C.

2.2.6. TRANSIENT TRANSFECTION EXPERIMENTS

Cells were transiently transfected either with the BMP7 or a mock (PeGFP or PvMyc) plasmid. Therefore, cells were plated in 6-well plates at a density depending on the cell type, in 2 ml complete medium per well. After 24 h, the medium was removed from the wells and 2 ml serum-free OPTIMEM was added. For each well, 1 µg of DNA was mixed with 3 µl of FUgene transfection reagent per µg of DNA and 100 µl OPTIMEM. This mix was incubated for 15 min at RT to allow the interaction between carrier molecules of the transfection reagent and DNA molecules. After incubation, 100 µl of the transfection mix was added to each well and carefully swirled to ensure an even distribution. Cells transfected with mock (empty) vectors served as controls. 5 to 8 h after transfection, the OPTIMEM was changed back to complete medium.

2.2.7. TRANSFECTION OF MPC AND MTT CELLS WITH SIRNA MOLECULES

Nucleofection of MPC/MTT was performed by the use of the Amaxa 4D-Nucleofector (Lonza, Cologne, Germany). Cells were plated on tissue culture dishes before they were trypsinized and counted, and the desired amounts of cells (2×10^6 cells per reaction) were centrifuged at 1000 rpm for 10 min. The supernatant was aspirated, and the cells were resuspended in SF solution and supplement mixtures according to the manufacturing instructions, in the presence or absence of 300 nM siRNA, and

transferred into the nucleofection cuvette. Nucleofection was conducted in the X-unit of the device, and electroporation was processed with the DS134 program settings in order to maximize transfection efficiency without significantly altering viability of the cells. Cells were then incubated at 37 °C for 10 min, resuspended in 400 µl of pre-warmed RPMI cell culturing medium and plated into tissue culture dishes. 24 h after transfection, efficiency and cell viability were assessed by immunoblotting or fluorescence microscopy as previously described.

2.2.8. WORK WITH LENTIVIRUS

Lentivirus:

Retroviridae family are viruses which are characterized by a long incubation period. Lentiviruses deliver genetic information into the host cell DNA and are able, unique among retroviruses, to replicate in non-dividing cells, so they display one of the most efficient methods to deliver gene vectors. We used a modified HIV virus.

In general, infectious viruses retain 3 main genes coding for the viral proteins in the order: 5´-gag-pol-env-3´. There can be additional genes depending on the virus (e.g., for HIV-1: vif, vpr, vpu, tat, rev, nef) whose products regulate the synthesis and processing of viral RNA .

RNA interference:

shRNA constructs were designed and cloned into the pGP vector (Anastasov et al. 2009) (Anastasov, Hofig et al. 2012). Specific shRNAs were designed by using bioinformatics tools publicly available from Invitrogen. The sequences (sh-BMP7) of the complementary oligonucleotides are:

sh*Bmp7* 1.8

Fw: 5'- GATCC **AGGCCTGATTGGACGGCAT** TTCAAGAGA **ATGCCGTCCAATCAGGCCT** TTTTTG-3'

Rev: 5'- AATTCAAAAA **AGGCCUGAUUGGACGGCAU** TCTCTTGAA **ATGCCGTCCAATCAGGCCT**G 3'.

sh*Bmp7* 2.9

Fw: 5'-GATCC**CGGGAGAUGCAGCGGGAAA**TTCAAGAGA**TTTCCCGCTGCATCTCCCG**TTTTTG-3'

Rev: 5'-AATTCAAAAA**CGGGAGAUGCAGCGGGAAA**TCTCTTGAA**TTTCCCGCTGCATCTCCCG**G-3'.

Double-stranded DNA encoding siRNA oligonucleotides for BMP7 were synthesized. The specific sequence contained a sense strand of 19 nucleotides (bold)

followed by a short spacer (TTCAAGAGA) and the reverse complement of the sense strand. As a stop signal 5 thymidines and 1 guanidine were added at the end of synthesized oligonucleotides as RNA polymerase III transcriptional stop signal. Each pair of oligos was annealed at 20 µM in annealing buffer (100 mM potassium acetate), for 4 min at 95 °C, followed by incubation at 70 °C for 10 min and slow cooling to 4 °c. 40 pM of annealed oligos were phosphorylated by T4 polynucleotide kinase before they were ligated into pGP vector digested by EcoR1 and Hind3. All constructs were checked by Bgl2 digestion. Positive clones should have inserts around 300 bp. An empty vector has an around 240 bp insert.

Virus production:

In a 10 cm Petri dish replication-defective lentiviral particles were generated by transient co-transfection of HEK293T cells with 16 µg, 8 µg and 4 µg of packaging plasmids pMDLg/pRRE, pRSV (Anastasov, Hofig et al. 2012). Rev and pMD2.G (a kind gift from D. Trono, École polytechnique fédérale de Lausanne) and 8 µg of lentiviral transduction vector pGreenPuro (pGP; System Biosciences, California) were transfected using Lipofectamine 2000 (Life Technologies, California) according to the manual instructions.

12 h after transfection the medium was changed and 48 h after transfection the supernatant containing the virus was harvested, cleared of debris by low-speed centrifugation, and filtered through 0.45 µm Stericup filters.

The lentivirus was concentrated by ultrafiltration using Amicon-20 100-kDa-molecular-weight cut-off columns according to guidline instructions and aliquots (100 µl) were stored at −80 °C. Virus titers (multiplicity of infection: MOI) were determined by fluorescence-activated cell sorting (FACS) analysis of a known number of HEK293T cells which were infected with serially diluted viral supernatant and GFP expression analysis was performed.

Infection of mouse pheochromocytoma cell line and primary rat pheo cells:

For infections, MPC, MTT (10^5 cells /ml) and primary tumor cells (25^5 cells /ml) were plated on 96-well or 6-well plates and 24 h later cells were infected by lentiviral vectors expressing the green fluorescence protein (GFP) or GFP and shRNA against BMP7. Therefore, the medium was changed to a conditional medium containing lentivirus-supernatant in the presence of polybrene (8 µg/ml). After the medium

exchange, the plates were centrifuged at 1000 g for 90 min to obtain a better infection rate. Conditional medium was changed back to normal medium 24 h after infection. The GFP fluorescent signal could be observed after further 24 h of incubation.

2.2.9. RNAI KNOCKDOWN EXPERIMENTS

Cells were transfected with siRNAs targeting certain genes. Cells were seeded in 6-well plates at a density of 5 x 10^5 cells in 2 ml complete medium per well. 24 h after plating, the medium was removed and low-serum medium was added. For transfection in 6-well plates, 100 pmol siRNA were mixed with 15 µl Lipofectamin transfection reagent (Qiagen). siRNA was handled under RNase-free conditions. Untransfected cells, cells treated with transfection reagent and cells transfected with scrambled siRNA served as controls. Five to 8 h after transfection, the medium was changed to normal medium. Cells were harvested after 48 h of transfection.

2.2.10. MTT ASSAY

Proliferation studies were performed using the MTT (3-(4, 5-Dimethylthiazol-2-yl)-2.5-diphenyltetrazoliumbromide) assay. MTT is reduced to colored compounds by all living, metabolically active cells and is used therefore, as a measure of cell viability. 10,000 cells were plated in 96-well plates in cell-specific medium. Cells were treated or transfected as usual. After the treatment or transfection the MTT solution (5 mg/ml MTT in PBS, 0.2 µM filter-sterilized) was added in a ratio of 1:10. After an incubation of 4 h, 200 µl of MTT lysis solution (0.04 M HCl in absolute isopropanol) was added to solubilize the purple formazan product. The absorbance was finally measured at 560 nm.

2.2.11. CELL VIABILITY AND PROLIFERATION

The effect of up or downregulation or treatment of drugs was tested on primary pheochromocytoma cell cultures or cell lines plated in 96-well plates. Cell viability was assessed 24 h, 48 h or 72 h after transfection or incubation with the test substances using WST-1 colorimetric assay (Roche, Mannheim, Germany) according to the manufacturer's recommendations.

2.2.12. CELLS APOPTOSIS ASSAY

The members of the caspase family play key effector roles in apoptosis of mammalian cells. Therefore, apoptosis rates of cells after treatment with DMH1 were assessed by measuring the activity of cysteine aspartic acid-specific proteases (caspase)-3/7 using the Caspase-Glo ® 3/7 Assay kit (Promega). This assay provides a luminogenic caspase-3/7 substrate, which contains the tetrapeptide sequence DEVD, in a reagent optimized for caspase activity, luciferase activity and cell lysis. Cells were plated in 96-well plates and treated with DMH1 (3 µM, 5 µM) or vehicle 24 h later. 24 h after treatment, reagent was added directly to the wells. This resulted in cell lysis, followed by the cleavage of the substrate by caspase-3/7 and generation of a luminescent signal. Luminescence was measured using a luminometer (Tecan).

2.2.13. TISSUE PREPARATION

Adrenals of age-matched wild-type and MENX-affected rats were fixed in 4% buffered formalin and paraffin-embedded. Four µm sections were cut and stained with haematoxylin and eosin (HE) for pathological examination, or used for immunohistochemistry or immunofluorescence. Rat serum samples were collected right after the rats were sacrificed.

2.2.14. IMMUNOHISTOCHEMICAL STAINING (IHC) ON PARAFFIN FIXED TISSUE SECTIONS

Immunohistochemical staining (IHC) is a method that was used to detect specific proteins in tissues or cells. The primary antibody binds to the specific antigen of the target protein, thus forming an antibody-antigen complex. This complex is then bound by a secondary, enzyme-conjugated antibody. In the presence of substrate and chromogen, the enzyme forms a coloured deposit at the sites of antibody-antigen binding. Paraffin sections were deparaffinized in two changes of xylol for 10 min each. After incubation in two changes of 100% ethanol for five minutes, the sections were incubated in 90% and 70% ethanol for 5 min each. Afterwards the slides were washed in distilled water and Tris- buffered saline, 0.05 % Tween (TBS-T, pH 7.0) for 5 min each. After rehydration the samples were incubated in hydrogen peroxide

(H_2O_2) solution (0.3% H_2O_2 in methanol) for 5 min to block endogenous peroxidase activity. This step minimized non-specific background staining. After washing the slides twice for five minutes in TBS buffer, the antigen retrieval was performed to enable antibody binding and staining intensity. For this the sections were microwaved for 30 min at 750 W in citrate acid monohydrate buffer (pH = 6.0) to break protein cross-links. After the slides were microwaved they were washed in TBS for 5 min to cool them down. To avoid unspecific binding the slides were blocked with normal goat serum for 30 min. Following the slides were incubated with primary antibodies against the specific proteins overnight at 4 °. In the avidin-biotin system we used, the secondary antibody is conjugated to biotin beads, which can bind to the avidin-enzyme complex. On the following day the samples were washed three times in TBS for 5 min and incubated with biotinylated secondary antibodies for 45 min, followed by a washing procedure (3 x 5 min) in TBS. After that the slides were incubated in streptavidin-horseradish peroxidase (of the Histo mark Biotin Streptavidin HRR-system) for 30 min. Then the slides were washed three times for 5 min in TBS. After washing the entire tissue section was covered with 1-5 drops of DAB staining solution and incubated for ca. 2 min to enable visualisation. After sufficient staining was affirmed under the microscope the slides were counterstained in haematoxylin for 2 min and then washed under running water for 4 min. Then the slides were dehydrated in increasing concentrations of ethanol (70%, 96% and 100%) with 60 times up and down moving in each concentration. Subsequently the sections were incubated in xylol twice for 10 min and mounted with cover slips.

Immunohistochemistry on TMA and human tissues was performed on an automated immunostainer (Ventana Medical Systems) according to the manufacturer's protocols with some modification. Conventional 4 µm sections of standard full mount human pheochromocytoma tissue blocks, or of the TMAs were used for immunohistochemistry. Paraffin sections were deparaffinized by hand as described before. Afterwards the slides were washed in distilled water and Tris- buffered saline, 0.05% Tween (TBS-T, pH 7.0) for 5 min each. The sections were microwaved for 23 min at 750 W in W-cap citrate acid monohydrate buffer (pH = 6.0) to break protein cross-links. After the slides were microwaved they were washed in TBS for 5 min. The samples were incubated in hydrogen peroxide (H_2O_2) solution (0.3% H_2O_2 in methanol) for 5 min to block endogenous peroxidase activity and washed in TBS-T buffer for 5 min. After this procedure, slides were inserted into the automated

immunostainer and the standard protocol including a 12 min avidin and 12 min biotin blocking step was used. The primary antibody was incubated for 12 h and the secondary antibody for 32 min.. Images were recorded using an Olympus BX microscope.

2.2.15. IMMUNOFLUORESCENCE ON PARAFFIN FIXED TISSUE SECTIONS

For the immunofluorescence staining, we used sections originated from paraffin embedded tissue samples. Before the tissues were stained, the sections had to be deparaffinized and then rehydrated and cooked as described for IHC. After boiling, the tissue sections were transferred rapidly into TBS-T. Then the primary antibody, diluted in Dako REAL solution, was added on the tissue sections. In case of the co-immunofluorescent staining, a mixture of both primary antibodies was applied. After the pre-treatment the slides were incubated with the first antibody dilutions in humid surroundings at 4 °C overnight. On the following day the samples were washed three times in TBS for 5 min. The secondary antibody was diluted in Dako REAL solution and incubated for 60 minutes, followed by a washing procedure (3 x 5 min) in TBS. For co-staining a mixture of both secondary antibodies was used. The nuclei were stained with DAPI in the dark for 3 min followed by 1 min washing in distilled water. Finally the tissue sections were covered with 1-3 drops of vectashield mounting medium and a cover glass. Tissue slides were stored at -20 °C in the dark.

2.2.16. IMMUNOFLUORESCENCE ON CELLS

The cells were plated and cultured on cover slips in 24-well plates in the appropriate medium. After washing the wells three times in PBS, they were fixed in 2% paraformaldehyde in PBS for 30 min and washed a further three times in PBS. To permeabilize the cell membrane a 3 min incubation step with 0.1 % Triton X-100 was performed. After washing the cells five times with PBS, the fixed cells were blocked in 5% normal goat serum for 30 min at RT to avoid unspecific antibody binding. The primary antibody (Table 4), diluted in 5 % normal goat serum, was then added for an overnight incubation step at 4 °C. After 3 times washing with warm PBS, the appropriate secondary antibody (Table 4), diluted 1:100 in 5% normal goat serum, was added to the coverslips and incubated for 1 h at RT. This incubation step was

performed in the dark to avoid a fading of the signal. After 3 further washing steps in warm PBS, the nuclei were stained with DAPI in the dark for 3 min. After a last washing step, the cover slips were mounted onto microscope slides with vectashield. For storage, the slides were frozen at -20 °C in the dark.

2.2.17. MIGRATION & INVASION ASSAY

A chemomigration assay was performed using 24-well plates with uncoated polycarbonate membrane inserts (8 µm pore size; BD BioCoat™ BD). To start, cells were plated and then transfected with BMP7 or mock vector. After 24 h incubation, cells were detached by trypsinization and collected in 1 ml medium containing 0.02% FBS and 0.1% horse serum to be counted. 50000 cells (PC12) or 100000 cells (MPC/MTT) were diluted in 750 µl of the same medium and the cell suspension was added onto the insert. The lower well was filled with 750 µl of the chemoattractant (medium supplemented with 2.5% FBS and 15% horse serum). Cells were incubated for 24 h at 37 °C, 5% CO_2. Cells and medium from the upper part of the insert were then removed using a water humidified cotton-tipped swab and the insert (with the cells that migrated through and adhered to the lower part of the membrane) was fixed in 100 % methanol for 10 min. After washing in Ampuwa water, cells were stained with 1.5% (w/v) toluidine blue in water. The membrane was washed in water, dried 1 h at 37 °C and then removed from the well with a needle and a forceps to be mounted onto a microscope slide. For migration following viral knockdown of BMP7 MPC and MTT cells were harvested after 72 h following infection. 50000 cells (PC12) or 100000 cells (MPC/MTT) were diluted in 750 µl of the same medium and the cell suspension was added onto the insert. Following procedure was performed as described before for transfected cells!

Invasion assay was performed with matrigel coated polycarbonate membrane inserts (8 µm pore size; BD BioCoat™ BD) according to the manufacturer's recommendations. 75000 cells (PC12) or 150000 cells (MPC/MTT) were used for this assay.

2.2.18. NUCLEIC ACIDS ANALYTICS

RNA isolation

RNA extraction of cells or tissues was performed by Maxwell 16 system. For RNA extraction Homogenization Solution and Lysis Buffer (components of the Maxwell® 16 simply RNA Tissue Kit) are added to the samples and processed as indicated in the manual instructions. After the lysis of the cell or tissue samples followed by transfer of the sample lysate to Maxwell 16 LEV Cartridge (component of the Maxwell® 16 simply RNA Tissue Kit), the remaining purification process was fully automated by the extractor in simply RNA Mode. The sample input of 200 µl and output of 40-60 µl were chosen based on the manufacturer's recommendation.

Nucleic acid quantification

Concentration and quality of RNA and DNA samples were spectrophotometrically analysed using a NanoDrop device. Conventionally, 1 OD at a wavelength of 260 nm corresponds to 50 µg/ml for double-stranded DNA and to 40 µg/ml for RNA. To assess the purity of a nucleic acid sample, the ratio of the absorbance at 260 nm and 280 nm is measured. Ideally, this ratio amounts to 1.8 for pure DNA and 2.0 for pure RNA.

Reverse transcription

In order to do PCR-based analysis on RNA extracts, reverse transcription was performed to generate cDNA from RNA templates. To this end, 0.1-1 µg of total RNA was incubated for 10 min at RT with 1 µg random primers in 11 µl reaction volume. After incubation, the following components were added per reaction batch:

Table 10. RT components

Reagents	Volume
5x first strand buffer	4 µl
DTT (0.1 M)	2 µl
dNTP Mix (10 mM each)	1 µl
RNaseOUT	1 µl
SuperScript™ II reverse transcriptase	1 µl

Mixtures were incubated for 1 h at 42 °C. The reaction was stopped by heating to 95 °C for 5 min. cDNA was stored at -20 °C until further use.

Polymerase chain reaction (PCR)

For polymerase chain reaction, the following mixtures were prepared in 0.2 ml tubes:

Table 11. PCR components

Reagents	Volume
PCR master-mix (see 2.1.4)	16.5 µl
forward primer (10 pmol/µl)	1 µl
reverse primer (10 pmol/µl)	1 µl
Taq polymerase	0.5 µl
cDNA template	1 µl

PCRs were run with the following program for 30-40 cycles (steps 2 to 4):

Table 12. PCR Setup

Step	Temperature [°C]	Time
1	94	5 min
2	94	45 sec
3	~ Tm	45 sec
4	72	1 min
5	72	7 min
6	4	Pause

The annealing temperature (step 3) was varied depending on the melting temperatures (T_m) of the primers. The temperature used was 2-3 °C beneath T_m.

Agarose gel electrophoresis

The reaction products of PCR runs were separated and examined on agarose gels. For this purpose, 1 µl of sample was mixed with 5 µl of 6x loading dye and loaded onto a 1% agarose gel containing 0.005% ethidium bromide. Samples were separated in 1x TBE alongside a DNA standard at 100 V. DNA bands were made visible under UV light.

Quantitative real time PCR (qPCR)

After reverse transcribing isolated RNA into cDNA (see above), specific genes were amplified by TaqMan PCR using gene expression assays from Applied Biosystems (Table 12). The following mix was prepared for each sample:

Table 13. qPCR components

Reagents	Volume
2x TaqMan master mix	10 µl
Assay-on-Demand	1 µl
Ampuwa	5 µl

16 µl of mixture were aliquoted into 96-well PCR plates. 4 µl of Ampuwa-diluted reverse transcription product was added. All samples were pipetted in duplicates. In parallel, negative control samples (16 µl mix plus 4 µl Ampuwa) and calibrator reverse transcription product were loaded. cDNA from αT-3 cells or rat brain (calibrator) was used to create standard curves for the genes of interest. Next to the genes of interest, an endogenous control, *B2m* (encoding β_2 microglobulin), was run for normalization of cDNA input. The 7300 Real Time PCR System was run for 40 cycles (steps 3 to 4) with the following program:

Table 14. qPCR set up

Step	Temperature [°C]	Time
1	50	2 min
2	95	10 min
3	94	15 sec
4	60	1 min
5	4	Pause

Table 15. List of TaqMan assays

Gene symbol	Assay ID
Bmp7 **(mouse)**	Mm00432102_m1
Bmp7 **(rat)**	Rn01528889_m1
Bmp7 **(human)**	Hs00233476_m1
B2m **(mouse)**	Mm00437762_m1
B2m **(rat)**	Rn00560865_m1
Cdkn1b **(rat)**	Rn00582195_m1
Cited1**(rat)**	Rn00821880_g1
Mcc **(rat)**	Rn01527265_m1
Smad6 **(rat)**	Rn01766978_m1
Smad6 **(mouse)**	Mm00484738_m1
Plaur **(rat)**	Rn00569290_m1
Plaur **(mouse)**	Mm00440911_m1
E2F5 **(rat)**	Rn01755728_g1
Stat5a **(rat)**	Rn00567011_m1

The system quantifies PCR reaction products during each cycle by calculating the cycle threshold (Ct) value for each sample. Relative quantification was performed using the pre-recorded standard curve and analysis data of the 7300 detection system. Linear regression analysis was used to calculate the relative amount of mRNA in samples. Values were normalized against *B2m*.

2.2.19. PROTEIN ANALYTICS

Protein isolation

After thawing frozen cell pellets on ice, they were resuspended in RIPA buffer with freshly added protease and phosphatase inhibitors. The volume of buffer varied from 25 µl to 80 µl, depending on the size of the cell pellet. Enough buffer was added to solubilize the whole pellet. After 15 min incubation on ice, the cell lysate was spun down at 13000 x g and 4 °C for 5 min to remove cell debris. The protein-containing supernatant was transferred to a fresh tube and protein extracts stored at -20 °C.

Protein quantification

Protein content was measured using the bicinchoninic acid (BCA) assay. A standard curve was created from BSA solutions with known concentrations. 5 µl of the protein sample was added to 95 µl H_2O bidest. 1 ml BCA solution (1:50 mixture of reagent A and B from Pierce kit) was added. The tube was closed and vortexed. To increase the sensitivity and accuracy of the assay, the 15 min incubation was carried out at 60 °C. The OD of the solution at 560 nm was spectrophotometrically determined. The amount of protein in the given sample was estimated by comparing the value for OD_{560} to the standard curve.

SDS-PAGE

Proteins were separated by discontinuous SDS gel electrophoresis. 35 µg (15-pocket comb) or 50 µg (10-pocket comb) of protein sample were mixed 1:1 with 2x Laemmli buffer plus 5% (v/v) β-mercaptoethanol and boiled for 5 min at 95 °C. Samples were electrophoretically separated in SDS running buffer on discontinuous gels, 4% stacking and 12% separating gels. Gels were run at 90 V until the tracking stain had passed the interface between stacking and separating gel, upon which voltage was increased to 130 V. A prestained protein ladder was run alongside the samples in each gel.

Western blot transfer

To target specific proteins from cell lysates, Western blot analysis was applied following SDS-PAGE. In order to make the proteins in the gel accessible to detection by antibodies, they were blotted from the gel onto a thin nitrocellulose membrane with non-specific protein-binding properties. All transfers performed during this work were carried out according to the so-called wet blot technique in a Bio-Rad system. Before

blotting, two filter pads, four sheets of Munktell filter paper and the membrane were equilibrated in Western blot transfer buffer for 5 to 10 min. The blotting sandwich was assembled as depicted in Figure 10:

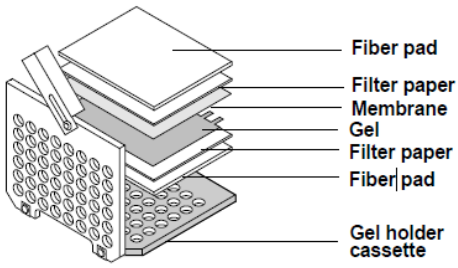

Figure 10. Western blot sandwich. Sandwich configuration for Western blot transfer in a Bio-Rad wet blot system. Adapted from Bio-Rad (Munich, Germany).

The blotting chamber was filled with transfer buffer and a constant electric field of either 50 V for overnight transfer or 100 V for 2 h transfer applied. Transfer occurred under stirring with a standard stir bar at 4 °C on ice. To determine the quality of the transfer, the membrane was reversibly stained with Ponceau S directly after transfer. The staining was removed by washing the membrane three times for 5 min in TBS-T.

Protein detection

To prevent non-specific binding between the membrane and the antibodies used for detection, non-specific binding was blocked with 5% (w/v) skimmed milk in TBS-T. The membrane was incubated in 5% milk in TBS-T for 1 h under gentle agitation at RT or overnight at 4 °C. After three 5 min washes in TBS-T, a dilution of the primary antibody specific for the protein of interest was added and incubated either 1 to 2 h at RT or overnight at 4 °C under gentle agitation. Unbound primary antibody was removed with three 5 min wash steps with TBS-T. Subsequently, a species-specific, horseradish peroxidase-coupled secondary antibody, diluted in 5% (w/v) skimmed milk in TBS-T, was added to the membrane. Incubation with the secondary antibody was carried out for 60 min at RT. Following three more washes with TBS-T, a chemiluminescent agent (1:1 Pico West solutions) was added and incubated for 5 min at RT in the dark. The membrane was exposed on a sheet of photo film.

Secondary probing

For reprobing of Western blot membranes with different primary antibodies, membranes were incubated with stripping buffer for 10 min at 37 °C. After three

washes for 5 min each at RT in 1x TBS-T, the whole detection-process described above starting from blocking with milk was repeated for different proteins of interest.

To allow correction for the total amount of protein on the membrane, the housekeeping gene α-tubulin was always probed as the loading control.

Enzyme linked immunosorbent assay (ELISA)

To measure the secreted Bmp7 in the serum of MENX affected and wild type rats or in the plasma of human patiens and healthy controls, the Bmp7 Enzyme-linked immunosorbent assay kit was used. To obtain the rat serum a red (EDTA) serum or separator tube was filled with rat blood. After mixing, the tube was centrifuged at RT for 4 min at 4000 rpm or 10 min at 3000 rpm. Serum was aliquoted and stored at -20 ^{o}C until use. Plasma which we received from the clinicians (as described before) was aliquoted and stored at -80 ^{o}C until use.

For the rat serum samples the microtiter plate from USCN Life Science Inc. provided in the kit had been pre-coated with a monoclonal antibody specific to Bmp7. Standards or samples were added to the microtiter plate wells and incubated as described in the manual instructions. After washing steps a biotin-conjugated polyclonal antibody was added to Bmp7. Next, avidin conjugated to Horseradish Peroxidase (HRP) was added. Then a TMB substrate solution was added to each well. Wells containing Bmp7, biotin-conjugated antibody and enzyme-conjugated avidin exhibited a change in color. The enzyme-substrate reaction was then terminated by the addition of stop solution and a color change could be measured spectrophotometrically at a wavelength of 450 nm. The concentration of Bmp7 in the samples could be calculated by comparing the OD of the serum samples to the standard curve.The protocol was performed as described in the manual instructions. For the human BMP7 Elisa the sigma BMP7 Elisa kit was used. Standards or samples (undiluted) were added to the microtiter plate wells and Elisa was performed as indicated in the manufacturing instructions.

2.2.20. IN VIVO EXPERIMENTS

Compound preparation

NVP-BEZ235 was kindly provided from Novartis Pharma. For *in vitro* studies, stock solutions of NVP-BEZ235 was prepared in 100% DMSO and stored at −20 °C. Dilutions to the final concentration were made in the culture medium immediately before use. For *in vivo* experiments, BEZ235 (20 mg/kg) was suspended in 1 volume of 1-methyl-2-pyrrolidone (Sigma–Aldrich) and 9 volumes of PEG300 (Sigma–Aldrich).

Animals and *in vivo* treatment

MENX-affected rats were maintained as previously reported (Frizer A, 2002). Animals were maintained and treated with BEZ235 or placebo in agreement with the procedures approved by the Helmholtz Zentrum München, by the Technische Universität München, and by the local government authorities (Bayerische Landesregierung).

For later molecular analysis, MENX-affected rats with 7-8 months were treated daily by oral administration of BEZ235 (20 mg/kg) or placebo (1 volume of 1-methyl-2-pyrrolidone and 9 volumes of PEG300) (Figure11).

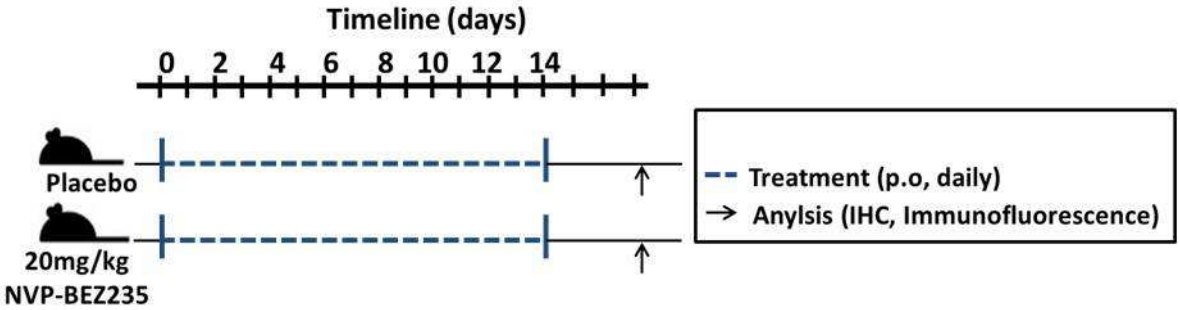

Figure 11. Scheme of experimental procedure. Rats were treated daily by oral administration of BEZ235 (20 mg/kg) or placebo (1 volume of 1-methyl-2-pyrrolidone and 9 volumes of PEG300) and after 2 weeks the rats were sacrificed.

3. *RESULTS*

3.1. *EXPRESSION OF BONE MORPHOGENETIC PROTEIN 7 (BMP7) IN RAT PHEOCHROMOCYTOMAS*

In earlier studies it was shown by transcriptome analysis and quantitative (q)RT-PCR that the *Bmp7* gene was overexpressed in pheochromocytomas developing in MENX rats when compared with normal adrenomedullary tissue (Molatore et al. 2010). Interestingly, the expression of *Bmp7* increased from adrenomedullary hyperplasia (+2.6 fold versus normal adrenal medulla) to tumors (+4.7 fold) (Molatore et al. 2010). Although both expression array and qRT-PCR analysis of rat pheochromocytomas quantify the amount of mRNA transcript, a correlation to the protein levels does not automatically follow. Therefore, we investigated whether the observed overexpression of the *Bmp7* mRNA transcript translates into higher amounts of the Bmp7 protein in rat tumor cells. Using immunohistochemistry we confirmed that a relationship exists between *Bmp7* gene transcript and protein levels. Thus, Bmp7 levels were much higher in pheochromocytoma cells of the MENX-affected rats when compared with the adrenal gland of wild-type animals. (Figure 12)

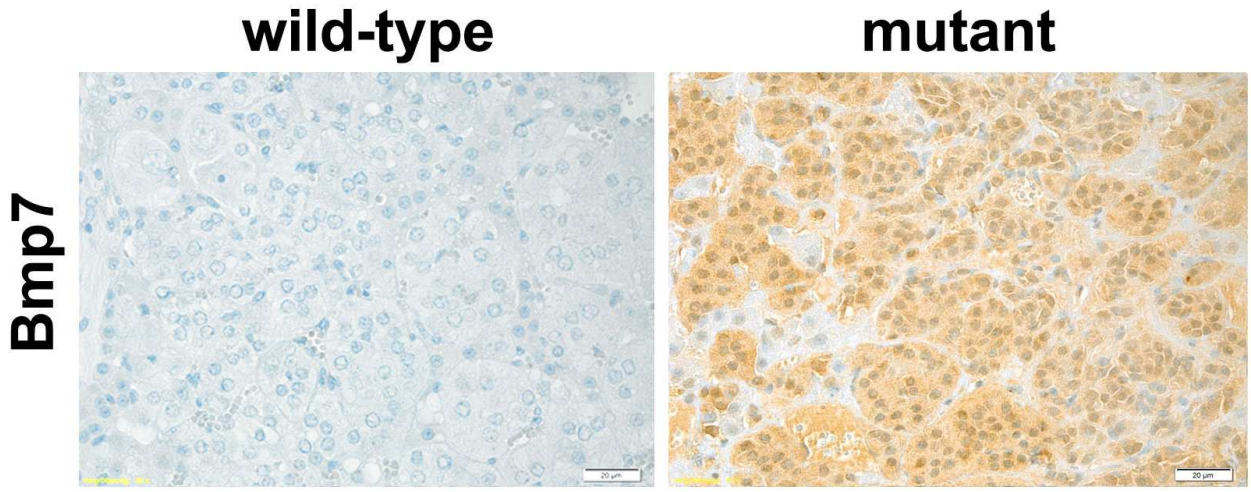

Figure 12. Immunohistochemistry of wild-type and mutant adrenal medullary tissue. Immunohistochemistry was performed on paraffin embedded formalin fixed tissue using rat anti-BMP7 antibody (1:100). The adrenal medulla of wild-type rats shows almost no positivity for Bmp7 whereas the hyperplasia of a mutant rat shows a strong cytoplasmic staining for Bmp7. While non-tumor tissue remains only very weakly positive (see arrows). Original magnification: 400x

Bone morphogenetic protein 7 is a secreted protein that acts by binding and activating BMP receptors on the surface of target cells. We wanted to investigate whether Bmp7 is secreted into the blood of affected rats, as this may be a biomarker whose detection could be used for the noninvasive diagnosis of cancer. Thus, we used a (rat) Bmp7-specific Enzyme-Linked Immunosorbent Assay (ELISA) to evaluate the serum levels of the protein in mutant and wild-type rats. Since tumor progression is directly proportional to the age of the MENX-rats we chose wild-type and mutant littermates at 8-9 months of age. The MENX-rats have already developed large pheochromocytomas at this age. The analysis of samples from seven mutant and seven wild type-rats showed a significantly elevated mean level of Bmp7 (2.3 fold) only in the MENX mutant rats. (Figure 13)

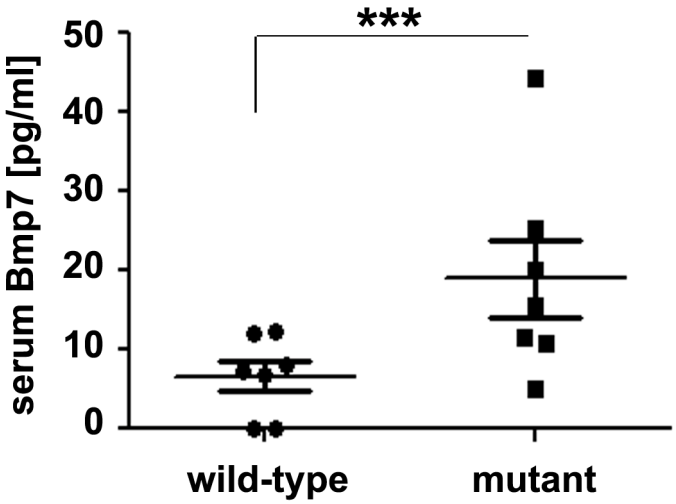

Figure 13. Bmp7 serum levels. Serum of 7 MENX mutant and 7 wild-type rats that were fasted for 12 h was collected, and Bmp7 levels were measured using a Bmp7 ELISA-KIT. Serum of mutant animals showed significantly higher Bmp7 levels compared with wild-type ones. Individual values are plotted, with mean ± SD shown for each group. ***P < 0.001

3.2. Expression of Bmp7 in human pheochromocytomas

Our previous study showed that the *BMP7* gene is upregulated in sporadic and familial human pheochromocytomas (Molatore, Liyanarachchi et al. 2010). To verify whether the transcript overexpression here also translates into a higher amount of the BMP7 protein, we extracted proteins from 10 sporadic pheochromocytomas and from one control adrenal medulla and performed western blotting using an anti-BMP7

antibody. The results show that the tumors, but not the control tissue, express a high level of the protein (Figure 14).

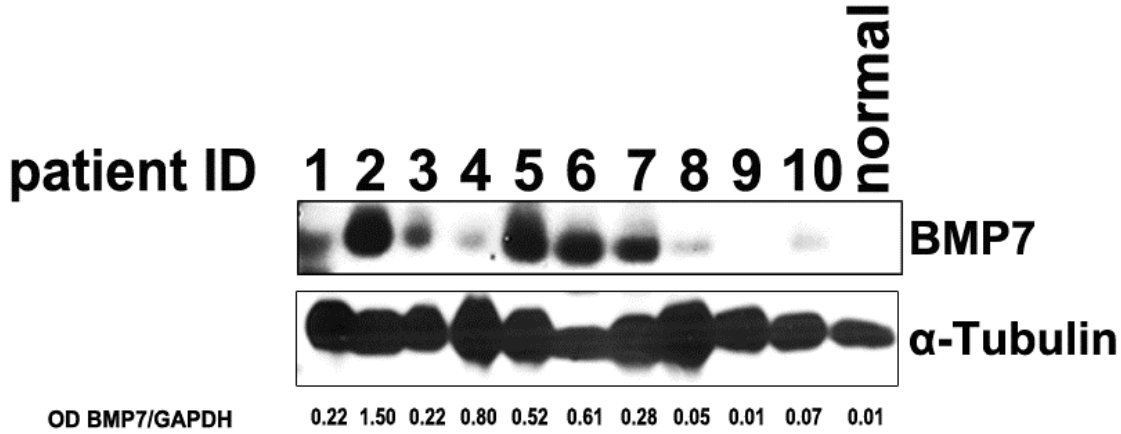

Figure 14. Western Blot analysis of BMP7 in human tumors. The figure shows the expression of BMP7 (1:500) and the loading control α-Tubulin (1:1000) in 10 human tumors (#1-10) and one human normal medulla (normal). Numbers at the bottom of the western blot represent the ratio of the quantification of band intensities (optical density = OD) of BMP7 normalized to the α-Tubulin loading control (OD BMP7/ α-Tubulin).

To confirm cellular localization we obtained formalin-fixed, paraffin-embedded (FFPE) tissue blocks from the same tumors analyzed by western blotting, and stained them for BMP7 using same antibody. While normal adrenal medulla show low to undetectable levels of BMP7, the tumor cells had quite a high expression level of BMP7, whereas other cells of the tumor tissue, such as endothelial cells, showed no BMP7 staining. (Figure 15)

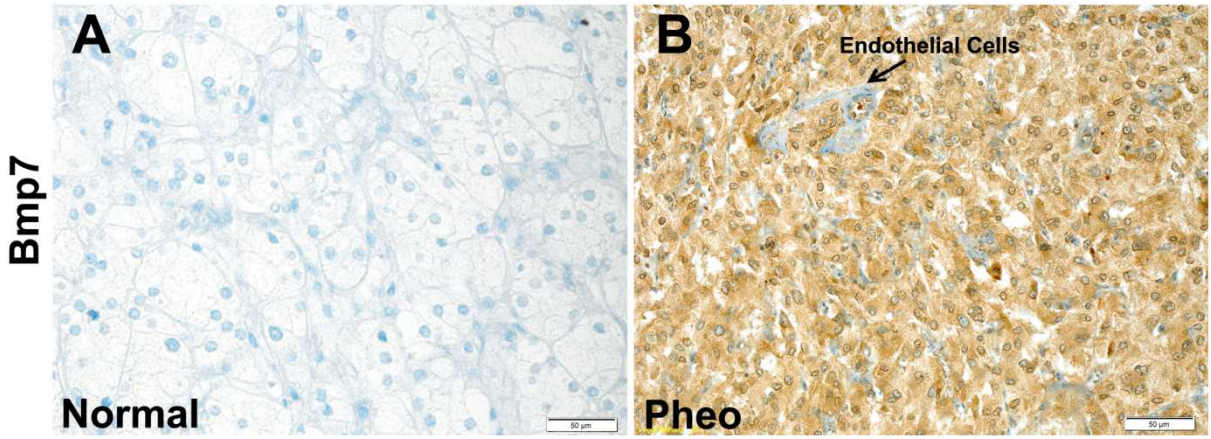

Figure 15. Immunohistochemistry for BMP7 in human pheochromocytoma. Immunohistochemistry was performed on human (A) normal and (B) tumorigenic adrenal medullary tissue using a human anti-BMP7 antibody (1:1000). The staining shows that non-tumorous cells (=endothelial cells) in the sample are negative for BMP7 staining (see arrow). Representative data from normal (n=3) and tumor (n=10) samples. Bar equals 50 µm.

To evaluate a larger series of pheochromocytomas we examined 5 paraffin-embedded formalin fixed tissue microarrays (TMAs) which were obtained from the ENS@T (European Network for the Study of Adrenal Tumors). These contained a total of 208 human pheochromocytomas, including 166 adrenal and 42 extra-adrenal tumors (paragangliomas). For each case, two different areas of the tumor were included for the TMA. The TMA sections were stained by immunohistochemistry using the automated immunostainer. The tumors were scored depending on the intensity of the staining from – to +++ (Figure 16). We only considered tumors for which both replicate samples could be scored and showed similar BMP7 expression. Therefore, 24 tumors did not fulfill our requirements and were excluded. Tumors that showed a staining scores "–" or "+"were considered to have "low" BMP7 levels, whereas tumors characterized by "++" and "+++" IHC staining were considered as having "high" BMP7 levels.

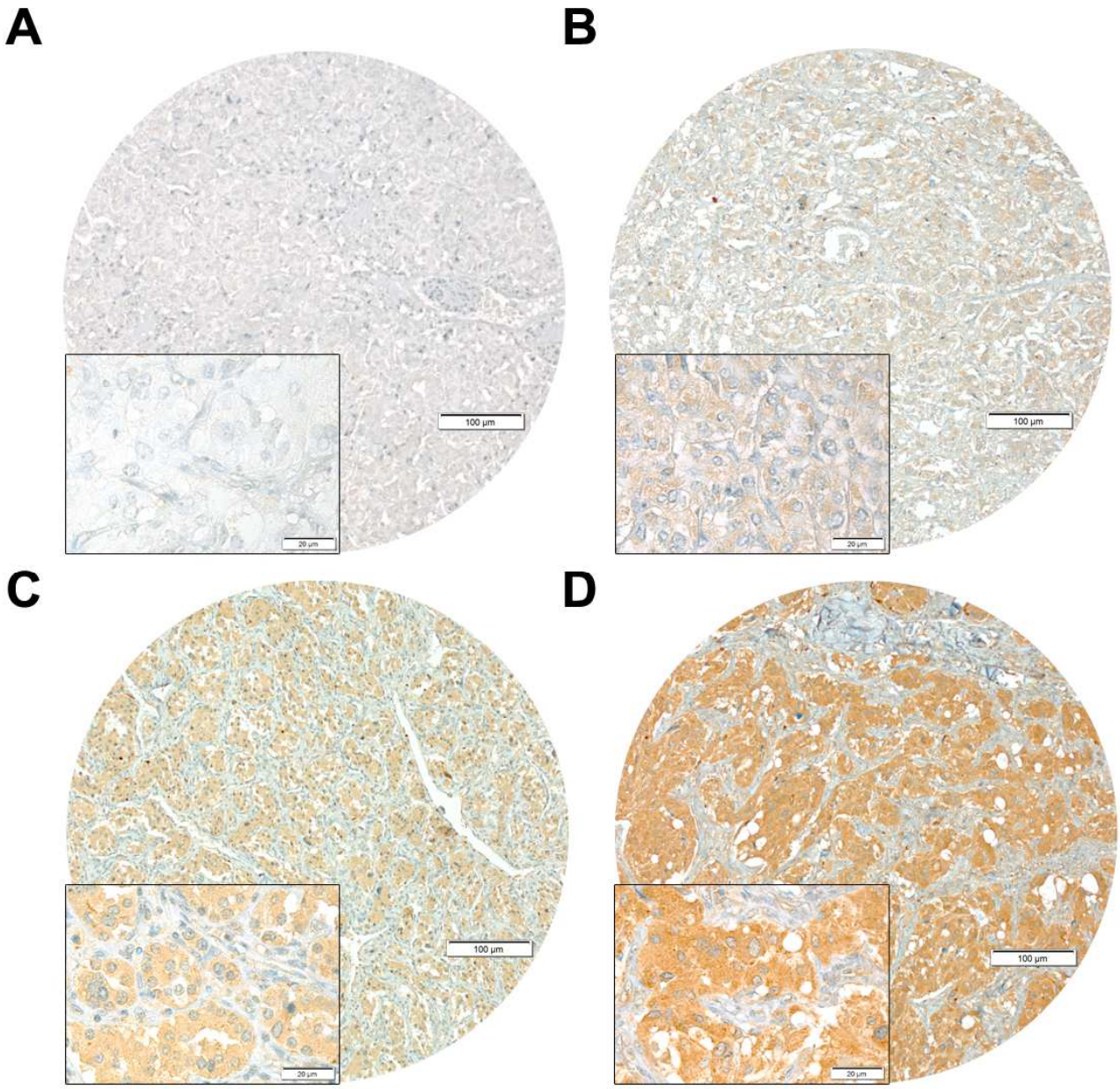

Figure 16. Representative fields of human pheochromocytoma tissue microarrays immunohistochemically stained with anti-BMP7 antibody. Immunohistochemistry was performed on formalin fixed paraffin embedded human normal and tumorigenic adrenal medullary tissue using a human anti-BMP7 antibody (1:1000). Low (original magnification, x40) and high (original magnification, x400) power views of 4 representative pheochromocytoma showing the range of BMP7 expression levels detected (A,-;B,+;C,++;D,+++).

Table 16. Clinical parameters of samples spotted on the tissue microarrays. The clinical parameters include location of the tumor (Pheochromocytoma, Paraganglioma), the gene expression cluster (cluster 1, 2) to which they belong indicating their germline predisposing mutation, the tumor size (>80mm; <35 mm) low and high catecholamine's (uMN; uNMN), malignancy (Metastasis), multiple tumor (multiple primaries, blood pressure (low/high) and chromogranin A expression. n= number of patients; uMN= urinary metanephrine; uNMN= urinary normetanephrine; chromo A= chromogranin A; low BMP7= tumors which show a – or + score for BMP7; high BMP7= tumors which show a ++ or +++ score for BMP7.

	total (n)	low BMP7 (n) / %	high BMP7 (n) / %
Tumors	184	52 / 28	132 / 72
Pheochromocytoma	150	48 / 32	102 / 68
Paraganglioma	34	4 / 12	30 / 88
cluster 1	53	3 / 19	43 / 81
VHL	21	5 / 24	16 / 76
SDHA	0	0 / 0	0 / 0
SDHB	13	5 / 38	8 / 62
SDHC	2	0 / 0	2 /100
SDHD	17	0 / 0	17 / 100
cluster 2	49	17 / 35	32 / 65
NF1	11	3 / 27	8 /73
TMEM	2	1 / 50	1 / 50
RET	24	10 / 42	14 / 58
MAX	4	0 / 0	4 / 100
Tumor > 80 mm	14	1 / 7	13 / 93
Tumor < 35 mm	34	15 / 44	19 / 56
low uMN	57	15 / 26	42 / 74
high uMN	63	25 / 40	38 / 60
low uNMN	62	15 / 24	47 / 76
high uNMN	43	13 / 30	30 / 70
Metastasis	11	2 / 18	9 / 82
multiple primaries	30	7 / 23	23 / 73
normal blood pressure	20	6 / 30	14 / 70
high blood pressure	64	25 / 39	39 / 61
chromo A high	10	2 / 20	8 / 80
chromo A low	19	3 / 16	16 / 84

We considered a total of 184 of the 208 pheochromocytomas, including 150 adrenal and 34 extra-adrenal tumors for which the two replicate samples could be scored and showed similar BMP7 expression (Table: 15). In total 72% of all tumors were characterized by high BMP7 levels. We then compared diagnostic markers which were reported by the different centers of the ENS@T (European Network for the Study of Adrenal Tumors) with the levels of BMP7. For markers such as plasma chatecholamines or chromogranin A we could not find any link to high or low BMP7

levels. We also could not detect any correlation between BMP7 levels and blood pressure or the presence of multiple primary tumors.

Compared to adrenal pheochromocytomas, of which only 10-25% are malignant, paragangliomas have a 60% risk of being malignant (Ayala-Ramirez, Feng et al. 2011); Kirmani, 1993). In our tumor series, 88% of paragangliomas exhibited high BMP7 levels and 12% low BMP7 levels, whereas 68% of the pheochromocytomas showed high levels of BMP7 and 32% low levels (p=0.02 by Fishers exact test) (Figure 17).

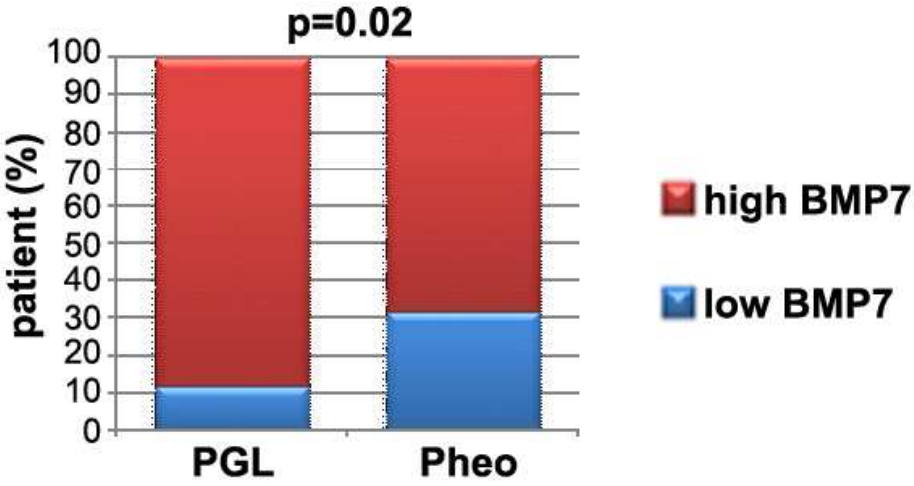

Figure 17. BMP7 levels from the TMA analysis correlated with the location of the tumors. The BMP7 levels of 150 pheochromocytoma and 34 paraganglioma are shown. 32% (n=48) of the pheochromocytoma showed low BMP7 levels whereas 68% (n=102) were characterized by high BMP7 levels. In Contrast only 12% (n=4) of the paraganglioma exhibit low levels and 88% (n=30) had high levels of BMP7.

Pheochromocytomas and paragangliomas can be divided into two different tumor clusters (cluster 1 or cluster 2) depending on their underlying germline mutation (Dahia 2014). Thus, cluster 1 pheochromocytomas are associated to mutations in the genes *VHL*, *SDHx* (*SDHA*, *SDHB*, *SDHC*, *SDHD*, *SDHAF2*), *HIF2α (Dahia, Ross et al. 2005)* and *FH* (Castro-Vega, Buffet et al. 2014); whereas cluster 2 tumors bear mutations in *NF1*, *RET*, *KIF1Bβ* and *TMEM127* (Gimenez-Roqueplo, Dahia et al. 2012, Vicha, Musil et al. 2013). Tumors due to mutations in *MAX* show a phenotype that is intermediate between cluster 1 and cluster 2 tumors (Burnichon, Cascon et al. 2012). BMP7 levels may be associated with specific genetic alterations,

since we found a trend showing that more cluster 1 tumors (92%) show high BMP7 levels when compared with cluster 2 pheochromocytomas (74%) (Figure 18), but this trend turned out not to be statistically significant (p=0.0773 by Fishers exact test). These observations could also be biased be the fact that many of the cluster 1 tumors were paragangliomas which had higher BMP7 levels. Twenty-seven out of 34 paragangliomas have a known genetic mutation and they all belong to cluster 1. Cluster 2 tumors having a mutation in *SDHB* are known to frequently metastasize. Five out of 13 *SDHB*-mutated tumors were malignant. Four of them showed high levels of BMP7 while only 4 out of the remaining 8 benign tumors had high BMP7 expression.

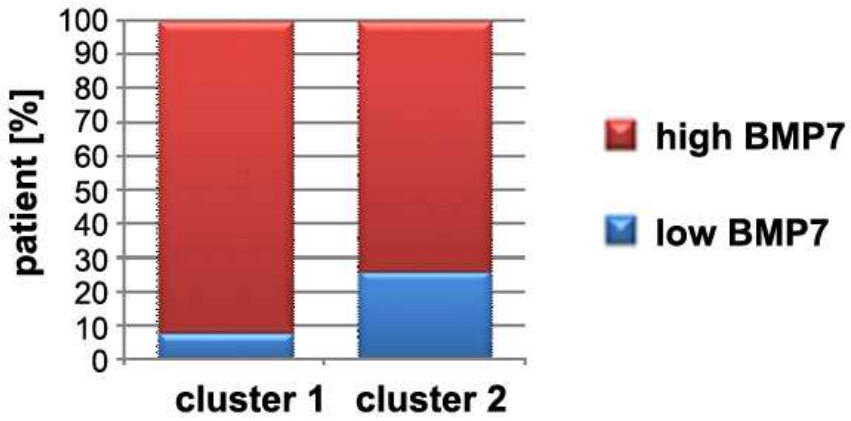

Figure 18. Higher BMP7 levels from our TMA analysis associates with cluster 2 genetic alteration. The BMP7 levels of 39 cluster 1 and 27 cluster 2 tumors are shown. 8% (n=3) of the cluster 1 tumors showed low BMP7 levels whereas 92% (n=36) were characterized by high BMP7 levels. In contrast 27% (n=7) of the cluster 2 tumors exhibit low levels and 72% (n=20) had high levels of BMP7.

The size of a tumor may be used to indicate the extent of tumor progression. It has been reported that the size of pheochromocytomas is a significant risk factor for metastasis and decreased overall survival (Ayala-Ramirez, Feng et al. 2011). In addition, bigger tumors are more difficult to remove bysurgery, and this correlates with a higher risk of recurrence. Most interestingly, the levels of BMP7 were strongly associated with tumor size: 93% of tumors larger than 80 mm had high BMP7 while only 56% of smaller tumors (<35 mm) had high BMP7 (p=0.018 by Fisher´s exact test) (Figure 19).

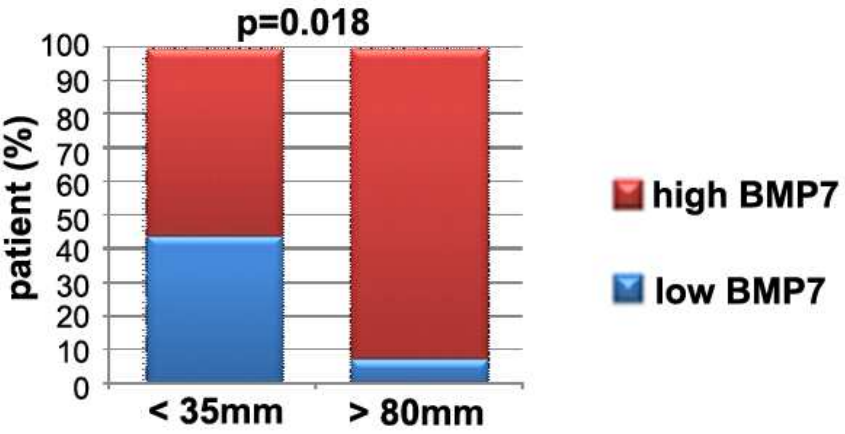

Figure 19. BMP7 levels from the TMA analysis associate with the size of the tumors. The BMP7 levels of 34 small tumors (<35 mm) and 14 big tumors (>80mm) are shown. Large tumors >80mm (n=14) and small tumors (<35 mm) (n=19) were compared by Fisher´s exact test. p=0.018

The presence of metastases is characteristic of malignant pheochromocytomas, which are associated with a worse outcome (Eisenhofer, Bornstein et al. 2004). Currently, no markers can predict the malignant potential of these tumors, and there is no effective treatment for malignant tumors. Therefore, it is important to identify new molecules and pathways that mediate the invasive phenotype of pheochromocytoma in order to find predictive biomarkers and new targets for treatment strategies. In our study we found that nine out of the 11 metastatic tumors showed high levels of BMP7. Due to the limited number of cases available this result was not statistically significant (p=0.7308 by Fisher´s exact test). (Figure 20)

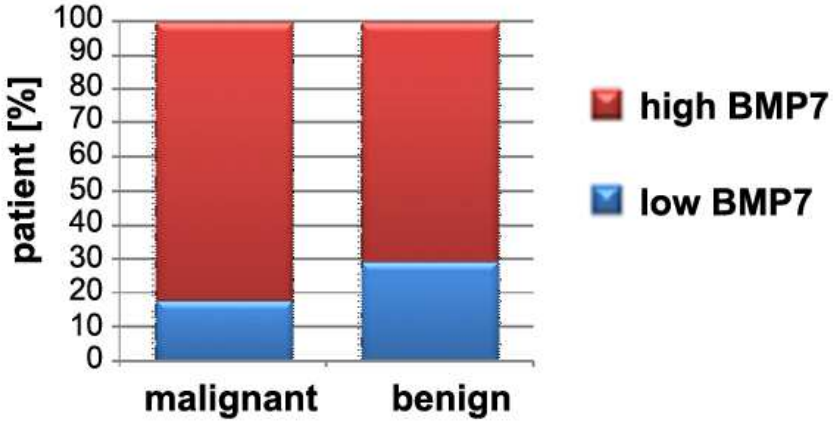

Figure 20. BMP7 protein expression indicates a link to a more malignant pheochromocytoma phenotype. The BMP7 levels of 11 malignant and 164 benign tumors are shown. 82% (n=9) of the malignant tumors showed high BMP7 levels. In contrast 71% (n=123) of benign tumors had high levels of BMP7.

BMP7 is a secreted protein (Constam and Robertson 1999) and we have shown (Figure 13) that BMP7 levels are elevated in MENX-rat serum levels. Therefore, we wanted to investigate whether BMP7 is secreted and can be detected in the blood in human patients. This would be a potential noninvasive tool for the diagnosis of cancer. We used a BMP7-detecting Enzyme-Linked Immunosorbent Assay (ELISA) to evaluate the plasma levels in pheochromocytoma patients (n=28) and healthy donors (n=31). We received pheochromocytoma plasma samples from Prof. Massimo Mannelli und control blood from Prof. Graeme Eisenhofer. Blood was taken a few days before the resection of the pheochromocytoma. The patients were neither starved nor was the blood taken at a specific time of the day. We found mildly elevated levels of BMP7 in the plasma of pheochromocytoma patients (Figure 21). In contrast to the results obtained on MENX rats, the elevated BMP7 in plasma of pheochromocytoma patients compared to that of healthy controls were not statistically significant (p=0.143 by t-test).This may be due to the high inter-individual variability or due to diet, time of sampling, medication or other uncontrolled variables. In addition, compared with our rats, the patients had not been fasted before blood was taken. This could impact BMP7 levels in the circulating blood. Another problem related to our analyses was that we did not have data regarding other phenotypic features that might influence BMP7 expression in the corresponding tumors of the

donor patients so that we were not able to draw conclusions if the tumors having high BMP7 also secrete higher levels of BMP7.

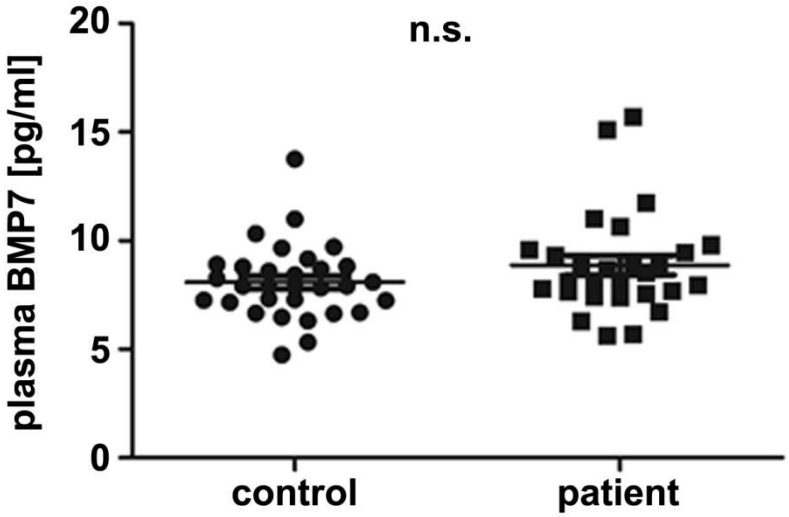

Figure 21. BMP7 plasma levels in human control individuals (non pheochromocytoma patients) and pheochromocytoma patients blood. Plasma of 31 controls and 28 pheochromocytoma patients was collected, and analyzed by human BMP7 ELISA kit. BMP7 levels of pheochromocytoma patients were mildly but not significantly elevated compared with controls. n.s. = not statistically significant.

3.3. Relationship between p27 and Bmp7

We previously showed that *Bmp7* overexpression occurs in the adrenomedullary cells of MENX-affected rats before histological alterations are detectable in the adrenal gland. This indicates that this change represents an early event in the tumorigenic transformation of these cells (Molatore et al. 2010). MENX-affected rats have a germline mutation in *Cdkn1b* which leads to an extremely reduced or absent level of the encoded p27 cell cycle inhibitor (Pellegata 2006). Thus, we wondered whether the overexpression of *Bmp7* might be causally linked with the lack of functional p27. To investigate a possible relationship between these two molecules, we analyzed Bmp7 expression in cells with different levels of p27 expression. Specifically, we established mouse embryonic fibroblasts (MEF) from mice with either heterozygous or homozygous deletion of *Cdkn1b* to generate p27+/+, p27+/- and p27-/- cell lines. Moreover, we generated rat embryonic fibroblast (REF) cell lines from mutant MENX-affected (homozygous p27mut/mut) or wild-type rats (p27wt/wt). The endogenous level of *Bmp7* expression was measured in these cell lines by qRT-

PCR and compared to p27 status. *Bmp7* expression in p27-/- MEFs was on average four times higher than that measured in p27+/+ MEFs, while the p27+/- cells express a level similar to p27 +/+ cells (Figure 22).

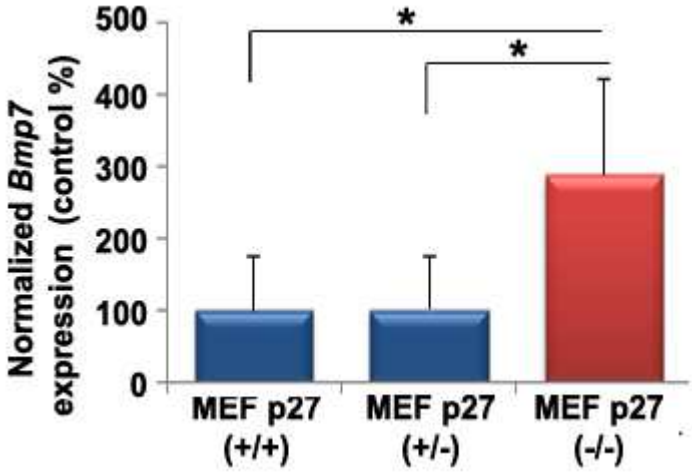

Figure 22. Bmp7 mRNA expression level in MEF cell lines from *Cdkn1b* (p27) wild- type (+/+), heterozygous (+/-), and mutant (-/-) mice. Total RNA was extracted with Trizol, reverse transcription was performed and the levels of *Bmp7* were assessed by TaqMan using specific primers and probes (Assay-on-Demand TM). β2-microglobulin served as the endogenous control for normalization of RNA input. The *Bmp7* mRNA level in p27 (-/-) and p27 (+/-) cells was normalized against the value obtained for the p27 (+/+) cells, whose average was arbitrarily set at 100%. The total absence of functional *Cdkn1b* (p27) results in a higher expression level of *Bmp7* mRNA. Data were analyzed independently with two biological and two technical replicates each and were expressed as the mean ±SD. *p < 0.05

Interestingly, the fact that the *Bmp7* mRNA levels in mouse p27+/- cells are similar to those of p27 +/+ cells suggests that the complete absence of p27 is required to activate pathways leading to higher *Bmp7* expression in these cells. In similar experiments, we used mutant-MENX-derived REF cells which do not have a knockout of p27 as the MEF cells but are characterized by a *Cdkn1b* (p27) having a 8 bp frameshift mutation. The cells are characterized by undetectable levels of p27 (Molatore, Kiermaier et al. 2010). We observed an almost 3-fold higher amount of *Bmp7* transcript in mutant REF cells when compared with that of wild-type REF cells (Figure 23). Altogether, these results confirm the mouse results and show that reduced *Cdkn1b* (p27) levels correlate with higher *Bmp7* expression.

We then investigated whether the induced knockdown of *Cdkn1b* in PC12 cells (having functional endogenous p27) can modulate the level of *Bmp7*. To this aim, cells were transfected with siRNA oligos directed against rat *Cdkn1b*. Downregulation

of *Cdkn1b* was verified by TaqMan analysis. Expression was reduced by up to 80 % with respect to the control (scrambled siRNA oligos) (Figure 24).

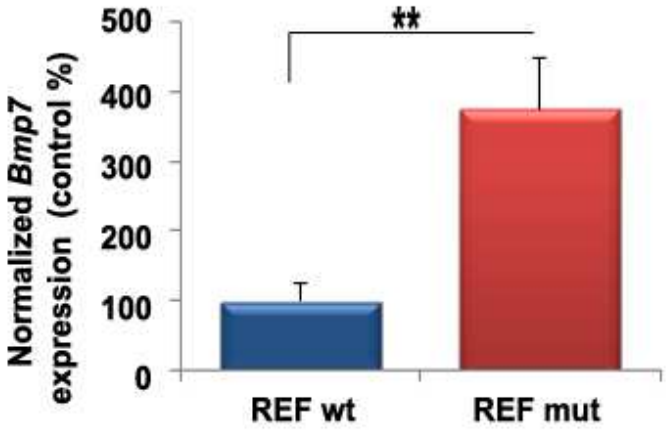

Figure 23. *mRNA* expression level of Bmp7 in REF cell lines of wild-type (REF wt) and mutant MENX-affected rats (REF mut). Total RNA was extracted with TRIzol, reverse transcription was performed and the levels of cDNA *Bmp7* was assessed by TaqMan using specific primers and probes (Assay-on-Demand TM). β2-microglobulin served as endogenous control for normalization of RNA input. The *Bmp7* mRNA level in REF mut cells was normalized against the value obtained for the REF wild-type (wt) cells, whose average was arbitrarily set at 100%. The absence of functional *Cdkn1b* (p27) results in a higher expression level of *Bmp7*. Data were analyzed independently with two biological and two technical replicates each and were expressed as the mean ±SD. **p < 0.01

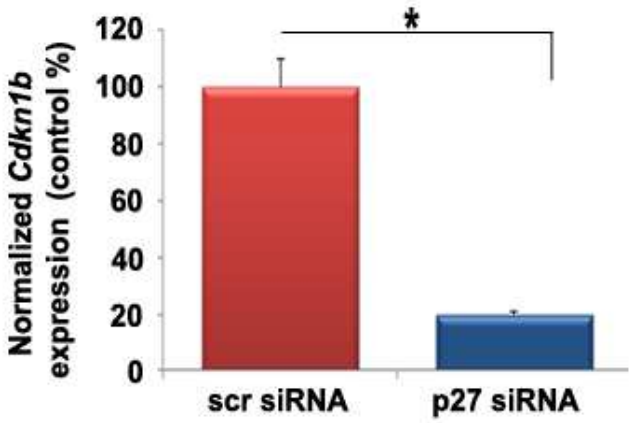

Figure 24. Knockdown of mRNA expression level of *Cdkn1b* in PC12 line following transfection with siRNA molecules targeting *Cdkn1b*. Cells were either transfected with a scrambled (scr) siRNA or with the siRNA targeting *Cdkn1b* (p27 siRNA). Total RNA was extracted with TRIzol, reverse transcription was performed and the levels of cDNA *Cdkn1b* (p27) was assessed by TaqMan using specific primers and probes (Assay-on-Demand TM). β2-microglobulin served as endogenous control for normalization of RNA input. The *Cdkn1b* mRNA level in scrambled- and p27-siRNA transfected PC12 cells was normalized against the value obtained for the untreated PC12 cells, whose average was arbitrarily set at 100%. sip27 transfected cells showed a 80% reduced expression level of *Cdkn1b*. Data were analyzed independently with two biological and two technical replicates each and were expressed as the mean ±SD. *p<0.05

p27 siRNA-transfected PC12 cells showed a 3.3 -fold higher expression level of endogenous *Bmp7* than scrambled siRNA-transfected cells (Figure 25). Taken together these data (Figure 22-25) suggest that there is a functional link between the amount of *Cdkn1b* (p27) and that of *Bmp7*.

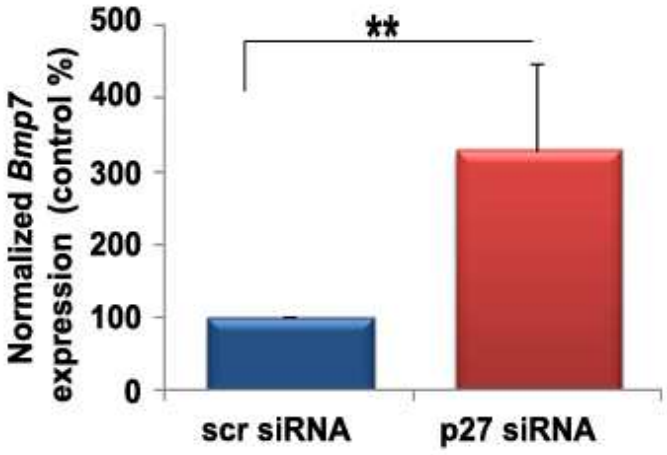

Figure 25. mRNA expression level of *Bmp7* in PC12 cell line with different p27 expression levels. Cells were either transfected with a scrambled (scr) siRNA or with the siRNA targeting p27. Total RNA was extracted with TRIzol, reverse transcription was performed and the levels of cDNA Bmp7 was assessed by TaqMan using specific primers and probes (Assay-on-Demand TM). β2-microglobulin served as endogenous control for normalization of RNA input. p27 siRNA transfected cells showed a 3.3-times higher expression level of *Bmp7*. The *Bmp7* mRNA level in scrambled and sip27- transfected PC12 cells was normalized against the value obtained for the untreated PC12 cells, whose average was arbitrarily set at 100%. Data were analyzed independently with two biological and two technical replicates each and were expressed as the mean ±SD. **$p < 0.01$

3.4. Expression of BMP receptors in pheochromocytoma cells and adrenal gland tissue

We found that Bmp7 is overexpressed and secreted in the serum of MENX rats and overexpressed in human pheochromocytoma. Next, we wanted to determine if there is an the effect of this endogenous BMP7 on primary pheochromocytoma cells of MENX rats and in pheochromocytoma cell lines (rat PC12, mouse MPC and MTT). Before performing functional analyses with these cells, we checked whether they express the most prominent *BMP* receptors *Alk2*, *ALK3 ALK6*, *AcVr2a, AcVr2b* and *BMPRII* to make sure that they are able to respond to BMP7 stimulation (Figure 26).

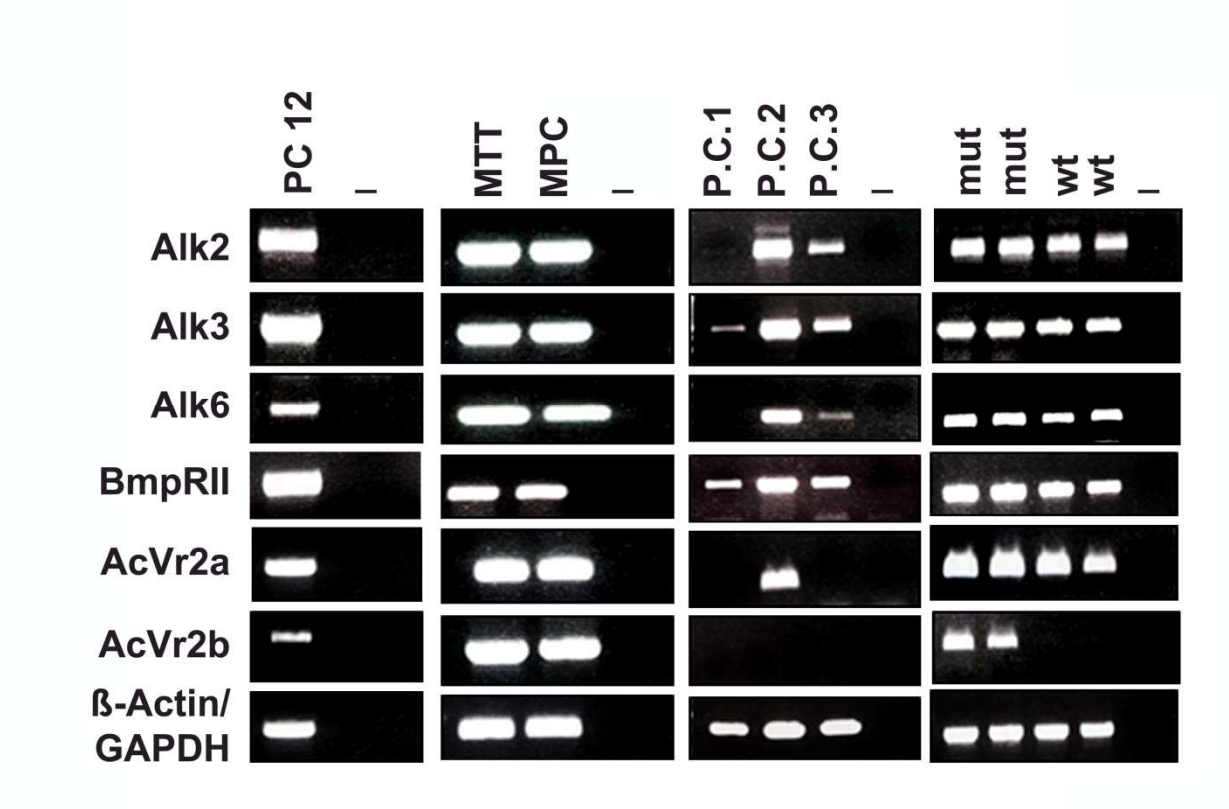

Figure 26. *Bmp7* receptor gene expression in pheochromocytoma cells and pheochromocytoma tissues. RNA was extracted from PC12, MPC and MTT cells, from three rat primary pheochromocytoma cell cultures (P.C. 1-3), and from adrenal medullas of mutant (mut) and wild-type (wt) rats. RNA was reverse transcribed into cDNA, and amplified by RT-PCR using primers specific for *Alk2, Alk3* and *Alk6*, *BmpRII*, *AcVr2a*,*b*, *ß-Actin* (for rat) and *GAPDH* (for mouse). The PCR product was detected on a 1% agarose gel following ethidium bromide staining. Mouse *Bmp* receptor transcripts were detected at the following sizes: *Alk2* (331bp)*, ALK3* (263bp) and ALK*6* (221bp), *BmpRII* (326bp), *AcVr2a* (318bp), *AcVr2b*(393bp). Rat Bmp receptor transcripts were detected at the following sizes: *Alk2* (323bp)*, ALK3* (464bp) and ALK*6* (221bp), *BmpRII* (326bp), *AcVr2a* (318bp), *AcVr2b* (264bp). Lanes marked (-) served as negative controls as no target template was added. PC12, MPC and MTT cells express all tested receptors. The individual primary cultures (P.C. 1-3) showed a variable expression pattern of *BMP* receptors.

We confirmed the expression of a range of *Bmp* receptors in rat PC12, mouse MPC and MTT cell lines, as well as in primary rat pheochromocytoma cells. The individual primary cultures of rat pheochromocytoma showed a variable expression pattern of *BMP* receptors, which might be due to a different stage of progression of the tumor or to the effects of *in vitro* manipulation. Further, we found that adrenal medulla from MENX rats (with tumors) expresses all tested types of *Bmp* receptors when compared with adrenal medulla from wild-type rats or the primary rat pheochromocytoma cells which do not express *AcVr2b*. In conclusion, we

demonstrated that pheochromocytoma cells are candidate models for assessing autocrine/paracrine effects upon Bmp stimulation as they express multiple *Bmp* receptors.

3.5. Endogenous overexpression of Bmp7 has neurotrophic effects on PC12 cells

PC12 cells have been extensively used as a model of neuronal differentiation and signal transduction. When treated with neurotrophic factors, such as nerve growth factor (NGF), these cells undergo growth arrest and form neurites resembling those of differentiated parasympathetic neurons (Greene & Tischler 1976). It has been reported that incubation with recombinant rhBMPs, including rhBMP7 (Di Liddo et al. 2010), enhances NGF-mediated neurite formation in PC12 cells. We then investigated whether ectopic Bmp7 overexpression can stimulate neurite formation through autocrine signaling in these cells since this would prove our hypothesis that BMP7 is able to affect the transfected cells via an autocrine loop. To this aim, PC12 cells were transfected with the Myc-BMP7 vector or with empty vector (mock) (Figure 27).

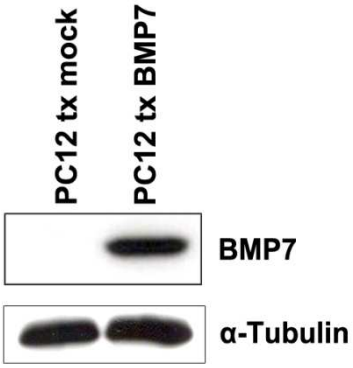

Figure 27. Validation of the overexpression of BMP7 in PC12 cells. PC12 cells were transfected with an empty Myc plasmid (PC12 tx mock) or transfected with an Myc-BMP7 plasmid (PC12 tx BMP7) and 24 h later cells were analyzed by western blotting using a specific anti Myc-antibody (1:500). α-Tubulin (1:1000) was used as loading control.

Twenty-four hours post-transfection the medium was changed to a “serum starvation” medium containing 0,1% horse serum and 0,02% FBS. Twenty-four hours later the cells were treated with NGF (100 ng/ml) for an additional 24 h or left untreated. Then, the shape of PC12 cells was assessed under the microscope following

immunofluorescent staining and western blot analysis for neurofilament H, a member of the intermediate filament subclass which is associated with neuronal differentiation (Takeda, Okabe et al. 1994). As illustrated in Figure 28, PC12 cells transfected with empty vector showed an unchanged rounded morphology. About 80 % of the PC12 that were transfected with the Myc-BMP7 vector showed high BMP7 expression. However, transfection of BMP7 resulted in an increase in the number of cells showing neurite-like outgrowth and higher neurofilament H levels (Figure 29), even in the absence of NGF. Mock-transfected cells incubated with NGF show a similar phenotype to BMP7 transfected cells as they also start forming neurites. Interestingly, mock-transfected cells incubated with NGF even show increased levels of endogenous Bmp7. In contrast mock-transfected cells without further treatment did not show neurite formation.

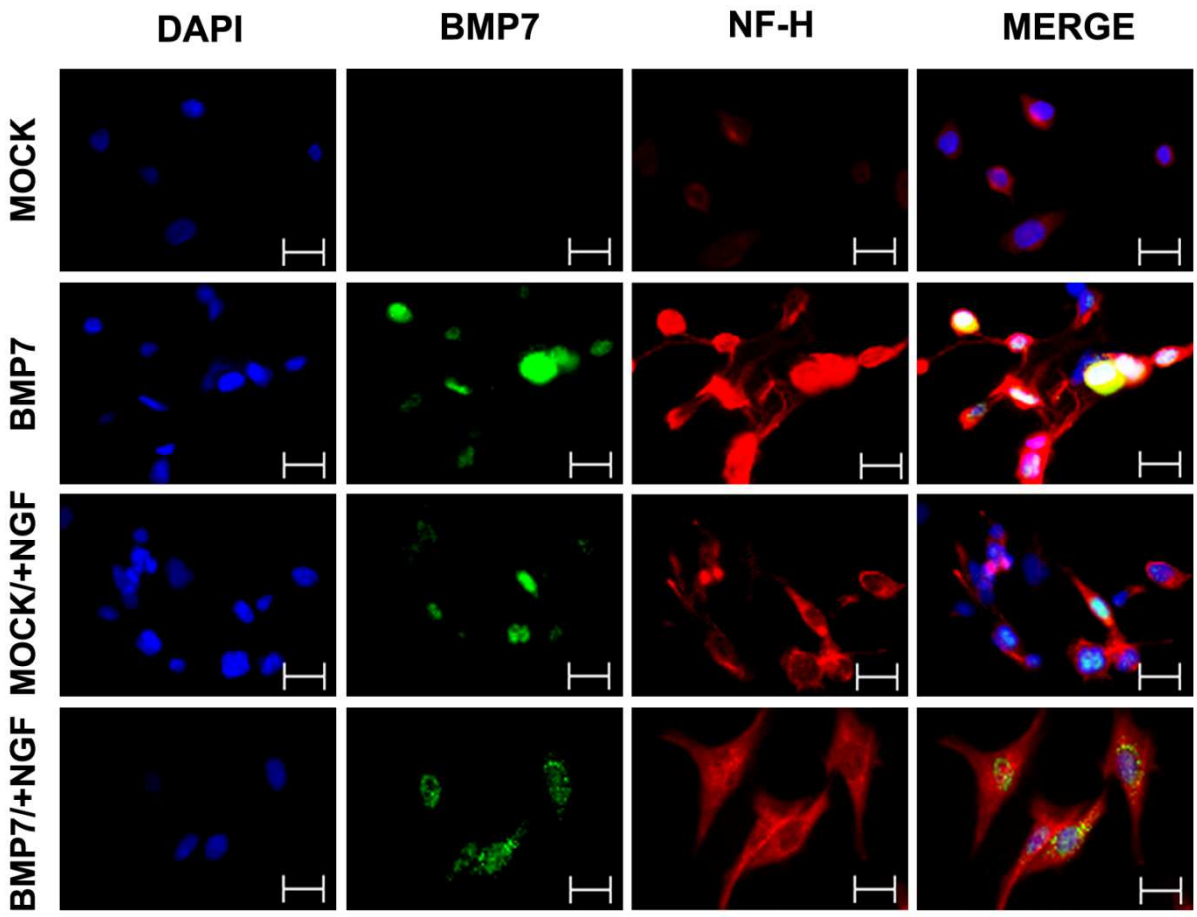

Figure 28. Neuronal differentiation of PC12 cells. Neurite outgrowth after transfection of PC12 cells with Myc-BMP7 or Mock vector and treatment with (+) NGF for 24h. Expression of neurofilament H (in red) and of Bmp7 (in green) was evaluated following immunofluorescent staining with specific antibodies (rat anti-Bmp7: 1:100; anti-NF-H 1:400). Nuclei were counterstained with DAPI. Pictures were taken by confocal microscopy. Original magnification: 400x; The bar equals 20 µm.

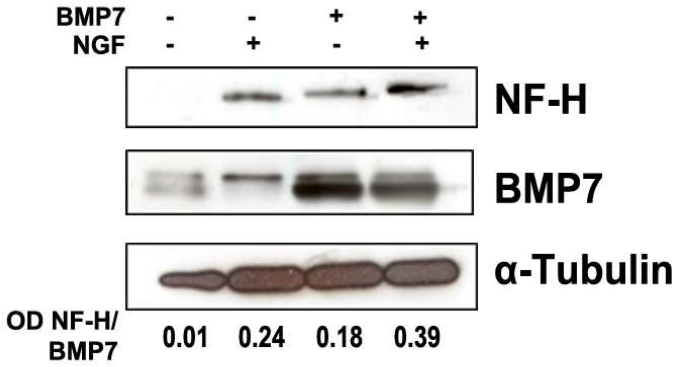

Figure 29. Western blotting showing neuronal differentiation of PC12 cells. Neurite formation after transfection of PC12 cells with Myc-BMP7 or Mock vector and treatment with (+) NGF for 24 h was determined by western blot analysis. Western blotting of PC12 cells transfected with Myc-BMP7 or Mock vector or treated with NGF was performed using a rat anti-Bmp7 (1:500) and anti-NF-H (1:500) antibody. α-Tubulin (1:1000) was used as loading control. Numbers at the bottom of the western blot represent the ration of the quantification of band intensities of NF-H normalized to α-Tubulin (OD NF-H/ α-Tubulin).

Altogether, these results suggest that overexpression of BMP7 promotes neurite outgrowth in PC12 cells concordantly with the results concerning the treatment with NGF or rhBMP7. Noteworthy, overexpression of endogenous BMP7 protein and treatment with NGF promote slightly more the formation of neurite-like processes in PC12 cells. In conclusion, our findings indicate that PC12 cells undergo neurite formation upon endogenous overexpression of BMP7.

3.6. BMP7 promotes migration and invasion of PC12 cells

Higher potential for cell migration and invasion are *in vitro* properties associated with malignancy and metastases. It was already reported that BMP7 can increase migration and invasion of human and mouse breast cancer cells (Alarmo, Korhonen et al. 2008). It has also been shown that other factors that are usually known to be major players in the migratory and invasion processes, such as the Urokinase receptor (UPAR) (Tang and Han 2013), have also been associated with the subsequent progression of NGF-driven differentiation (Farias-Eisner, Vician et al. 2000). Thus, we decided to assess whether BMP7 plays a role in the migration and invasion of pheochromocytoma cells. PC12 cells transfected with the Myc-BMP7 vector or with the empty vector (mock) were allowed to migrate through a 8 µm pore

membrane from low to high serum concentration. The migrated cells were then stained and the percentage of migrated cells was then determined by counting migrated cells five random fields at 200 x magnification. We observed that elevated levels of BMP7 expression stimulate the migration of PC12 cells by +1.8 fold compared to mock-transfected cells assayed under identical conditions (Figure 30).

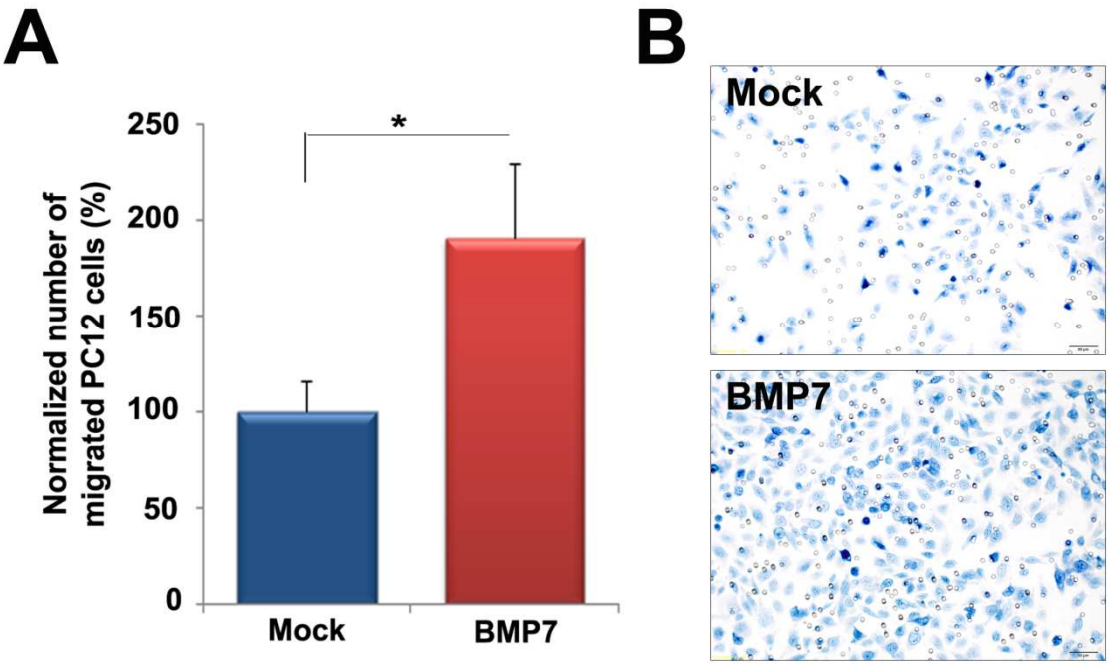

Figure 30. Migration assay following overexpression of Bmp7 in PC12 cells. We transfected PC12 with a Myc plasmid (Mock) or with an Myc-BMP7 plasmid (BMP7) and 24 h later assessed migration. (A) The level of migration of BMP7-transfected cells was normalized against the value obtained for mock-transfected cells, whose average was arbitrarily set to 100%. The experiment was performed with two biological and two technical replicates (±SD). Five random fields of each membrane at 400× magnification were counted. **p < 0.01 (B) Here representative pictures of migration assay membranes of PC12 cells transfected either with a Myc plasmid (Mock) or with a Myc-BMP7 plasmid (BMP7) are shown.

PC12 cells were also subjected to an invasion assay by measuring their movement through a matrigel basement membrane matrix. As illustrated in Figure 31, BMP7-transfected PC12 cells show higher invasion potential (+2.8 fold) compared with mock-transfected cells (Figure 31).

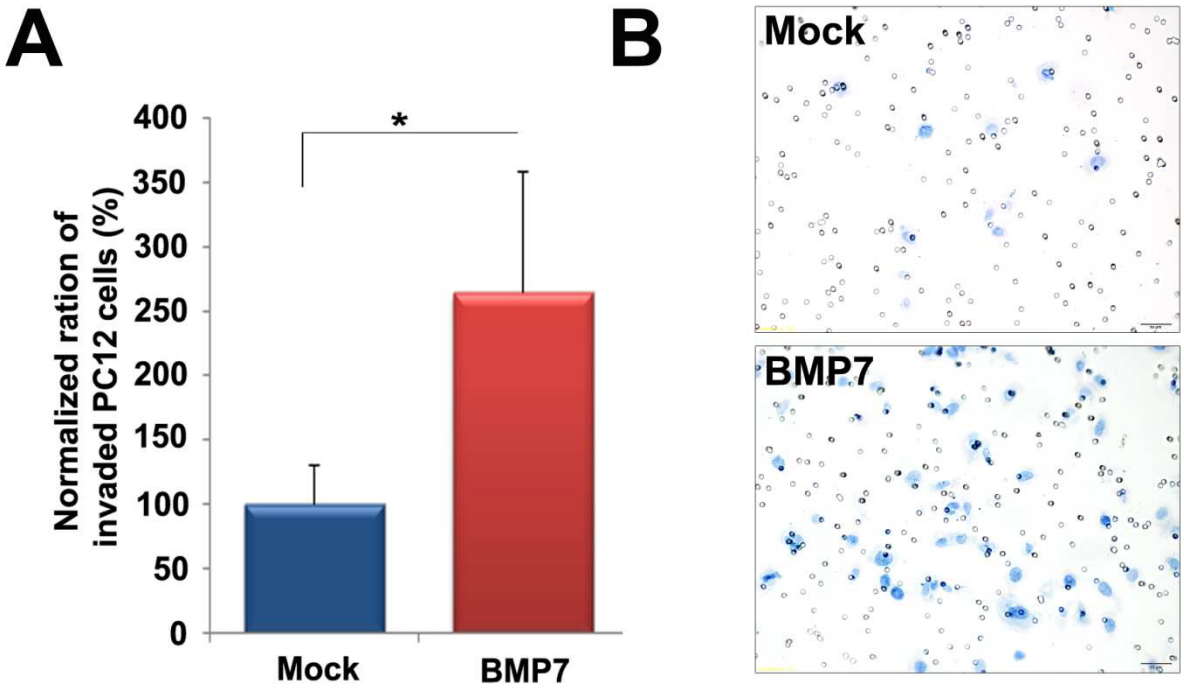

Figure 31. Invasion assay following overexpression of *Bmp7* in PC12 cells. We transfected PC12 with a Myc plasmid (Mock) or with an Myc-BMP7 plasmid (BMP7) and 24 h later invasion was assessed. (A) The level of invasion of BMP7-transfected cells was normalized against the value obtained for mock- transfected cells, whose average was arbitrarily set to 100%. The experiment was performed with two biological and two technical replicates (±SD). Five random fields of each membrane at 400x magnification were counted. **p < 0.01 (B) Here representative pictures of migration assay membranes of PC12 cells transfected either with a Myc plasmid (Mock) or with a Myc-BMP7 plasmid (BMP7) are shown.

Altogether, these data show that increased autocrine BMP7 signaling promotes both migration and invasion of PC12 cells.

3.7. Transfections of MPC/MTT and primary pheo cells with lentiviral vectors

MPC and MTT cells express high levels of Bmp7, like rat primary pheochromocytoma cells. When we tried to transfect MPC/MTT and primary rat pheochromocytoma cells we realized that general liposome transfection-based reagents were not successful for siRNA or plasmid DNA transfer. For this reason, we decided to generate a lentiviral vector with a sh*BMP7* sequence to enable the knockdown of *Bmp7* in these hard to transfect cells. This work was done in cooperation with N. Anastasov. In order to find the right shRNA sequence to clone into the lentiviral vectors, we examined the effect of 4 siRNA oligos on PC12 cells. All four siRNAs showed an efficient knockdown of *Bmp7* in PC12 cells upon transfection using Lipofectamine (Figure 32).

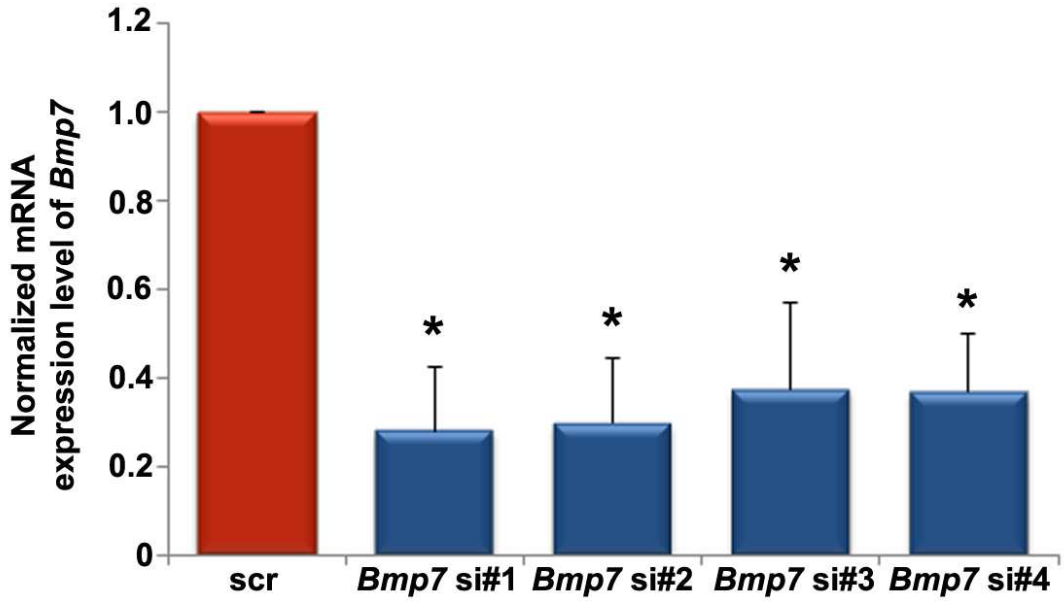

Figure 32. mRNA expression level of *Bmp7* in PC12 cell line transfected with si*BMP7* or scr siRNA. Cells were either transfected with a control scrambled siRNA (scr) or with 4 different siRNAs targeting *Bmp7* (*BMP7* si#1-4). Total RNA from the cells was then extracted, reverse transcription was performed and the levels of *Bmp7* transcript was analyzed in a PCR cycler using specific TaqMan primers and probes (Assay-on-Demand TM). β2-microglobulin served as endogenous control for normalization of RNA input. *Bmp7* level in si*BMP7*- transfected PC12 cells was normalized against the value obtained for the scrambled siRNA-transfected PC12 cells, whose average was arbitrarily set to 1. Data were analyzed independently with two biological and two technical replicates each and were expressed as the mean ±SD; *p<0.05

The sequences that showed the highest knockdown of *Bmp7* (*Bmp7* si#1 and *Bmp7* #2) were cloned into the lentiviral vectors (pGP) containing a GFP sequence and named sh*Bmp7 1.8* and sh*Bmp7 2.9*. After virus production the infection efficiency of the virus was tested in HEK293 cells. The cells were either infected with the undiluted virus (stock concentration) or with virus diluted 10^{-1} with cell specific medium. Therefore, HEK293 cells were infected with lentiviruses containing either an empty pGP-Vector or a pGP-Vector containing one of the small hairpin (sh)RNA sequences directed against *Bmp7* (sh*Bmp7 1.8* and sh*Bmp7 2.9*). Seventy-two hours after infection, GFP intensity in the cells was measured by FACS analysis. As indicated in Figure 33, we can monitor proper integration of the virus in the control HEK293 cells in a concentration dependent manner. Thus, for all three vectors the undiluted virus batch gave the highest infection efficiency with 99% of cells showing a fluorescent signal by FACS analysis. Moreover, 99% of the cells which were infected with the 10^{-1} diluted virus batch containing the empty pGP or the sh*Bmp7 2.9* vector were GFP

expressing, whereas only 87% of the cells infected with the lentivirus containing sh*Bmp7 1.8* showed a green fluorescent signal (Figure 33).

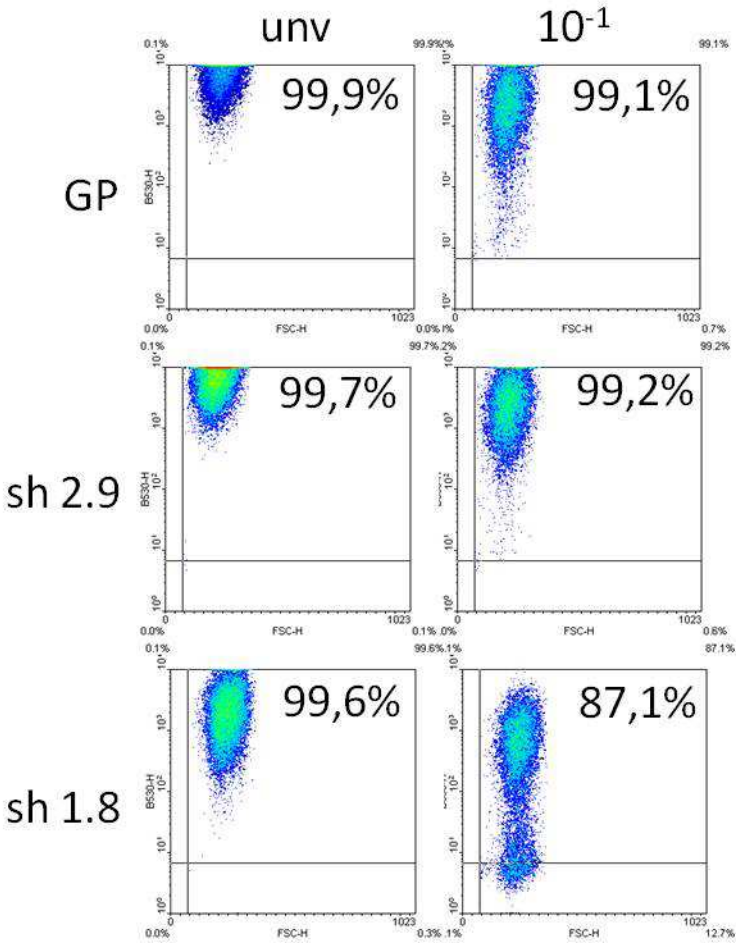

Figure 33. HEK293 cells infected with undiluted (unv) or diluted (10^{-1}) viral vectors containing either the empty control pGP vector or the vector containing the sequence sh*Bmp7 2.9* (sh2.9) or sh*Bmp7 1.8* (sh1.8). Whole population in side (Y) and forward (X) scatter with fluorescent levels at 530 nm (green). Undiluted infection showed for all three infections after 72 h after infection >99% of cells had the fluorescent signal. The 10^{-1} diluted virus, infected more than 99% of the cells with the empty pGP or the sh2.9, whereas for sh1.8 only 87% of the cells showed the green fluorescent signal.

In order to check whether the lentivirus-mediated *Bmp7* knockdown was efficient using the lentiviruses, we transfected the primary pheochromocytoma cells, MPC and MTT cells with the viruses containing the different vectors. Seventy-two hours after transfection cells were harvested and RNA was extracted, followed by TaqMan RT-PCR analysis to assess *Bmp7* expression.

In the primary cells and in MPC cells, but not in MTT cells, downregulation of *Bmp7* using sh*Bmp7 1.8* was successful while the downregulation mediated by 2.9 was

efficient in all tested cells and the reduction was estimated to be between -40% and -80% (Figure 34).

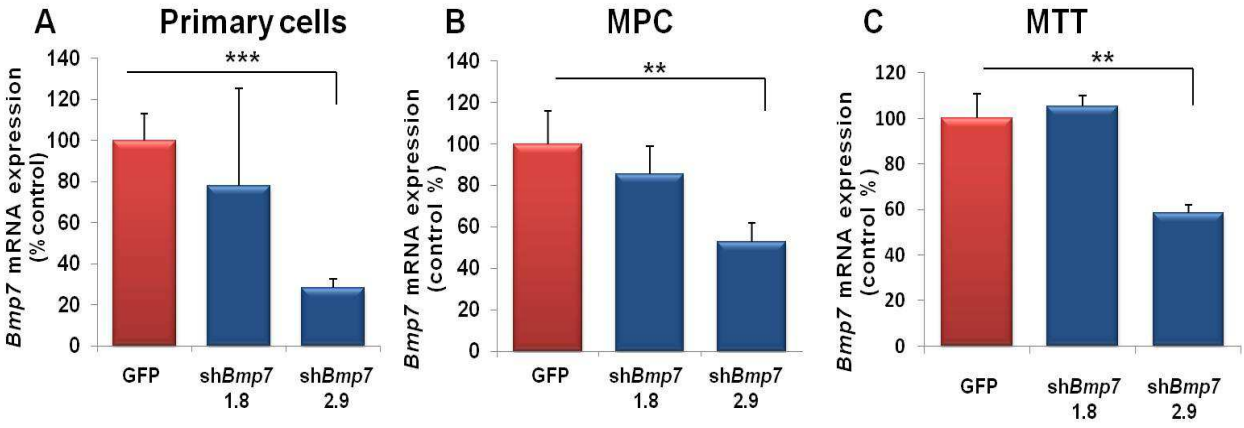

Figure 34. Knockdown of mRNA expression level of *Bmp7* in cells infected with sh-containing lentiviral vectors. Primary cells (A), MPC (B) or MTT (C) cells were either infected with a lentiviral vector containing the empty pGP plasmid (GFP) or the sh*Bmp7 2.9* or *1.8* sequences. Total RNA from the cells was extracted with the Maxwell machine, reverse transcription was performed and the levels of *Bmp7* were analyzed in a PCR cycler using specific TaqMan primers and probes (Assay-on-DemandTM). β2-microglobulin served as the endogenous control for normalization of RNA input. *Bmp7* level in sh*Bmp7* infected cells were normalized against the value obtained for the GFP infected cells, whose average was arbitrarily set to 100%. Data were analyzed independently with two biological and two technical replicates each and were expressed as the mean ±SD. **p < 0.01; ***p < 0.001

Based on this data we decided to use the viral vector with the sh*Bmp7 2.9* sequence for further studies (sh*Bmp7*).

3.8. Loss of BMP7 promotes proliferation, migration and invasion of MPC and MTT cells

The effective sh-mediated knockdown of *Bmp7* mRNA was confirmed by quantifiying Bmp7 encoded protein by western blotting in shBmp7-infected and GFP vector-infected cells (Figure 35).

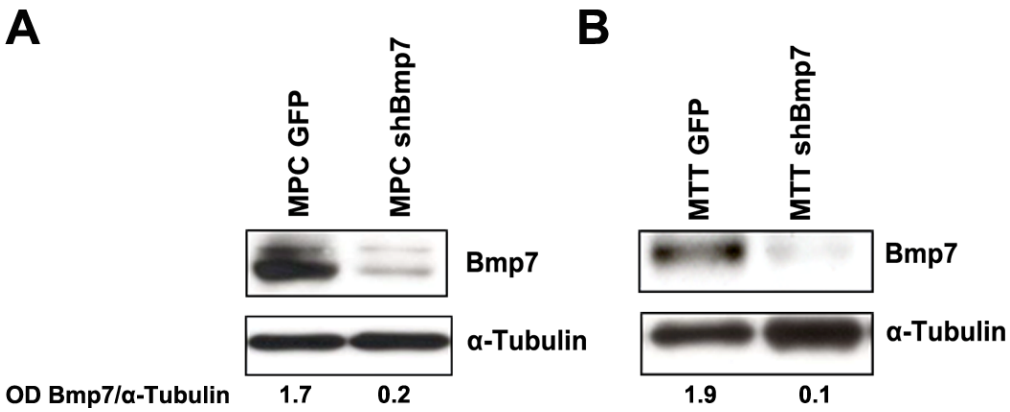

Figure 35. *Bmp7* knockdown in (A) MPC and (B) MTT cells. Cells were infected with lentiviral vectors containing sh*Bmp7*-GFP or GFP alone. Western blotting was performed using an anti-BMP7 antibody (1:500). α-Tubulin (1:1000) was used as loading control. Numbers at the bottom of the western blot represent the quantification of band intensities of Bmp7 normalized to α-Tubulin (OD Bmp7/ α-Tubulin).

We already showed that BMP7 can both enhance neuronal differentiation and confer increased tumorigenic properties such as migration and invasion in PC12 cells. In order to better understand the effect of Bmp7 on pheochromocytoma cell proliferation we dowregulated *Bmp7* in MPC (-86%) and MTT cells (-96%) and assessed proliferation. Upon downregulation of endogenous *Bmp7* expression we observed impaired proliferation of MPC cells (-30%) and, to a lesser extent, also of MTT cells (-20%) (Figure 36).

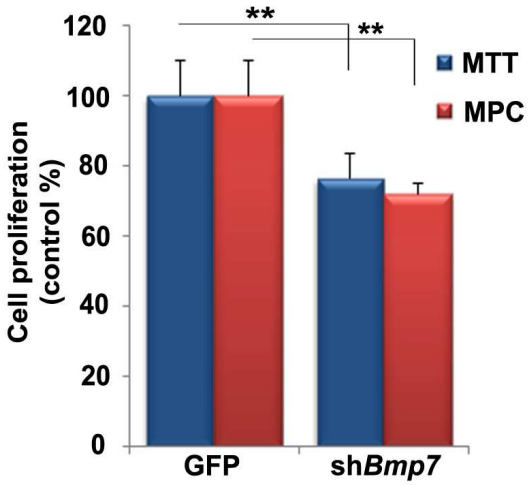

Figure 36. Effect of *Bmp7* knockdown in MPC (red) and MTT (blue) cells. Cells were infected with lentiviral vectors containing GFP or sh*Bmp7* and 72 h later proliferation was assessed using the WST-1 assay. The values are referred to GFP-infected cells set to 100%. The experiment was performed with two (MPC) or three (MTT) biological and 6 technical replicates each and were expressed as the mean ±SD. *p<0.05

Since Bmp7 promotes migration and invasion of PC12 pheochromocytoma cells, we next investigated whether Bmp7 knockdown can inhibit these processes in MPC and MTT cells. Following infection with sh*Bmp7* or GFP-only viral vectors, cells were allowed to migrate through a membrane and those that migrated were counted.

In MTT cells, knockdown of Bmp7 expression reduced their migration ability (average -77%) when compared with GFP-infected cells (Figure 37).

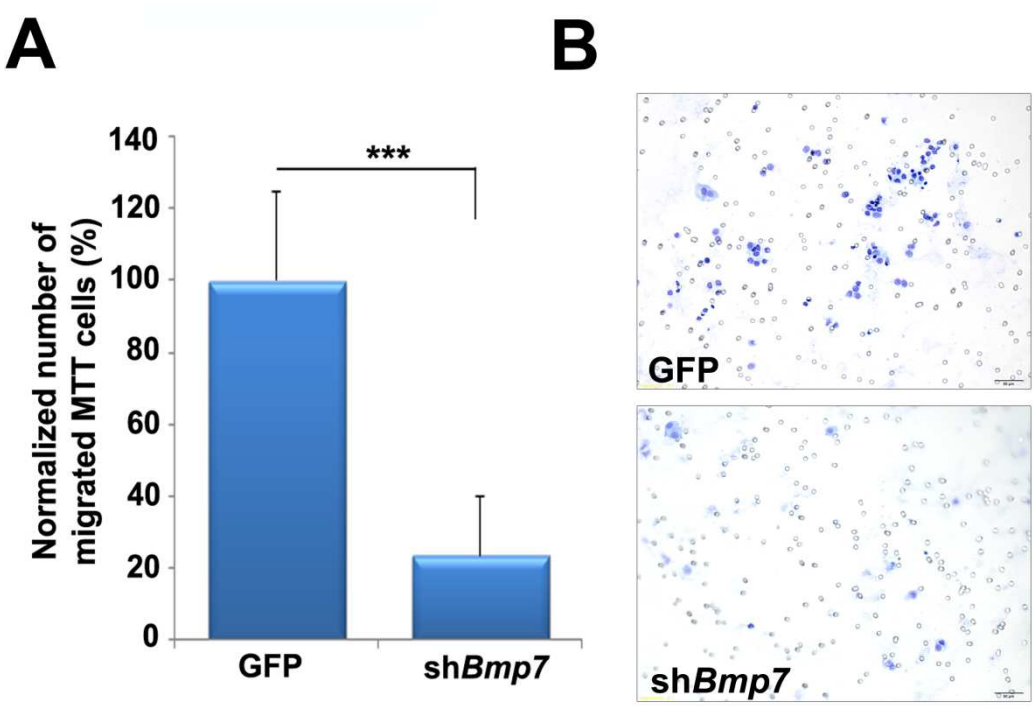

Figure 37. Migration of MTT cells following downregulation of *Bmp7*. Cells were infected with lentiviral vectors containing GFP or sh*Bmp7* and 72 h later migration was assessed. (A) Values of migrated cells were normalized against those of GFP-infected cells set to 100%. The experiment was performed with two biological and two technical replicates (±SD). Five random fields of each membrane at 400× magnification were counted. ***p < 0.001 (B) Here representative pictures of migration assay membranes of MTT cells transfected either with lentiviral vectors containing GFP or sh*Bmp7* are shown.

A similar effect was also observed for MPC cells. Thus, knockdown of *Bmp7* expression in MPC cells decreased migration (average -77%) when compared with GFP-infected cells (Figure 38).

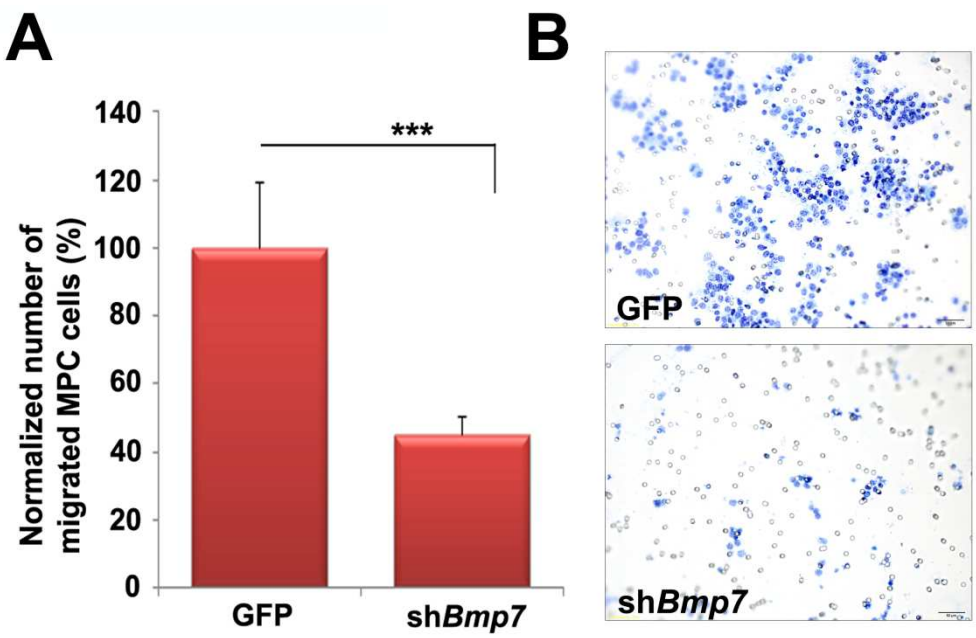

Figure 38. Migration of MPC cells following downregulation of *Bmp7*. Cells were infected with lentiviral vectors containing GFP or sh*Bmp7* and 72 h later migration was assessed. (A) Values of migrated cells were normalized against those of GFP-infected cells set to 100%. The experiment was performed with two biological and two technical replicates (±SD). Five random fields of each membrane at 400× magnification were counted. ***p < 0.001 (B) Here representative pictures of migration assay membranes of MPC cells transfected either with lentiviral vectors containing GFP or sh*Bmp7* are shown.

When invasion assays through matrigel basement membrane matrix were performed on both cell lines, *Bmp7* downregulation markedly decreased the invasion capacity of MTT cells (Figure 39) (average -83%) and MPC (average -77%) (Figure 40) when compared with control GFP-infected cells. In conclusion, Bmp7 can stimulate the migration and invasion of mouse pheochromocytoma cells, inhibition of Bmp7 by knockdown has the reverse effect, preventing migration and invasion.

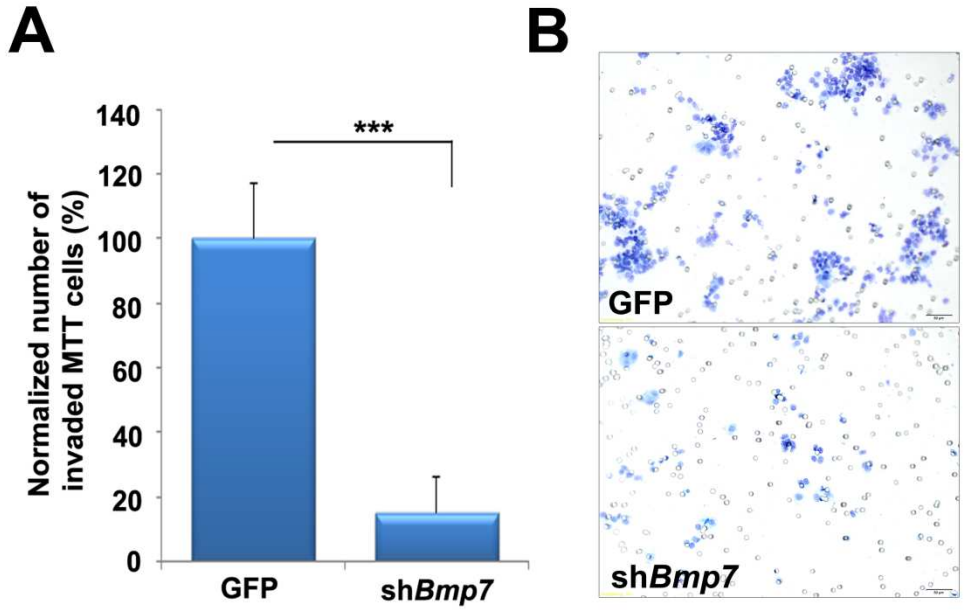

Figure 39. Invasion of MTT cells following downregulation of *Bmp7*. Cells were infected with lentiviral vectors containing GFP or sh*Bmp7* and 72 h later migration was assessed. (A) Values of invaded cells were normalized against those of GFP-infected cells set to 100%. The experiment was performed with two biological and two technical replicates. Five random fields of each membrane at 400× magnification were counted. ***p < 0.001 (B) Here representative pictures of migration assay membranes of MTT cells transfected either with lentiviral vectors containing GFP or sh*Bmp7* are shown.

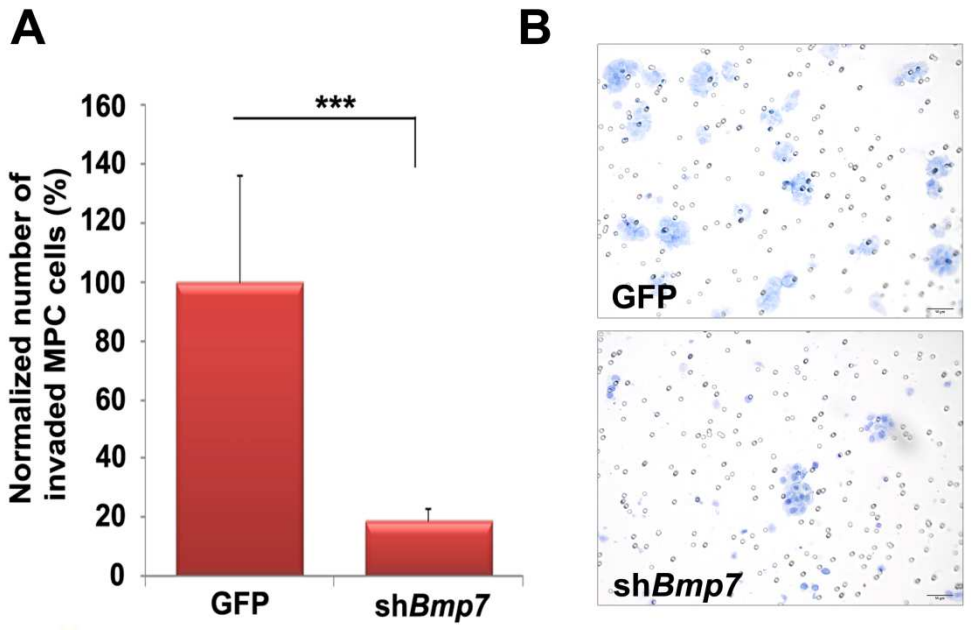

Figure 40. Invasion of MPC cells following downregulation of *Bmp7*. Cells were infected with lentiviral vectors containing GFP or sh*Bmp7* and 72 h later migration was assessed. (A) Values of invaded cells were normalized against those of GFP-infected cells set to 100%. The experiment was performed with two biological and two technical replicates (±SD). Five random fields of each membrane at 400× magnification were counted. ***p < 0.001 (B) Here representative pictures of migration assay membranes of MPC cells transfected either with lentiviral vectors containing GFP or sh*Bmp7* are shown.

3.9. BMP7 promotes cell viability of rat primary adrenomedullary cells

We then evaluated the role of Bmp7 in tumorigenesis using a model system that is physiologically closer to the intact tissue: primary cultures of pheochromocytoma cells from MENX-affected rats, which have high levels of Bmp7. We employed the lentiviral vectors previously described expressing a shRNA molecule directed against rat *Bmp7* (sh*Bmp7*). Tumor cells from three independent MENX mutant rats were dispersed in culture plates and infected with the sh*Bmp7* vectors or with the GFP control vector (Figure 41). The infection with the empty vector and the sh*Bmp7* containg vector both showed similar transfection efficiencies of about 70%.

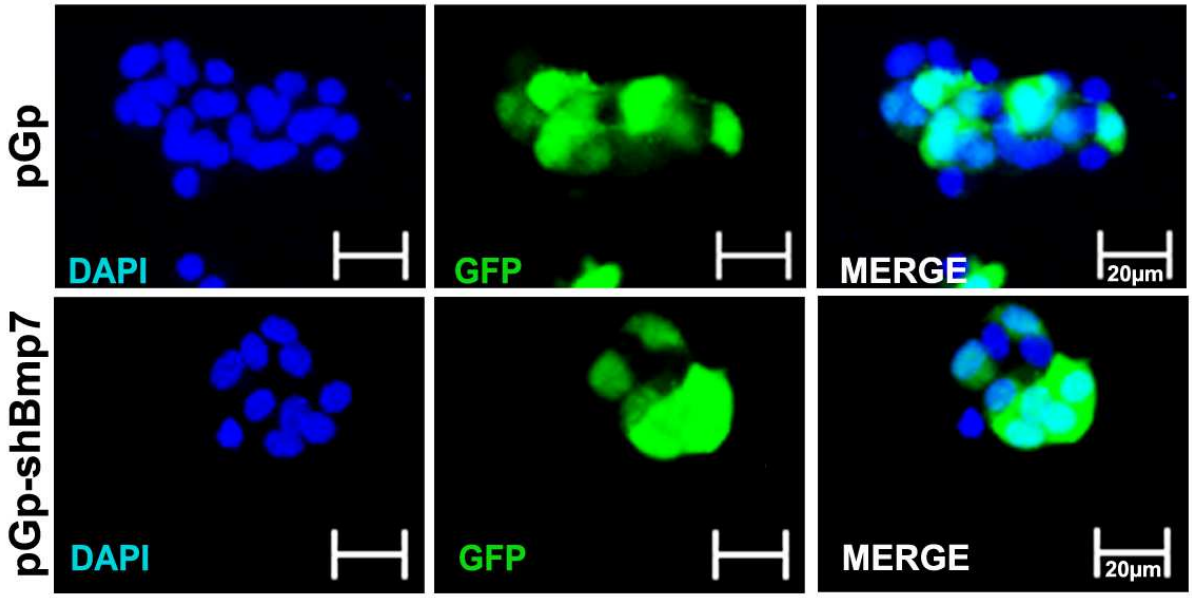

Figure 41. Lentiviral infection of rat primary pheochromocytoma cells. Rat primary tumor cells were infected with lentiviral vectors containing GFP or sh*Bmp7* and 72 h later we assed GFP expression (in green) using immunofluorescent. Nuclei were counterstained with DAPI. Pictures were taken by confocal microscopy.

Cell viability was assessed 72 h later. Concomitantly with a reduction in *Bmp7* expression (-65%) (Figure 42) we observed a decrease in primary cell viability upon infection with sh*Bmp7* (-35% to -45% versus control GFP alone). Therefore, the data suggests that autocrine Bmp7 signaling sustains the survival of rat primary adrenomedullary tumor cells. Although the data is very promising we cannot exclude that the decrease in primary cell viability seen in primary cells could be due to

cytotoxic effects of the sh*RNA*, since we did not use a scrambled sh*RNA* control vector but an empty GFP expression vector.

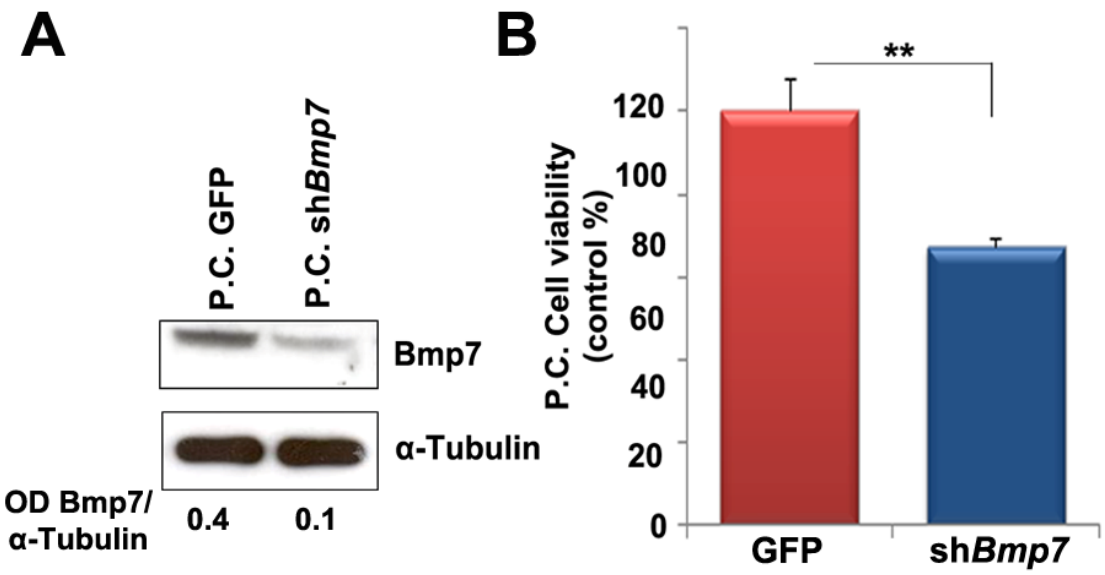

Figure 42. Effect of knockdown of *Bmp7* on viability of primary rat pheochromocytoma cells. (A) primary rat tumor cells (P.C.) were infected with lentiviral vectors containing sh*Bmp7*-GFP or GFP alone. Western blotting was performed 72 h post infection using an anti-BMP7 antibody. α-Tubulin (1:1000) was used as loading control. Numbers at the bottom of the western blot represent the quantification of band intensities of Bmp7 normalized to α-Tubulin (OD Bmp7/ α-Tubulin). (B) Cell viability was measured 72 h after infection of rat P.C. cells. Shown is the average of 3 independent cultures from 3 mutant rats. ***P* < 0.01

3.10. BMP7-directed pheochromocytoma cell migration involves integrin β1

Because BMP7 overexpression stimulates pheochromocytoma cell migration/invasion, we investigated the involved mechanisms mediating these effects. Integrin's are cell surface receptors and known to build interactions between cells and the extracellular matrix and are critical players in regulating cell motility (Hynes 2002). Therefore, we focused on integrins in order to evaluate their influence in migratory processes in pheochromocytoma cells. Among the integrin subunits, integrin β1 has been associated with the progression of several cancer types (Ju and Zhou 2013, Nistico, Di Modugno et al. 2014). As integrin β1 was expressed in all three pheochromocytoma cell lines (Figure 43), it was selected for further studies.

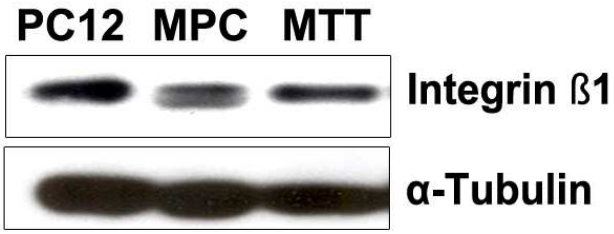

Figure 43. Western blot analysis of basal integrin β1 expression in PC12, MPC and MTT cells. Western blotting was performed on protein extracts of PC12, MPC and MTT cells using an anti-integrin β1 antibody (1:500). α-Tubulin (1:1000) was used as loading control.

If integrin β1 was indeed involved in the Bmp7-mediated increase in PC12 cell migration/invasion, we expected it to be induced by activated Bmp receptor signaling. Thus, PC12 cells were transfected with BMP7-vector or empty-vector, and integrin β1 levels were determined by western blotting. Ectopic BMP7 overexpression increased not only PC12 cell migration/invasion (Figure 30-31) but also the amount of integrin β1 (Figure 44B).

By immunofluorescence, BMP7 upregulation enhanced integrin β1 expression in transfected and nearby untransfected cells, consistent with a paracrine signaling mechanism (Figure 44A). In contrast, mock-vector transfected cells exhibited no or very faint staining for integrin β1. As shown in Figure 44A only a few cells show an overexpression of BMP7 but interestingly both transfected cells and cells located nearby BMP7-transfected cells show upregulated integrin β1 expression while cells more distantly located had lower but still detectable levels of integrin β1. This suggests a paracrine signaling mechanism is triggered by the secretion of BMP7 from the transfected cells.

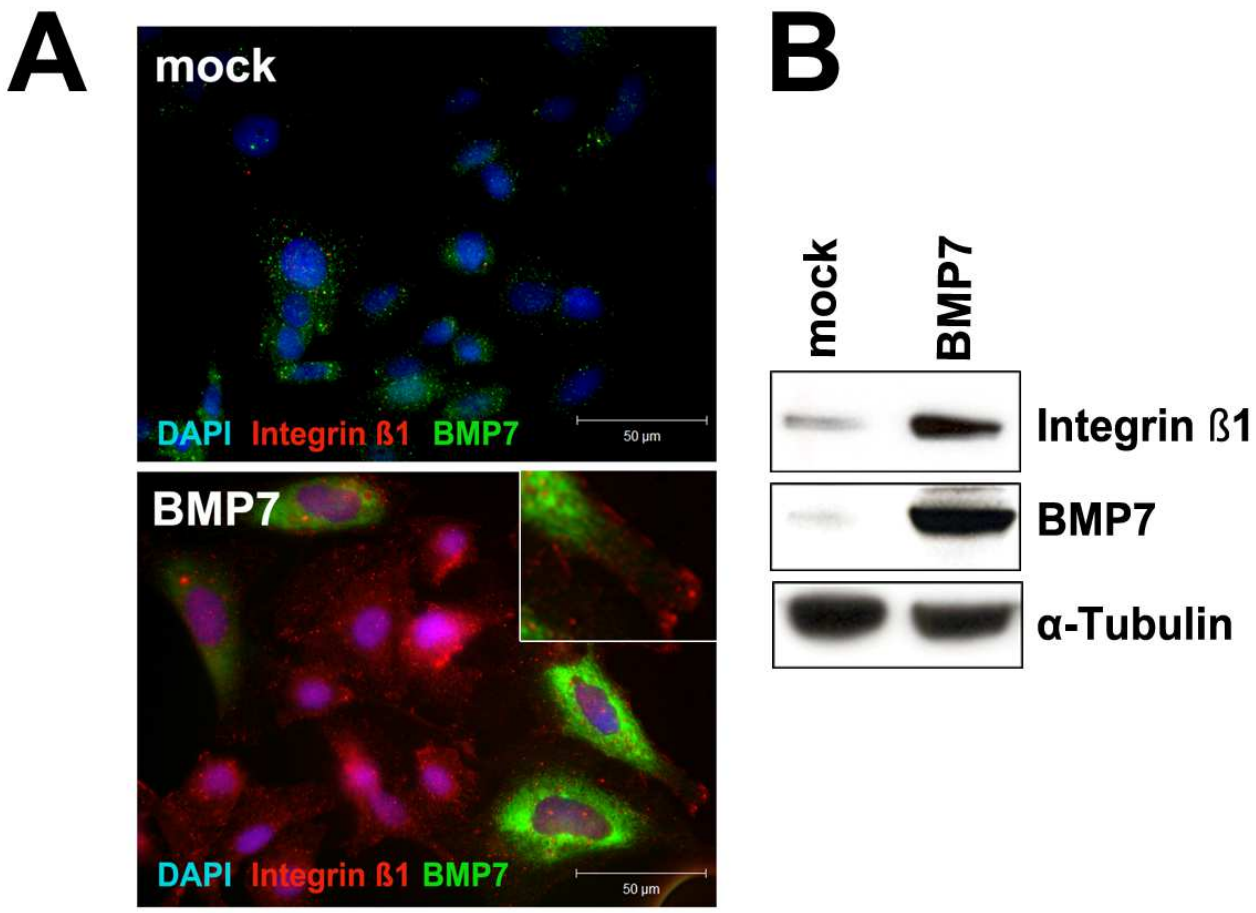

Figure 44. Integrin β1 expression increases upon overexpression of BMP7 in PC12 cells. PC12 cells were transfected with the BMP7-containing Myc-BMP7 or mock-vector. Twenty-four h post-transfection, immunofluorescence (A) or western blotting (B) using specific antibodies targeting Interinß1 (1:400; 1:500), and BMP7 (1:100; 1:500) was performed. DAPI staining was used for detection of cell nuclei by immunofluorescence. α-Tubulin (1:1000) was used as loading control in the western blot.

3.11. BMP7 activates downstream signaling pathways

In addition to the transfection experiments in PC12 cells, PC12 cells were also treated with recombinant human (rh) BMP7, which upregulates the canonical downstream pathways (i.e., P-Smad1/5/8) similar to *BMP7* overexpression (Figure 45).

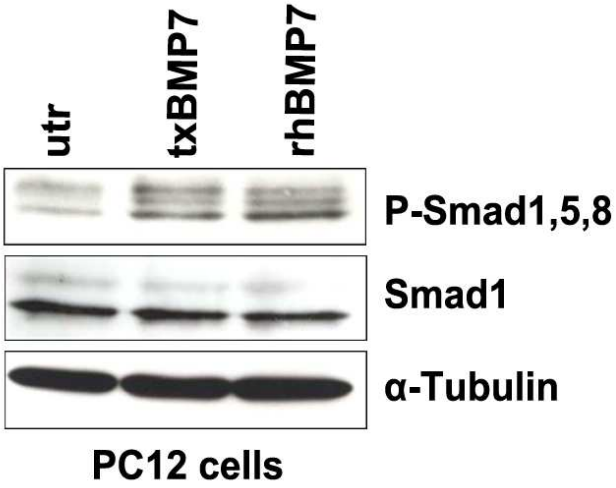

Figure 45. Canonical downstream signaling in response to BMP7. PC12 cells were treated 24 h with recombinant human BMP7 (rhBMP7) or transfected with the myc-BMP7 vector for 24 h (txBMP7) or left untreated. Western blot analysis was performed using specific antibodies raised against P-Smad1,5,8 (1:500), Smad1 (1:500) and α-Tubulin (1:1000) was used as loading control.

Following rhBMP7, integrin β1 expression was assessed at different time points. Treatment with rhBMP7 stimulated the expression of the integrin β1 protein with a very rapid kinetic of induction: it was found to be induced already 15 min later (Figure 46).

In addition, we observed that upregulation of integrin β1 following treatment of PC12 cells with rhBMP7 is accompanied by an increase in the ratio of phosphorylated (p, activated) p-AKT/AKT (Figure 46A,B). Similar results have been reported for chondrosarcoma cells following treatment with rhBMP2 (Fong, Li et al. 2008). Specifically, we observed a biphasic response of PC12 cells to rhBMP7. The P-AKT/AKT ratio increased between 5 min and 15 min post-treatment and decreased at 30 min and then increased again between 45 min and 60 min. These data suggest that integrin β1 is a downstream target of BMP7 signaling.

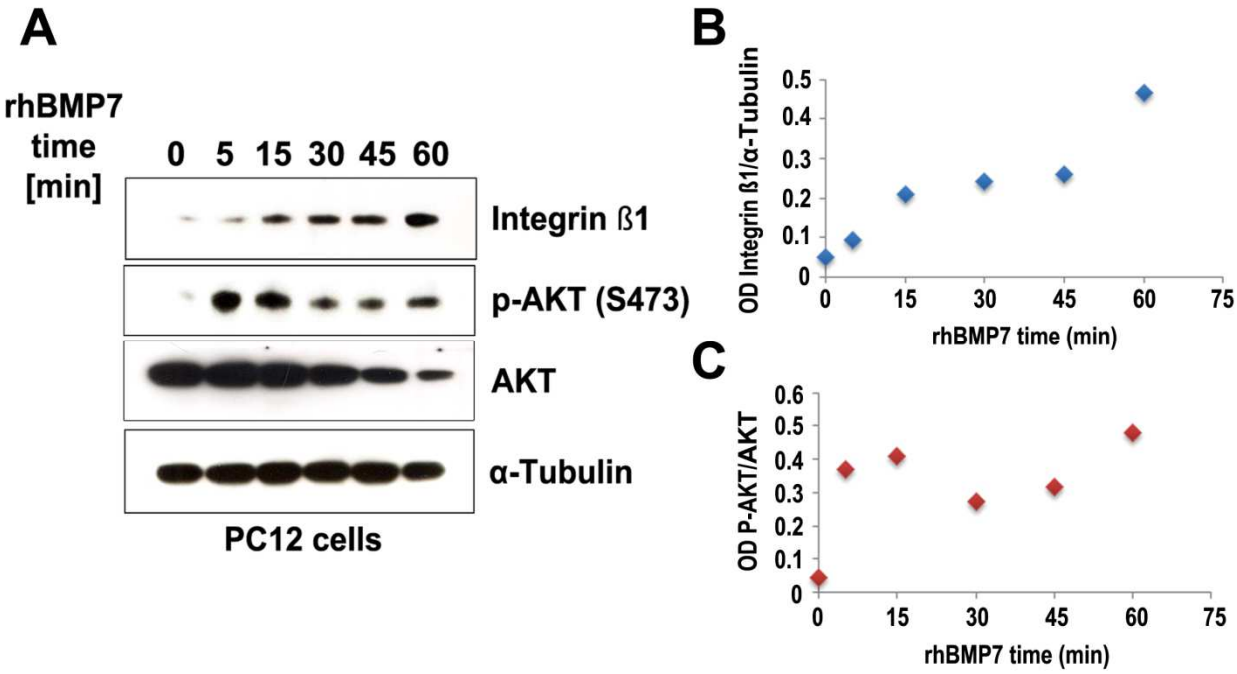

Figure 46. Downstream molecules activated by BMP7 signaling in PC12 cells. Cells were treated with recombinant human BMP7 (rhBMP7) for 5, 15, 30, 45, or 60 min.(A) Western blot analysis was performed using antibodies raised against integrin β1 (1:500), phospho-AKT (p-AKT;1:500) and AKT (1:500). α-Tubulin (1:1000) was used as loading control. Quantification of the bands of the western blotting was performed and the ration of the optical density (OD) of (B) integrin ß1 to α-Tubulin and of (C) P-AKT to AKT were calculated and shown in a histogram in a time dependent manner upon rhBMP7 treatment.

Integrin β1 is regulated by PI3K/AKT/mTOR signaling in various cancer types (Adelsman, McCarthy et al. 1999, Fong, Li et al. 2008). Therefore, we investigated whether this also occurs in pheochromocytoma. PC12 cells with active BMP7 signaling (following BMP7 transfection) were incubated with the selective AKT kinase inhibitor GSK690693 (Rhodes, Heerding et al. 2008). We observed that GSK690693 prevented the increase in integrin β1 levels in PC12 transfected cells (Figure 47), consistent with a role for AKT in modulating integrin β1 expression. In PC12 cells, as previously observed in other cancer cells, P-AKT did not decrease following GSK690693 treatment because of the blockade of a negative feedback loop downstream of AKT (Panupinthu, Yu et al. 2014).

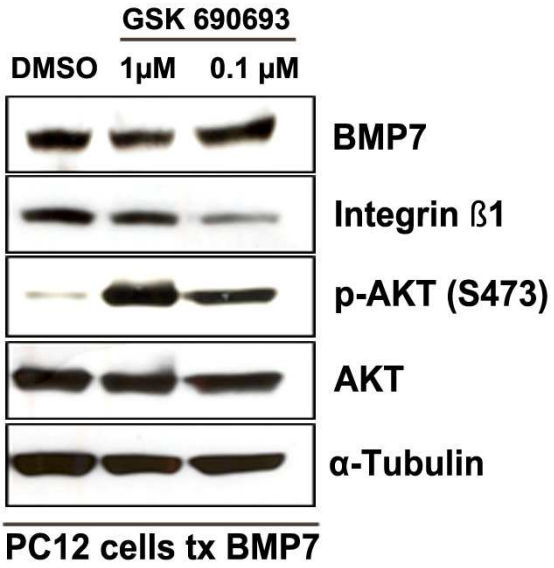

Figure 47. Western blot analysis of PC12 cells with active BMP7 signaling (following BMP7 transfection) treated with the AKT kinase inhibitor GSK690693. PC12 cells were transfected with the myc-BMP7 vector and 24 h later treated with the indicated concentrations of the AKT inhibitor GSK690693 dissolved in DMSO. Western blot analysis was conducted using specific antibodies raised against myc (BMP7; 1:500), integrin β1 (1:500), Phospho-AKT (P-AKT;1:500) and AKT (1:500). α-Tubulin was used as a loading control.

To verify whether integrin β1 mediates BMP7-dependent increase in cell migration and invasion, PC12 cells were co-transfected with Myc-BMP7 and scrambled siRNA oligos (scr-siRNA), or with Myc-BMP7 and siRNA oligos against the *Itgb1* gene (siRNA-*Itgb1*) encoding integrin β1. Efficient integrin β1 knockdown was confirmed by western blotting and the ectopic overexpression of BMP7 was verified using an anti-myc antibody (Figure 48). Phospho-AKT and AKT levels did not change upon downregulation of *Itgb1* (Figure 48).

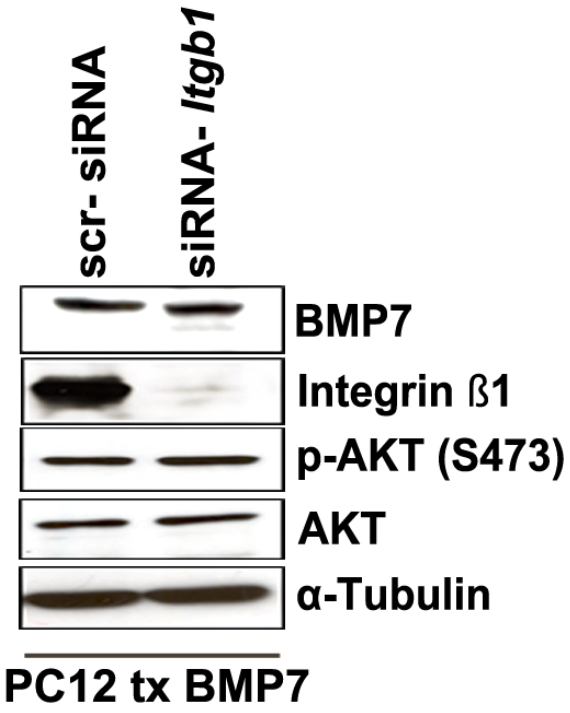

Figure 48. Western blot analysis of PC12 cells following knockdown of *Itgb1*. PC12 cells were co-transfected with BMP7 and scr-siRNA or siRNA-*Itgb1* and 24 h later western blot analysis was conducted using specific antibodies raised against myc (BMP7; 1:500), integrin β1 (1:500), Phospho-AKT (P-AKT;1:500) and AKT (1:500). α-Tubulin was used as a loading control.

Following *Itgb1* silencing, PC12 cells overexpressing BMP7 were analyzed for their migration and invasion capacity (Figure 49). We observed that both invasion (average -72%) and migration (average -46%) were significantly reduced upon downregulation of *Itgb1* (-90%), whereas scr-siRNA oligos had no effect on cell motility or invasion.

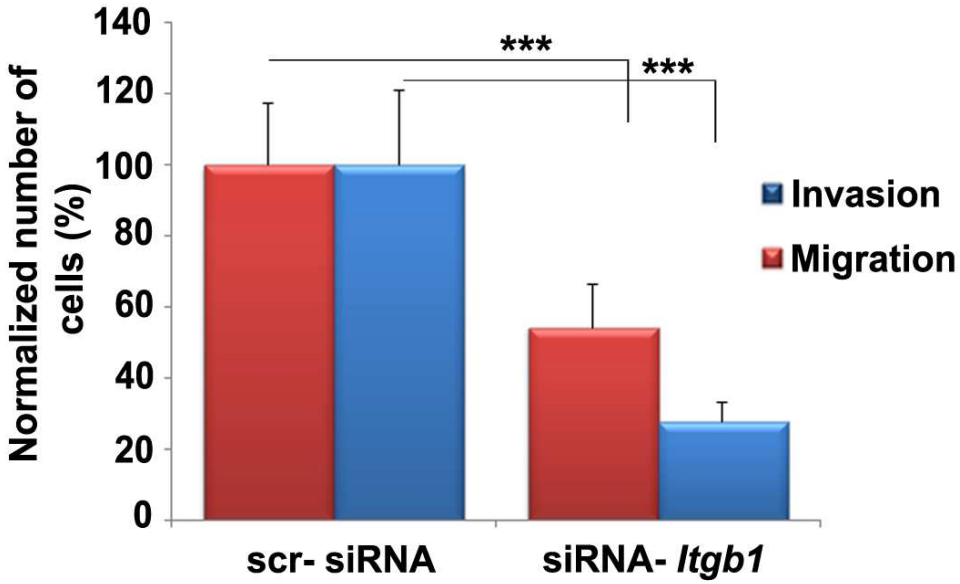

Figure 49. Invasion and migration assays following knockdown of *Itgb1* in PC12 cells. PC12 cells were co-transfected with BMP7 and scr-siRNA or siRNA-Itgb1 and 24 h later migration and invasion were assessed. Five random fields of each mambrane at 400× magnification were counted. Migration and invasion of cells with knockdown of *Itgb1* were normalized against the values of scr-siRNA-transfected cells arbitrarily set to 100%. The experiment was performed with two biological and three technical replicates (±SD). ***p<0.001.

As no data were available on integrin β1 expression in human pheochromocytomas, 10 tumors with enough frozen material and one normal tissue were analyzed by western blotting. Samples were also probed for BMP7 and P-AKT expression. The results revealed that integrin β1 is expressed in pheochromocytoma; its level tends to correlate with that of BMP7. Although there was no perfect correlation between the levels of BMP7, integrin β1 and P-AKT, 4 out of 5 tumors having high BMP7 levels were also characterized by high levels of integrin β1 and P-AKT (Figure 50). Curiously, normal adrenal medulla showed also a high P-AKT/AKT ratio. This could be explained by the fact that what we employed as control tissue was the non-tumorous area adjacent to tumor #10. Thus, this tissue may not be “normal” but may have already started to accumulate genetic alterations. Potentially, this tissue has already started to switch on tumorigenic molecular pathways and therefore does not represent an ideal control tissue.

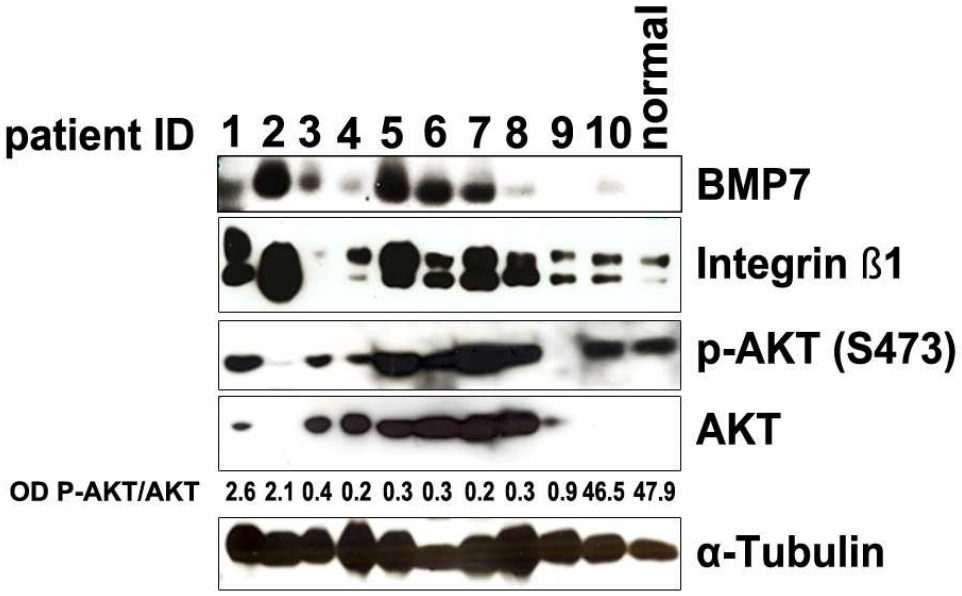

Figure 50. Western blot analysis of BMP7 and downstream molecules in human tumors. The figure shows the expression of BMP7 (1:500), integrin β1(1:500), P-AKT (1:500), AKT (1:500) and the loading control α-Tubulin (1:1000) in 10 human tumors and one human normal medulla (normal). Numbers below the AKT panel represent the ratio of the band intensities of P-AKT normalized to AKT (P-AKT/AKT) for each sample.

In conclusion, these data suggest that BMP7-promoted migration/invasion of pheochromocytoma cells may involve the activation of the PI3K/AKT pathway and ultimately of the integrin β1 receptor.

3.12. Bmp7 can be a predictor of response to treatment of pheochromocytoma cells with PI3K inhibitors

If the overexpression of *Bmp7* in rat primary tumor cells, as already postulated, leads to activation of the BMP pathway, and this is important for adrenomedullary cells survival and the ability to invade and migrate, then blockage of the pathway should affect these phenotypes.

In pheochromocytoma cells, we assume that BMP7 signals by binding to the receptors and activating downstream the PI3K/AKT/mTOR pathway, as indicated by the increase in P-AKT upon the paracrine stimulation with rhBMP7 treatment in PC12 cells (Figure 46). The PI3K/AKT/mTOR pathway has been previously suggested to be associated with the pathogenesis of adrenal tumors (Fassnacht, Weismann et al. 2005, De Martino, van Koetsveld et al. 2010). Targeting this pathway could offer a

promising new therapeutic strategy. Since pheochromocytomas have high levels of P-AKT we postulated that pheochromocytomas would respond well to PI3K inhibitors. Our group and others have shown that drugs targeting the PI3K pathway are indeed effective against both pheochromocytoma cell lines and primary rat pheochromocytoma cells (Lee, Waser et al. 2012, Nolting, Garcia et al. 2012). Whether the activation of the PI3K signaling cascade previously reported in pheochromocytomas (Fassnacht, Weismann et al. 2005) is also in part due to upregulation of BMP7 expression and to the triggering of an autocrine stimulatory pathway is currently unknown. This point is important because if this were the case, BMP7 might be considered as a predictor of the response of these tumors to a PI3K inhibitor drug.

To test this hypothesis, we took advantage of our *in vivo* model of endogenous pheochromocytoma and, in collaboration with Dr. M. Lee, we treated MENX-affected rats (n=4) for 2 weeks with the dual PI3K/mTOR inhibitor, BEZ235, or with a PEG vehicle (n=4). At the end of the treatment, we performed a detailed *ex vivo* analysis of the adrenal glands by assessing inhibition of the PI3K pathway, changes in P-S6 (a downstream target of P-Akt) and integrin β1 levels, induction of apoptosis (Annexin 5 and cleaved caspase 3) and proliferation rates (Ki67). We observed that in the rat tumors there were less proliferating cells following BEZ235 administration compared to vehicle alone (Figure 51). In parallel, a reduction of P-S6 and integrin β1, as well as an increase in apoptotic cells, could be seen in the tumors of drug-treated but not PEG-treated rats (Figure 51). These *in vivo* findings recapitulate the signaling pathway that we identified in pheochromocytoma cells *in vitro*, wherein active BMP7 signaling induces integrin β1 expression through PI3K/AKT/mTOR pathway activation. Moreover, they demonstrate that targeting the PI3K signaling cascade elicits antitumor effects in pheochromocytomas *in vivo*.

Altogether, these results suggest that the treatment of tumors having high endogenous levels of BMP7 (such as rat pheochromocytoma) with PI3K inhibitors could be a valuable approach to inhibit tumor growth and spread.

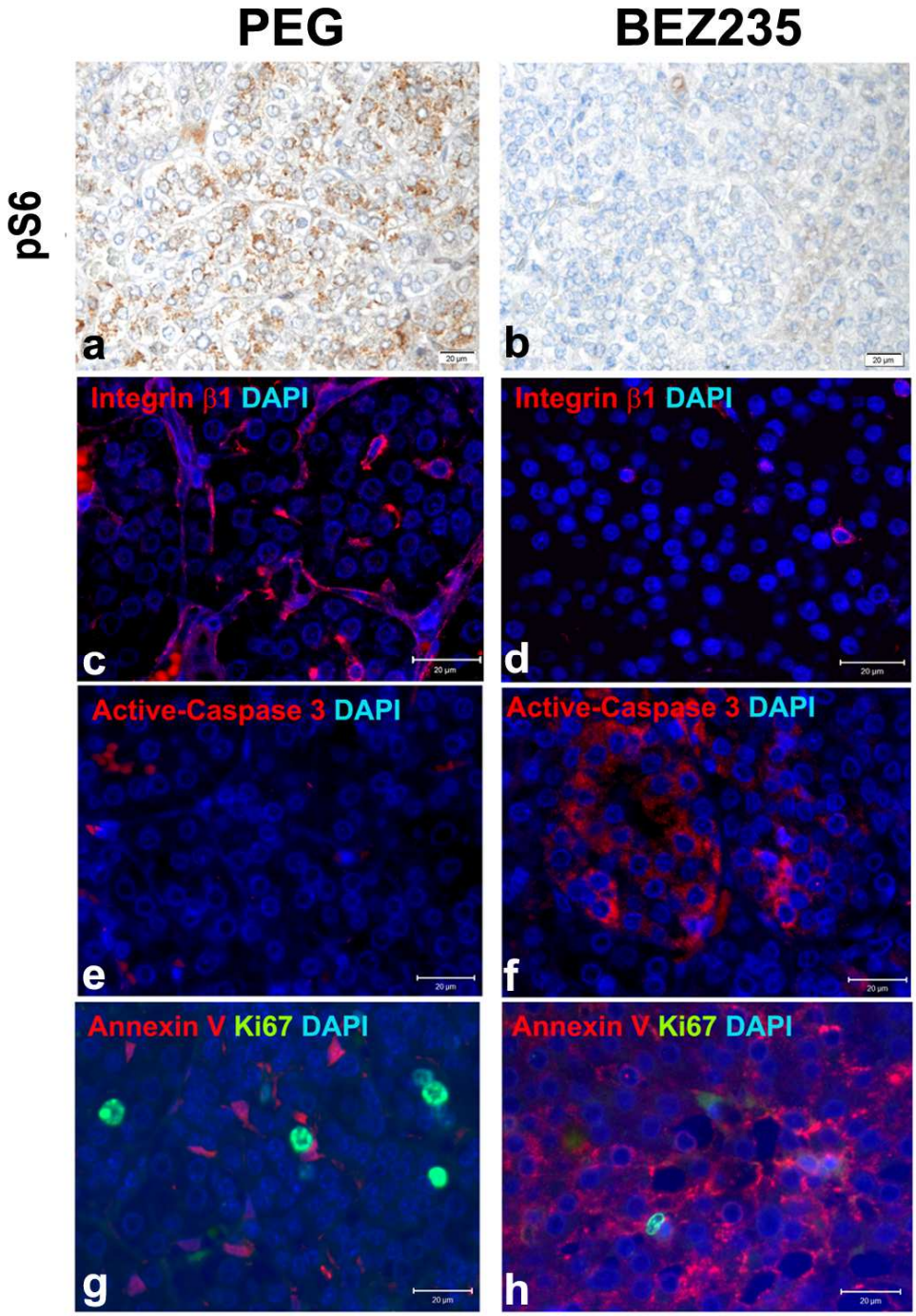

Figure 51. Immunofluorescence and IHC on pheochromocytoma of mutant rats following placebo or BEZ235 treatment. MENX-affected rats (n=4) were treated with a dual PI3K/mTOR inhibitor, BEZ235, or with PEG vehicle (n=4) by oral gavage for 2 weeks. Immunofluorescence or IHC on paraffin embedded tissues of these rats was performed using specific antibodies targeting integrin β1 (1:300), pS6 (1:100), active-caspase 3 (1:100), Ki67 (1:100) or Annexin V (1:100). DAPI staining was used for detection of cell nuclei in immmunoflourescent stainings. For IHC, haematoxylin was used as counterstaining. pS6, integrin β1 and Ki67 is reduced in BEZ235 treated rats whereas active-caspase 3 and Annexin V increase. (bar equals 20 µM).

3.13. DMH1 treatment impairs tumor progression by blocking BMP signaling in pheochromocytoma cells

Given its involvement in human cancers, the BMP pathway has been considered for therapeutic intervention, and small-molecule BMP antagonists are being evaluated in preclinical studies. Among them, DMH1, a second-generation analog of dorsomorphin, highly selectively inhibits BMP type I receptors (see introduction) and has no known off-target receptors (Hao, Ho et al. 2010, Cross, Thomason et al. 2011). DMH1 has been shown to reduce the growth of lung cancer cells in xenograft models (Hao, Lee et al. 2014) and human and mouse mammary tumor cells (Owens, Polikowsky et al. 2013), and could therefore represent a novel drug targeting Bmp7 in pheochromocytomas. To verify whether blocking BMP receptor signaling might be a potential strategy for targeted therapy of pheochromocytoma, we performed *in vitro* experiments in collaboration with A. Richter using DMH1 on MPC and primary rat pheochromocytoma cells assuming DMH1 is active against rat Bmp receptors. We treated MPC cells, which are characterized by high endogenous Bmp7 levels with DMH1 and then assessed cell proliferation. DMH1 treatment significantly suppressed MPC cell proliferation in a dose- and time-dependent manner (Figure 52). We observed that both the 3 µM and 5 µM concentrations of DMH1 significantly reduce MPC cell growth about -20% 24 h after treatment and -50% 48 h after treatment.

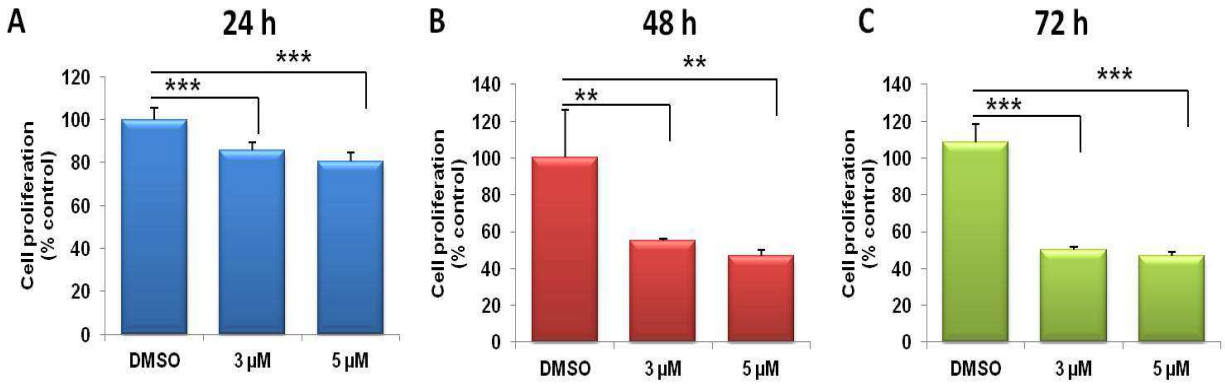

Figure 52. DMH1 reduces MPC cell proliferation. MPC cells were treated with DMH1 (3 and 5 µM) or DMSO for (A) 24, (B) 48 or (C) 72 h and cell proliferation was assessed using the WST-1 assay. The values are normalized against DMSO-treated cells set to 100%. Data were analyzed with three biological and six technical replicates each and were expressed as the mean for the 3 experiments ±SD. *p<0.05 **p<0.01 ***p<0.001

Concomitantly, we observed a dose- and time-dependent downregulation of the expression of P-Smad1/5/8, molecules of the canonical pathway of BMP7, and integrin β1 which are both readouts of active BMP signaling in pheochromocytoma cells (Figure 53). While the P-AKT/AKT ratio increased slightly upon DMH1 treatment, P-S6, a downstream effector of mTOR, was slightly downregulated attesting to a blockade of downstream PI3K effectors. The increase of P-AKT could be due to a negative feedback mechanism. Another explanation of the upregulation of P-AKT is that the signaling of other BMP family members is also blocked by DMH1 and this could have an impact on the P-AKT pathway.

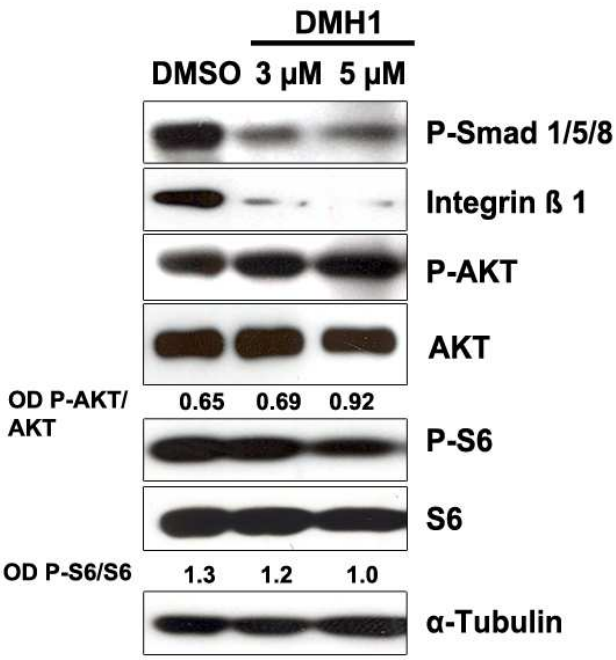

Figure 53. Western blot analysis of MPC cells treated with DMH1. MPC cells were treated with DMH1 (3 µM or 5 µM) or with DMSO vehicle for 48 h. Proteins were then collected and probed for the expression of integrin β1, P-Smad1/5/8, P-S6 (1:500) and α-Tubulin was used as a loading control. Numbers below AKT and S6 represent the quantification of band intensities of P-AKT to AKT (OD P-AKT/ AKT) and P-S6 to S6 (OD P-S6/S6) to determine the activity of the proteins.

To determine whether DMH1 may have a cytotoxic activity on pheochromocytoma cells, as reported for lung cancer (Langenfeld, Calvano et al. 2003), apoptosis was measured 24 h after treatment by assessing the activity of cleaved caspase-3/7. We observed that apoptosis was induced in a dose-dependent manner following DMH1 but not vehicle administration (Figur: 54).

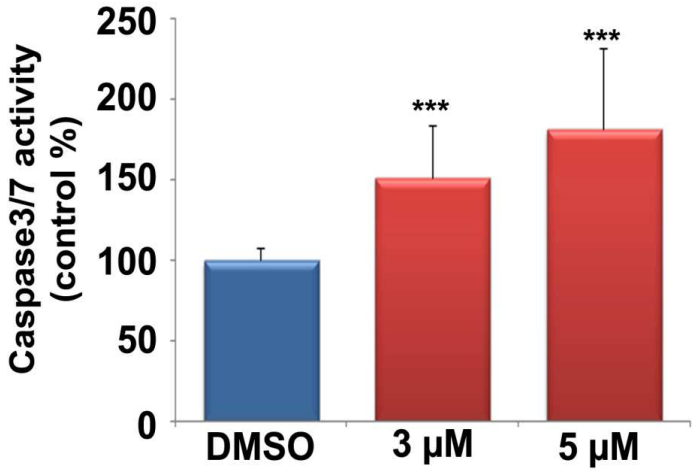

Figure 54. DHM1 induces apoptosis of MPC cells. Apoptosis was measured 24 h after treatment by assessing the activity of caspase-3/7. The experiment was performed with three biological and six technical replicates and is expressed as the mean ±SD. ***p<0.001

In order to study the effect of the drug in a “more" physiological system, we examined primary cultures of the pheochromocytomas and treated them with 3 µM or 5 µM DMH1 for 48 h or 72 h. Upon treatment with DHM1 we could notice a dose-dependent reduction of cell proliferation of up to -18% at both timepoints. Due to the variability in the response of the independent primary cultures, only the treatment with 5 µM DMH1 for 72 h showed a statistically significant reduction in cell viability (Figure 55).

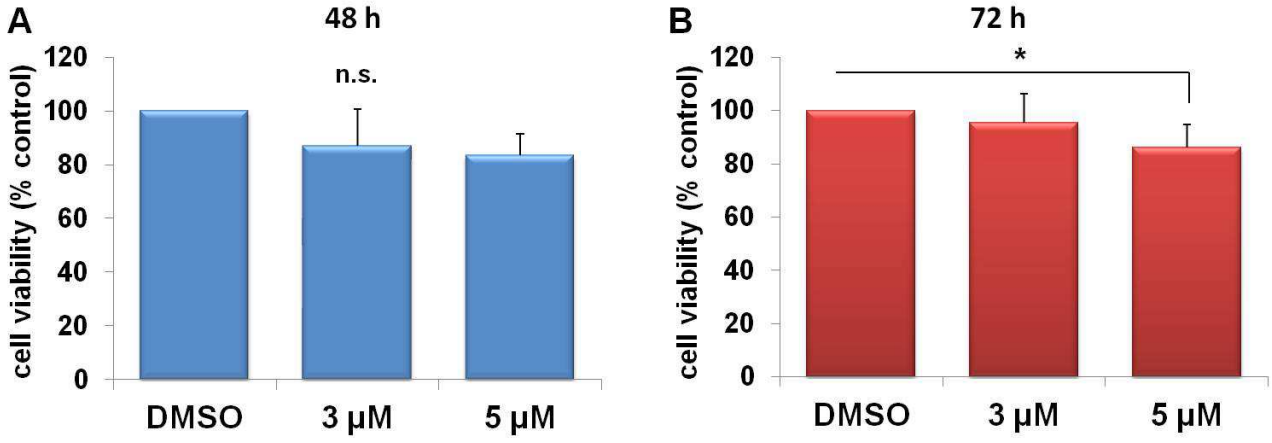

Figure 55. DMH1 reduces rat primary pheochromocytoma cell proliferation. Rat primary tumor cells were treated with DMH1 (3 and 5 µM) or DMSO for 48 or 72 h and cell viability was assessed using the WST-1 assay. Shown is the average of 3 independent cultures from 3 mutant rats. The values are normalized to the DMSO treated cells which were set to 100%. n.s. = not statistically significant; *p < 0.05

These results suggest that inhibition of BMP signaling by DMH1 significantly reduces pheochromocytoma cell proliferation and increases apoptosis *in vitro*. In conclusion, a small-molecule BMP antagonist elicits anti-proliferative and pro-apoptotic responses in pheochromocytoma cells *in vitro*.

4. DISCUSSION

4.1. The role of BMP7 in Pheochromocytoma Tumorigenesis

The medulla of the adrenal gland is responsible for the production of the hormones noradrenaline and adrenaline (Unsicker 1993). Tumors that arise from the chromaffin cells, the major cell type of the adrenal medulla, are termed pheochromocytomas (Pick 1912). Although, these tumors are usually benign, approximately 10% of all pheochromocytomas are malignant (Eisenhofer, Bornstein et al. 2004). For patients with these malignant tumors the survival rate is below 50% (Eisenhofer, Bornstein et al. 2004, Nomura, Kimura et al. 2009). Therefore, a better understanding of the molecular mechanisms regulating pheochromocytoma tumorigenesis, and especially of those processes that lead to an aggressive phenotype, would help to develop novel treatment strategies to cure the disease. Hereditary pheochromocytoma (33% of cases) has been associated with the deregulation of several different genes, but the changes in sporadic tumors have been less well elucidated at the molecular level (Favier, Amar et al. 2015) thereby hampering the identification of novel therapeutic targets for this occasionally aggressive tumor. Based on our studies, it seems that hereditary rat pheochromocytomas in the MENX rat have a genetic signature of sympathoadrenergic precursor cells; characterized by high expression of developmental genes (Pellegata, Quintanilla-Martinez et al. 2006, Molatore, Liyanarachchi et al. 2010).

Among the gene expression changes in MENX is the prominent upregulation of the *Bmp7* gene, encoding a growth factor that plays an important role during the embryonic development of the adrenal medulla by promoting the migration and differentiation of sympathoadrenal precursors. Until now, our understanding of the contribution of BMP signaling to cancer biology remains limited. So far, *BMP7* has been implicated in various human tumors such as breast cancer (Alarmo, Rauta et al. 2006), prostate cancer (Morrissey, Brown et al. 2010), gastric cancer (Aoki, Ishigami et al. 2011), malignant melanoma (Rothhammer, Poser et al. 2005), colorectal cancer (Motoyama, Tanaka et al. 2008), osteosarcoma (Sulzbacher, Birner et al. 2002) and renal cell cancer (Kwak, Park et al. 2007), where it plays either a pro- or anti-oncogenic role depending on the cell type. To date, the contribution of BMP7 signaling to pheochromocytoma pathogenesis has not been addressed. Our studies

demonstrate that activation of endogenous BMP7 signaling promotes oncogenic features in pheochromocytoma in a manner consistant with the role in early developement.

This thesis work stemmed from the observation that overexpression of the *Bmp7/BMP7* genes at the mRNA level was associated with both rat and human pheochromocytoma. We have now demonstrated here that these high gene expression levels translate to an elevated expression of the encoded proteins. This suggests direct read out of elevated Bmp7 RNA to protein.

It has been reported that serum levels of the bone morphogenetic protein 2 (BMP2), another BMP family member, are associated with migration and invasion of advanced non-small cell lung cancer (NSCLC) and therefore they may be a biomarker for assessing the progression of this tumor type. It has been speculated that serum BMP2 could also be a novel marker for assessing the response to a cisplatin-based chemotherapy in NSCLC patients (Choi, Kim et al. 2012). Therefore, we wanted to investigate whether circulating Bmp7 levels are increased due to its release by pheochromocytoma cells in MENX rats with tumors. We could demonstrate that circulating Bmp7 levels are indeed significantly elevated in peripheral blood of MENX-affected rats when compared with the wild-type rats, suggesting that serum Bmp7 could be a novel tumor marker for pheochromocytoma patients. Analysis of a small sample number of sera from pheochromocytoma patients and control individuals showed less clear results. We observed a slight trend that pheochromocytoma patients had higher BMP7 serum levels but this was not statistically significant. Nevertheless some patients had elevated levels so it is worth pursuing this in a large collective and comparing BMP7 levels to outcome. Most likely our results were due to the performance of the ELISA assay, which has not been extensively tested for diagnostic purposes, and to the heterogeneity of the serum sampling in the pheochromocytoma patients since the patients were not starved and the blood was not taken in a fixed diurnal rhythm. A greater number of patients with a diurnal und repeated blood collection would be necessary to better characterize the potential clinical relevance of circulating BMP7 in the peripheral blood of pheochromocytoma patients. Conversely we can speculate that the BMP7 produced by pheochromocytoma cells may be too highly diluted in the peripheral blood to serve as a biomarker.

Our human tissue microarray data demonstrated that the BMP7 protein is highly expressed in 72% of human tumors and that its expression correlated with tumor location (more frequently elevated in paragangliomas, extra adrenal location, than in pheochromocytomas) and most interesting, with the tumor size (higher in large pheochromocytomas). Of note, both these features have been associated with an increased risk of malignancy. Indeed, tumor size positively correlates with a higher malignancy risk for pheochromocytoma (Ayala-Ramirez, Feng et al. 2011), and an increased malignancy rate has been reported for paragangliomas compared with pheochromocytomas (Ayala-Ramirez, Feng et al. 2011). Additionally, we could see that 9 out of 11 malignant pheochromocytomas have high tissue BMP7 levels, but again due to the small number of cases this was not statistically significant. Cluster 1 tumors, carrying *VHL* and *SDHx* (*SDHA*, *SDHB*, *SDHC*, *SDHD*, *SDHAF2*), *HIF2α* or *FH* mutations, tend to show higher levels then cluster 2 tumors, which have mutations in the susceptibility genes *NF1*, *RET* (Eisenhofer, Huynh et al. 2004), *KIF1Bβ* (Yeh, Lenci et al. 2008), and *TMEM127* (Qin, Yao et al. 2010). This data is also not statistically significant. Given the high levels of endogenous BMP7 observed in human pheochromocytoma and the association of BMP7 levels with poor survival factors such as tumor size, location of the tumors and metastasis, it is tempting to speculate that BMP7 is an oncogene that triggers tumor progression of pheochromocytoma towards a more aggressive phenotype which may lead to malignancy and worse prognosis. This data is consistent with observations made for gastric cancer patients, for whom the BMP7 expression level correlates with tumour size and invasion potential of the tumors. Furthermore, the expression of BMP7 was negatively associated with postoperative outcome of gastric cancer patients (Aoki, Ishigami et al. 2011). This is an important fact since patients having high BMP7 levels should be monitored more carefully after resection of the tumors in order to detect relapse at an early stage. Personalized medicine targeting BMP7 (see below) could help to cure pheochromocytoma or other tumor patients having high BMP7 levels.

So far, most of the work focusing on BMP ligands and their receptors has been performed by administering BMPs to the cells as exogenous growth factors. This may elicit signaling pathways different from those induced by endogenous overexpression of these proteins (Haubold, Weise et al. 2010, Lim, Chuong et al. 2011, Zhang, Chen et al. 2014). Thus, in order to elucidate the functional role of the

elevated expression of BMP7 in pheochromocytoma, we manipulated its endogenous level in cell lines and primary rat tumor cells. Our assumption was that the Bmp7 produced by the pheochromocytoma cells will lead to an autocrine stimulation of the canonical and other related tumorigenic pathways. To investigate whether the above mentioned cells are suitable for signal transduction analysis, we evaluated the rat PC12, and mouse MPC and MTT cell lines and the rat primary pheochromocytoma cells for the expression of the most common BMP-receptors. It has already been shown that PC12 cells express the BMP receptors, *Alk2* and *ALK3*, *AcVr2a*, *AcVr2b* but not *Alk6*. (Goto, Otsuka et al. 2009) We demonstrated that PC12, MPC and MTT cell lines, pheochromocytoma primary cells of MENX-affected rats, as well as rat medullary tumor tissues express most of the most prominent BMP receptors *Alk2, Alk3* and *Alk6*, *BmpRII*, *AcVr2a* and *AcVr2b* although not all cells showed the same expression pattern. Thus the BMP7 secreted by the tumor cells has the potential to interact with multiple receptors located on these cells and initiate downstream signalling as it has also been reported for the bone morphogenetic protein 4 (BMP4), another BMP family member, in human dendritic cells (Martinez, Hidalgo et al. 2014). Due to the different expression pattern of BMP receptors the downstream effects of BMP signaling could vary between the cell types.

It has already been reported that rhBMP7 can initiate neuronal differentiation of PC12 cells (Di Liddo, Grandi et al. 2010). In our experimental set up, a *BMP7* expressing vector was transfected in PC12 cells and neurite formation was assessed in transfected cells and in cells located in the vicinity of the transfected cells. We observed that BMP7 transfection can increase the neuronal differentiation of the PC12 chromaffin cells, thereby defining another characteristic of endogenous BMP7 overexpression (i.e. triggering neurite growth). This is in agreement with the observation that recombinant BMP2 and BMP4 can induce neuronal differentiation of PC12 (Iwasaki, Hattori et al. 1996, Althini, Usoskin et al. 2003). In addition, these experiments demonstrate that transfected Bmp7 may be secreted and can act directly as an autocrine signal and as a paracrine signal on nearby cells.

By manipulating endogenous Bmp7 levels in pheochromocytoma cell lines such as PC12 (overexpression), MPC and MTT (knockdown) and in primary rat tumor cells (knockdown), we could demonstrate that endogenous BMP7 overexpression promotes not only the differentiation of PC12 cells, as discussed

before, but also oncogenic features in these cells. Specifically, PC12 cells expressing low endogenous levels of Bmp7 were found to migrate and invade at higher rates upon overexpression of the gene. These results resemble those of a study reporting enhanced migration and invasion of the breast cancer cell line MDA-MB-231 upon exogenous BMP7 stimulation (Alarmo, Parssinen et al. 2009). The more tumorigenic phenotype is contrary to the increased differentiation phenotype seen in PC12 cells transfected with BMP7. It has been reported that other factors such as UPAR (Farias-Eisner, Vician et al. 2000) or NGF (Zhu, Kleeff et al. 2002) are able to promote the differentiation of PC12 cells and trigger invasion properties in other cancers. We speculate that BMP7 mediated neuronal differentiation of PC12 cells could be more a morphological change while still retaining tumorigenic properties of the cells. MPC and MTT, having high endogenous expression of *Bmp7*, show decreased migration, invasion and proliferation upon gene knockdown. Although the data is very promising we cannot exclude the unlikely possibility that the decrease in migration, invasion and proliferation upon gene knockdown seen in MPC and MTT could be due to cytotoxic effects of the shRNA, since we did not use a scrambled shRNA control vector. Considering the collective data about the tumorigenic features of BMP7, the protein plays a pro-oncogenic role in pheochromocytoma cells, similarly to that reported for other human cancers. Specifically, BMP7 was reported to play an important role in controlling lung cancer cell motility and invasiveness, while it has limited effect on cell proliferation (Liu, Chen et al. 2012). In addition, BMP7 is associated with malignant melanoma (Rothhammer, Poser et al. 2005) and induces migration and invasion in breast cancer cells (Alarmo, Parssinen et al. 2009, Liu, Chen et al. 2012).

We have evaluated the role of Bmp7 in tumorigenesis in a near-physiological system using primary cultures of pheochromocytoma cells from MENX-affected rats. Upon shRNA-mediated knockdown of the elevated *Bmp7* levels we observed a reduction in the gene expression and concomitantly a decrease in primary cell viability. Therefore, autocrine Bmp7 signaling sustains the survival of rat primary adrenomedullary tumor cells. Due to their nature, primary cells are not suitable for invasion and migration assays and therefore we cannot address the effect of Bmp7 on these oncogenic features in primary pheochromocytoma cells.

Because of the specific effect of BMP7 on migration/invasion in the pheochromocytoma cell lines, we looked at the molecular mechanism that could mediate this effect. Our first candidate was the cell surface receptor for extra cellular matrix protein, integrin β1 (Hynes 1987), whose expression has been extensively associated with the invasive capacity of tumor cells (Masumoto, Arao et al. 1999, Arao, Masumoto et al. 2000, Berry, Goode et al. 2003) and which was found to be activated following treatment of chondrosarcoma cells with recombinant BMP2 (Fong, Li et al. 2008). Integrins belong to a diverse family of glycoproteins that form heterodimeric (α,β) receptor complexes for interacting with ECM molecules (Knudsen, Horwitz et al. 1985, Hynes 1987, Burke 1999, Hynes 2002). They activate kinases that phosphorylate cytoskeletal proteins (Guan 1997), mediate cell shape (Lai, Hermann et al. 2015) and migration (Huttenlocher, Ginsberg et al. 1996) or mobilize signaling proteins that control integrin adhesiveness to the ECM (Chen, Kinch et al. 1994). No data were available up to now on integrin β1 involvement in pheochromocytomas. We extended the observations made on chondrosarcoma cells with recombinant BMP2 to include not only the treatment of pheochromocytoma cells with recombinant (rh) BMP7, but also the overexpression of ectopic BMP7 in pheochromocytoma cells. Indeed, an increase in endogenous BMP7 levels in PC12 cells obtained by transfecting the cells with an myc-BMP vector or the treatment with rhBMP7 lead to higher amounts of integrin β1. Interestingly, by immunofluorescent staining we observed that cells located in the vicinity of BMP7-transfected cells also showed an increase in integrin β1 levels, suggesting again a paracrine signalling of secreted BMP7. Selective blockade of BMP signaling by DMH1, a selective inhibitor of the BMP type-1 receptors, causes a drastic reduction in integrin β1 expression in MPC cells. Of note, knockdown of *Itgb1* (integrin β1) significantly decreases BMP7-mediated (myc-BMP7 transfected) migration and invasion of PC12 cells. These findings provide experimental evidence to support the functional link between the BMP pathway and integrin β1. In conclusion, we identified integrin β1 as a downstream target of BMP-dependent signaling in pheochromocytoma and as a tumor progression driver.

Stimulation of integrin β1 expression in PC12 cells by BMP7 is accompanied by an increase in phosphorylated (=activated) serine/threonine-specific protein kinase (P-AKT) similar to that reported for chondrosarcoma cells following treatment

with recombinant BMP2 (Fong, Li et al. 2008). Noteworthy, when we analyzed human pheochromocytoma and normal adrenal medulla for the expression of integrin β1, its expression positively correlated with that of p-AKT and BMP7 although we could not see a perfect match of the proteins in the pheochromocytomas, but this could also be due the various stages of disruption of cancer related pathways in these tumors. Although the BMP canonical pathway molecules (Smads), are known to be critical for the signaling of BMP family members, recent data suggest that multiple non-Smad pathways, including PI3K/AKT, NF-κB, and RAS/ERK pathways are involved in mediating BMP signaling (Beck and Carethers 2007). It has been shown that BMP4 and BMP7 can signal through “non-canonical” (= non Smad-related) pathways involving PI3K/AKT or RAS/ERK signalling cascades in granulosa cells (Shimizu, Kayamori et al. 2012). Moreover BMP4 and BMP7 were also found to suppress granulosa cell apoptosis via PI3K and P-AKT signaling (Shimizu, Kayamori et al. 2012). Phosphorylated AKT is a central player in signal transduction activated by growth factors, and is known to contribute to many important functions such as cell growth, survival and motility (Vasko, Saji et al. 2004, Woodgett 2005). In addition, human primary pheochromocytoma cells are characterized by the hyperactivation of PI3K/AKT pathway (Fassnacht, Weismann et al. 2005, Favier, Amar et al. 2015). Here we report that over half of pheochromocytomas are characterized by high BMP7 expression and that active BMP-dependent pathways associate with P-AKT levels in pheochromocytoma cells. Thus, it is tempting to speculate that the PI3K pathway activation observed in pheochromocytomas might be, at least in part, due to BMP7 expression upregulation and the triggering of a cell autonomous stimulatory pathway. Mechanistically, we postulate that BMP7 signaling activates the PI3K/AKT/mTOR pathway, which in turn leads to the upregulation of integrin β1 (Figure 56). Indeed, inhibiting AKT or PI3K/mTOR activities with a selective AKT kinase inhibitor, GSK690693, in the context of active BMP7-mediated pathways, reduced integrin β1 expression in pheochromocytoma cells *in vitro*. Integrin β1 upregulation by the activated PI3K/AKT pathway has been also documented in other cancers, including breast (Adelsman, McCarthy et al. 1999) and prostate carcinomas (Tsaur, Makarevic et al. 2012), where it accounts for enhanced cell motility and invasion.

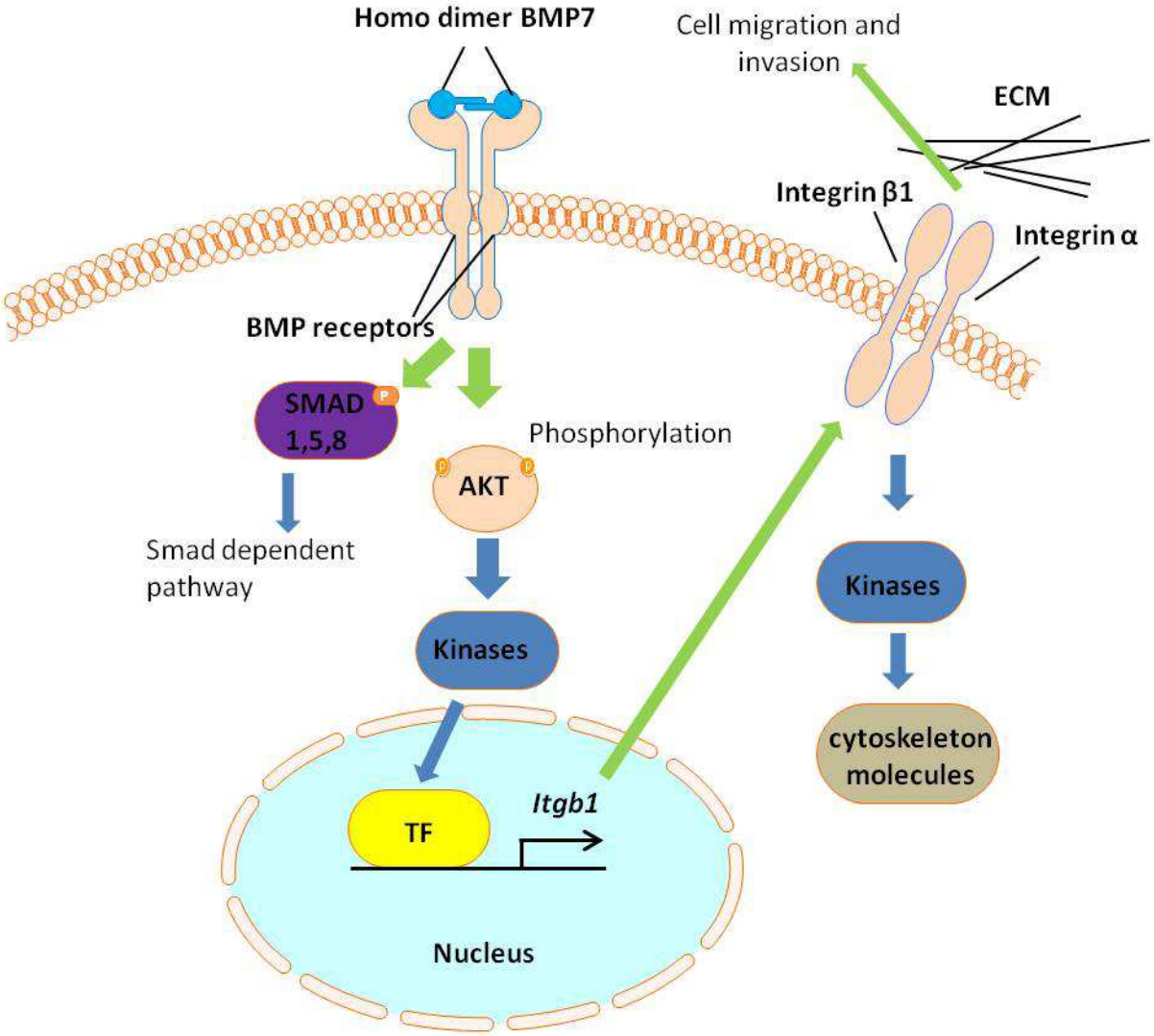

Figure 56. Schematic representation of the signaling pathways mediating BMP7-induced migration and invasion in pheochromocytoma cells. The BMP7 homodimer binds to the BMP receptors and activates them. Activated receptors mediate either Smad-dependent pathways or the phosphorylation of P-AKT in a direct or indirect fashion. AKT in turn induces the activation of unknown kinases and transcription factors (TF). These TFs initiate the transcription of *Itgb1* expression and the protein forms a heterodimeric complex with an integrin α subunit. This receptor complex regulates cytoskeletal molecules through the activation of kinases, and associates with extra cellular matrix molecules (ECM) thereby leading to increased migration and invasion of PC12 cells.

Our data uncover downstream effectors of active BMP signaling that could be the target of novel therapeutic strategies for pheochromocytomas. Since we observed that BMP7 signals through the PI3K/AKT/mTOR pathway in PC12 cells and the activation of the PI3K signaling cascade in pheochromocytomas has been demonstrated (Fassnacht, Weismann et al. 2005), we postulated that pheochromocytomas expressing high levels of BMP7 would respond well to PI3K inhibitors. Our group (Lee, Waser et al. 2012) and others (De Martino, van Koetsveld

et al. 2010, Nolting, Garcia et al. 2012) have previously shown that drugs targeting the PI3K pathway are effective against pheochromocytoma cell lines and primary rat pheochromocytoma cells. However, whether this is in part due to upregulation of BMP7 expression is not known. We exploited our MENX rat model to study the response of endogenous pheochromocytomas to a dual PI3K/mTOR inhibitor (BEZ235) that is bioavailable and in clinical trials. BEZ235 displays antitumor effects against pheochromocytoma cell lines and primary rat pheochromocytoma cells *in vitro* (Lee, Waser et al. 2012, Nolting, Garcia et al. 2012). We treated MENX-affected rats with the PI3K/mTOR inhibitor BEZ235 for two weeks and checked the effect on rat adrenal tumors *in vivo*. By *ex vivo* analysis of the adrenal glands we could show a reduction of cells stained for P-S6 (a downstream target of P-Akt) and of integrin β1 (downstream of P-AKT in pheochromocytoma cells) expression supporting our hypothesis that BMP7 activated P-AKT leads to increased levels of integrin β1 in human pheochromocytoma which could lead to increased invasion of tumor cells. We also found an increase in apoptosis in the tumors of drug-treated but not PEG-treated rats as these tissues showed more cells having cleaved capase 3/7 and annexin 5 staining. In addition proliferation was reduced in tumors of BEZ235-treated rats as the Ki67 expressing cells were reduced in the tissues of these rats. Altogether, these results suggest that the treatment of tumors having high endogenous levels of BMP7 (such as rat pheochromocytoma or human pheochromocytoma having high BMP7 levels) with PI3K inhibitors seems a valuable approach to inhibit tumor growth and spread. To date, everolimus (a rapamycin analog targeting mTOR) was evaluated in a few patients with progressive/malignant pheochromocytomas, but exhibited low efficacy (Yao, Phan et al. 2008). This lack of tumor control could be due to the activation of a feedback loop reactivating AKT signaling upstream of mTOR, a well-documented mechanism of resistance to rapamycin and its analogs in various human cancers (Hosoi, Dilling et al. 1998, Tan and Yu 2013). To escape the feedback resistance, compounds able to inhibit both mTOR and the upstream PI3K kinase were generated, including BEZ235 (Maira, Stauffer et al. 2008). Our preclinical *in vivo* trial provides the rationale for targeting the PI3K pathway in patients with progressive/inoperable pheochromocytomas using dual PI3K/mTOR inhibitors instead of single-molecule inhibitors.

While drugs inhibiting the PI3K pathway have reached the clinical trial stage or are already approved for treatment as rapalogues (everolimus; temsirolimus) (Wander, Hennessy et al. 2011), BMP antagonists are currently still in preclinical development (Hao, Lee et al. 2014), but may be available for clinical applications in future. Since the BMP pathway has been found to be important for adrenomedullary cells survival and for their ability to invade and migrate, a blockade of the pathway should affect these phenotypes. The anti-tumor effect elicited by DMH1, a second-generation inhibitor of BMP type-1 receptors (which are expressed in our cells), hold great promise for targeted therapies of adrenomedullary cells. Specifically, we could demonstrate that blocking Bmp7 signaling with DMH1 induces apoptosis and reduces cell proliferation in MPC cells and to a lesser extend in cultures of MENX rat primary pheochromocytoma cells. The difference we see in the efficiency of DMH1 treatment on the cell proliferation of MPC cells and the viability of primary cells could be due to the different expression of BMP receptors between the two cell systems. More likely is the fact that primary cells proliferate less compared with MPC cells, so that a greater effect on the proliferation of MPC cells compared with the primary cells is to be expected. Studies of other cancer types on animal models have shown that DMH1 successfully reduces the growth of lung (Hao, Lee et al. 2014) and mammary tumors *in vitro* and *in vivo* (Owens, Polikowsky et al. 2013). Therefore, these studies indicate that small molecule inhibitors of BMP receptors may offer a promising novel strategy for pheochromocytoma treatment.

4.2. Conclusion

In this study, we show that BMP7 protein is highly expressed in human pheochromocytomas and can be released into the blood as a potential biomarker. Expression correlates with the location of the tumor (extra adrenal), and with the tumor size and most likely with the malignancy of human pheochromocytomas. In these tumors, BMP7 promotes pro-oncogenic features through autocrine- and paracrine-mediated activation of PI3K/AKT/mTOR signaling cascade and of integrin β1 expression. We demonstrated that this knowledge may be exploited for therapeutic purposes, in proof-of-principle studies using BMP-receptor and P-Akt signaling blockers in *in vitro* and *in vivo* pheochromocytoma models.

In summary, our work identifies BMP7 as a novel pro-oncogenic factor in pheochromocytomas and provides leads for novel therapeutic approaches against pheochromocytomas targeting downstream effectors of BMP7-mediated signaling. These may be of greatest use in disrupting the BMP7/Integrin pathway associated with malignant progression.

5. LIST OF FIGURES

6. LIST OF TABLES

7. REFERENCES

Adelsman, M. A., J. B. McCarthy and Y. Shimizu (1999). "Stimulation of beta1-integrin function by epidermal growth factor and heregulin-beta has distinct requirements for erbB2 but a similar dependence on phosphoinositide 3-OH kinase." Mol Biol Cell **10**(9): 2861-2878.

Adelsman, M. A., J. B. McCarthy and Y. Shimizu (1999). "Stimulation of beta 1-integrin function by epidermal growth factor and heregulin-beta has distinct requirements for erbB2 but a similar dependence on phosphoinositide 3-OH kinase." Molecular Biology of the Cell **10**(9): 2861-2878.

Akiyama, S. K. (1996). "Integrins in cell adhesion and signaling." Hum Cell **9**(3): 181-186.

Alarmo, E. L., T. Korhonen, T. Kuukasjarvi, H. Huhtala, K. Holli and A. Kallioniemi (2008). "Bone morphogenetic protein 7 expression associates with bone metastasis in breast carcinomas." Annals of oncology : official journal of the European Society for Medical Oncology / ESMO **19**(2): 308-314.

Alarmo, E. L., J. Parssinen, J. M. Ketolainen, K. Savinainen, R. Karhu and A. Kallioniemi (2009). "BMP7 influences proliferation, migration, and invasion of breast cancer cells." Cancer Lett **275**(1): 35-43.

Alarmo, E. L., J. Rauta, P. Kauraniemi, R. Karhu, T. Kuukasjarvi and A. Kallioniemi (2006). "Bone morphogenetic protein 7 is widely overexpressed in primary breast cancer." Genes Chromosomes & Cancer **45**(4): 411-419.

Allen, J. A. and I. C. Roddie (1972). "The role of circulating catecholamines in sweat production in man." J Physiol **227**(3): 801-814.

Althini, S., D. Usoskin, A. Kylberg, P. ten Dijke and T. Ebendal (2003). "Bone morphogenetic protein signalling in NGF-stimulated PC12 cells." Biochemical and biophysical research communications **307**(3): 632-639.

Anastasov, N., I. Hofig, I. G. Vasconcellos, K. Rappl, H. Braselmann, N. Ludyga, G. Auer, M. Aubele and M. J. Atkinson (2012). "Radiation resistance due to high expression of miR-21 and G2/M checkpoint arrest in breast cancer cells." Radiat Oncol **7**: 206.

Annes, J. P., J. S. Munger and D. B. Rifkin (2003). "Making sense of latent TGFbeta activation." J Cell Sci **116**(Pt 2): 217-224.

Aoki, M., S. Ishigami, Y. Uenosono, T. Arigami, Y. Uchikado, Y. Kita, H. Kurahara, M. Matsumoto, S. Ueno and S. Natsugoe (2011). "Expression of BMP-7 in human gastric cancer and its clinical significance." Br J Cancer **104**(4): 714-718.

Arao, S., A. Masumoto and M. Otsuki (2000). "Beta1 integrins play an essential role in adhesion and invasion of pancreatic carcinoma cells." Pancreas **20**(2): 129-137.

Astuti, D., A. Agathanggelou, S. Honorio, A. Dallol, T. Martinsson, P. Kogner, C. Cummins, H. P. Neumann, R. Voutilainen, P. Dahia, C. Eng, E. R. Maher and F. Latif (2001). "RASSF1A promoter region CpG island hypermethylation in phaeochromocytomas and neuroblastoma tumours." Oncogene **20**(51): 7573-7577.

Astuti, D., F. Latif, A. Dallol, P. L. Dahia, F. Douglas, E. George, F. Skoldberg, E. S. Husebye, C. Eng and E. R. Maher (2001). "Gene mutations in the succinate dehydrogenase subunit SDHB cause susceptibility to familial pheochromocytoma and to familial paraganglioma." American journal of human genetics **69**(1): 49-54.

Ayala-Ramirez, M., L. Feng, M. M. Johnson, S. Ejaz, M. A. Habra, T. Rich, N. Busaidy, G. J. Cote, N. Perrier, A. Phan, S. Patel, S. Waguespack and C. Jimenez (2011). "Clinical risk factors for malignancy and overall survival in patients with pheochromocytomas and sympathetic paragangliomas: primary

tumor size and primary tumor location as prognostic indicators." J Clin Endocrinol Metab **96**(3): 717-725.

Baysal, B. E., R. E. Ferrell, J. E. Willett-Brozick, E. C. Lawrence, D. Myssiorek, A. Bosch, A. van der Mey, P. E. Taschner, W. S. Rubinstein, E. N. Myers, C. W. Richard, 3rd, C. J. Cornelisse, P. Devilee and B. Devlin (2000). "Mutations in SDHD, a mitochondrial complex II gene, in hereditary paraganglioma." Science **287**(5454): 848-851.

Beck, S. E. and J. M. Carethers (2007). "BMP suppresses PTEN expression via RAS/ERK signaling." Cancer Biol Ther **6**(8): 1313-1317.

Beck, S. E., B. H. Jung, A. Fiorino, J. Gomez, E. D. Rosario, B. L. Cabrera, S. C. Huang, J. Y. Chow and J. M. Carethers (2006). "Bone morphogenetic protein signaling and growth suppression in colon cancer." American journal of physiology. Gastrointestinal and liver physiology **291**(1): G135-145.

Bellis, S. L., J. T. Miller and C. E. Turner (1995). "Characterization of tyrosine phosphorylation of paxillin in vitro by focal adhesion kinase." J Biol Chem **270**(29): 17437-17441.

Berry, M. G., A. W. Goode, J. R. Puddefoot, G. P. Vinson and R. Carpenter (2003). "Integrin beta1-mediated invasion of human breast cancer cells: an ex vivo assay for invasiveness." Breast Cancer **10**(3): 214-219.

Besson, A., M. Gurian-West, A. Schmidt, A. Hall and J. M. Roberts (2004). "p27Kip1 modulates cell migration through the regulation of RhoA activation." Genes Dev **18**(8): 862-876.

Besson, A., H. C. Hwang, S. Cicero, S. L. Donovan, M. Gurian-West, D. Johnson, B. E. Clurman, M. A. Dyer and J. M. Roberts (2007). "Discovery of an oncogenic activity in p27Kip1 that causes stem cell expansion and a multiple tumor phenotype." Genes Dev **21**(14): 1731-1746.

Blagosklonny, M. V. (2002). "Are p27 and p21 cytoplasmic oncoproteins?" Cell Cycle **1**(6): 391-393.

Blanco Calvo, M., V. Bolos Fernandez, V. Medina Villaamil, G. Aparicio Gallego, S. Diaz Prado and E. Grande Pulido (2009). "Biology of BMP signalling and cancer." Clin Transl Oncol **11**(3): 126-137.

Blank, U., A. Brown, D. C. Adams, M. J. Karolak and L. Oxburgh (2009). "BMP7 promotes proliferation of nephron progenitor cells via a JNK-dependent mechanism." Development **136**(21): 3557-3566.

Brandi, M. L., R. F. Gagel, A. Angeli, J. P. Bilezikian, P. Beck-Peccoz, C. Bordi, B. Conte-Devolx, A. Falchetti, R. G. Gheri, A. Libroia, C. J. Lips, G. Lombardi, M. Mannelli, F. Pacini, B. A. Ponder, F. Raue, B. Skogseid, G. Tamburrano, R. V. Thakker, N. W. Thompson, P. Tomassetti, F. Tonelli, S. A. Wells, Jr. and S. J. Marx (2001). "Guidelines for diagnosis and therapy of MEN type 1 and type 2." The Journal of clinical endocrinology and metabolism **86**(12): 5658-5671.

Bravo, E. L. and R. Tagle (2003). "Pheochromocytoma: state-of-the-art and future prospects." Endocrine reviews **24**(4): 539-553.

Breuer, H. W., A. Skyschally, R. Schulz, C. Martin, M. Wehr and G. Heusch (1993). "Heart rate variability and circulating catecholamine concentrations during steady state exercise in healthy volunteers." Br Heart J **70**(2): 144-149.

Brown, M. A., Q. Zhao, K. A. Baker, C. Naik, C. Chen, L. Pukac, M. Singh, T. Tsareva, Y. Parice, A. Mahoney, V. Roschke, I. Sanyal and S. Choe (2005). "Crystal structure of BMP-9 and functional interactions with pro-region and receptors." J Biol Chem **280**(26): 25111-25118.

Buijs, J. T., N. V. Henriquez, P. G. van Overveld, G. van der Horst, P. ten Dijke and G. van der Pluijm (2007). "TGF-beta and BMP7 interactions in tumour progression and bone metastasis." Clinical & experimental metastasis **24**(8): 609-617.

Buijs, J. T., C. A. Rentsch, G. van der Horst, P. G. van Overveld, A. Wetterwald, R. Schwaninger, N. V. Henriquez, P. Ten Dijke, F. Borovecki, R. Markwalder, G. N. Thalmann, S. E. Papapoulos, R. C. Pelger, S. Vukicevic, M. G. Cecchini, C. W. Lowik and G. van der Pluijm (2007). "BMP7, a putative regulator of epithelial homeostasis in the human prostate, is a potent inhibitor of prostate cancer bone metastasis in vivo." Am J Pathol **171**(3): 1047-1057.

Burke, R. D. (1999). "Invertebrate integrins: structure, function, and evolution." Int Rev Cytol **191**: 257-284.

Burnichon, N., J. J. Briere, R. Libe, L. Vescovo, J. Riviere, F. Tissier, E. Jouanno, X. Jeunemaitre, P. Benit, A. Tzagoloff, P. Rustin, J. Bertherat, J. Favier and A. P. Gimenez-Roqueplo (2010). "SDHA is a tumor suppressor gene causing paraganglioma." Hum Mol Genet **19**(15): 3011-3020.

Burnichon, N., A. Cascon, F. Schiavi, N. P. Morales, I. Comino-Mendez, N. Abermil, L. Inglada-Perez, A. A. de Cubas, L. Amar, M. Barontini, S. B. de Quiros, J. Bertherat, Y. J. Bignon, M. J. Blok, S. Bobisse, S. Borrego, M. Castellano, P. Chanson, M. D. Chiara, E. P. Corssmit, M. Giacche, R. R. de Krijger, T. Ercolino, X. Girerd, E. B. Gomez-Garcia, A. Gomez-Grana, I. Guilhem, F. J. Hes, E. Honrado, E. Korpershoek, J. W. Lenders, R. Leton, A. R. Mensenkamp, A. Merlo, L. Mori, A. Murat, P. Pierre, P. F. Plouin, T. Prodanov, M. Quesada-Charneco, N. Qin, E. Rapizzi, V. Raymond, N. Reisch, G. Roncador, M. Ruiz-Ferrer, F. Schillo, A. P. Stegmann, C. Suarez, E. Taschin, H. J. Timmers, C. M. Tops, M. Urioste, F. Beuschlein, K. Pacak, M. Mannelli, P. L. Dahia, G. Opocher, G. Eisenhofer, A. P. Gimenez-Roqueplo and M. Robledo (2012). "MAX mutations cause hereditary and sporadic pheochromocytoma and paraganglioma." Clin Cancer Res **18**(10): 2828-2837.

Burnichon, N., L. Vescovo, L. Amar, R. Libe, A. de Reynies, A. Venisse, E. Jouanno, I. Laurendeau, B. Parfait, J. Bertherat, P. F. Plouin, X. Jeunemaitre, J. Favier and A. P. Gimenez-Roqueplo (2011). "Integrative genomic analysis reveals somatic mutations in pheochromocytoma and paraganglioma." Hum Mol Genet **20**(20): 3974-3985.

Cacciari, E., L. Mazzanti, D. Tassinari, R. Bergamaschi, C. Magnani, F. Zappulla, G. Nanni, C. Cobianchi, T. Ghini, R. Pini and et al. (1990). "Effects of sport (football) on growth: auxological, anthropometric and hormonal aspects." Eur J Appl Physiol Occup Physiol **61**(1-2): 149-158.

Carethers, J. M., S. E. Beck, B. H. Jung, A. Fiorino, J. Gomez, E. Del Rosario, B. L. Cabrera, S. C. Huang and J. Y. C. Chow (2006). "Bone morphogenetic protein signaling and growth suppression in colon cancer." American Journal of Physiology-Gastrointestinal and Liver Physiology **291**(1): G135-G145.

Carty, S. E., A. K. Helm, J. A. Amico, M. R. Clarke, T. P. Foley, C. G. Watson and J. J. Mulvihill (1998). "The variable penetrance and spectrum of manifestations of multiple endocrine neoplasia type 1." Surgery **124**(6): 1106-1113; discussion 1113-1104.

Cascon, A., S. Ruiz-Llorente, M. F. Fraga, R. Leton, D. Telleria, J. Sastre, J. J. Diez, G. Martinez Diaz-Guerra, J. A. Diaz Perez, J. Benitez, M. Esteller and M. Robledo (2004). "Genetic and epigenetic profile of sporadic pheochromocytomas." Journal of medical genetics **41**(3): e30.

Cassar, L., H. Li, A. R. Pinto, C. Nicholls, S. Bayne and J. P. Liu (2008). "Bone morphogenetic protein-7 inhibits telomerase activity, telomere maintenance, and cervical tumor growth." Cancer research **68**(22): 9157-9166.

Castro-Vega, L. J., A. Buffet, A. A. De Cubas, A. Cascon, M. Menara, E. Khalifa, L. Amar, S. Azriel, I. Bourdeau, O. Chabre, M. Curras-Freixes, V. Franco-Vidal, M. Guillaud-Bataille, C. Simian, A. Morin, R. Leton, A. Gomez-Grana, P. J. Pollard, P. Rustin, M. Robledo, J. Favier and A. P. Gimenez-Roqueplo (2014). "Germline mutations in FH confer predisposition to malignant pheochromocytomas and paragangliomas." Hum Mol Genet **23**(9): 2440-2446.

Castro-Vega, L. J., E. Letouze, N. Burnichon, A. Buffet, P. H. Disderot, E. Khalifa, C. Loriot, N. Elarouci, A. Morin, M. Menara, C. Lepoutre-Lussey, C. Badoual, M. Sibony, B. Dousset, R. Libe, F. Zinzindohoue, P. F. Plouin, J. Bertherat, L. Amar, A. de Reynies, J. Favier and A. P. Gimenez-Roqueplo (2015). "Multi-omics analysis defines core genomic alterations in pheochromocytomas and paragangliomas." Nat Commun **6**: 6044.

Celeste, A. J., J. A. Iannazzi, R. C. Taylor, R. M. Hewick, V. Rosen, E. A. Wang and J. M. Wozney (1990). "Identification of transforming growth factor beta family members present in bone-inductive protein purified from bovine bone." Proc Natl Acad Sci U S A **87**(24): 9843-9847.

Chandrasekharappa, S. C., S. C. Guru, P. Manickam, S. E. Olufemi, F. S. Collins, M. R. Emmert-Buck, L. V. Debelenko, Z. Zhuang, I. A. Lubensky, L. A. Liotta, J. S. Crabtree, Y. Wang, B. A. Roe, J. Weisemann, M. S. Boguski, S. K. Agarwal, M. B. Kester, Y. S. Kim, C. Heppner, Q. Dong, A. M. Spiegel, A. L. Burns and S. J. Marx (1997). "Positional cloning of the gene for multiple endocrine neoplasia-type 1." Science **276**(5311): 404-407.

Chen, Q., M. S. Kinch, T. H. Lin, K. Burridge and R. L. Juliano (1994). "Integrin-mediated cell adhesion activates mitogen-activated protein kinases." J Biol Chem **269**(43): 26602-26605.

Cho, K. W. and I. L. Blitz (1998). "BMPs, Smads and metalloproteases: extracellular and intracellular modes of negative regulation." Curr Opin Genet Dev **8**(4): 443-449.

Choi, Y. J., S. T. Kim, K. H. Park, S. C. Oh, J. H. Seo, S. W. Shin, J. S. Kim and Y. H. Kim (2012). "The serum bone morphogenetic protein-2 level in non-small-cell lung cancer patients." Med Oncol **29**(2): 582-588.

Clutter, W. E. and P. E. Cryer (1980). "Plasma dose-response studies with noradrenaline and adrenaline in man." Prog Biochem Pharmacol **17**: 84-89.

Cochard, P., M. Goldstein and I. B. Black (1978). "Ontogenetic appearance and disappearance of tyrosine hydroxylase and catecholamines in the rat embryo." Proc Natl Acad Sci U S A **75**(6): 2986-2990.

Collard, J. G. (2004). "Cancer: Kip moving." Nature **428**(6984): 705-708.

Comino-Mendez, I., F. J. Gracia-Aznarez, F. Schiavi, I. Landa, L. J. Leandro-Garcia, R. Leton, E. Honrado, R. Ramos-Medina, D. Caronia, G. Pita, A. Gomez-Grana, A. A. de Cubas, L. Inglada-Perez, A. Maliszewska, E. Taschin, S. Bobisse, G. Pica, P. Loli, R. Hernandez-Lavado, J. A. Diaz, M. Gomez-Morales, A. Gonzalez-Neira, G. Roncador, C. Rodriguez-Antona, J. Benitez, M. Mannelli, G. Opocher, M. Robledo and A. Cascon (2011). "Exome sequencing identifies MAX mutations as a cause of hereditary pheochromocytoma." Nat Genet **43**(7): 663-667.

Constam, D. B. and E. J. Robertson (1999). "Regulation of bone morphogenetic protein activity by pro domains and proprotein convertases." J Cell Biol **144**(1): 139-149.

Coupland, R. E. (1965). "Electron microscopic observations on the structure of the rat adrenal medulla: II. Normal innervation." J Anat **99**(Pt 2): 255-272.

Cripps, H. and D. P. Dearnaley (1972). "Vascular responses and noradrenaline overflows in the isolated blood-perfused cat spleen: some effects of cocaine, normetanephrine and -blocking agents." J Physiol **227**(3): 647-664.

Cross, E. E., R. T. Thomason, M. Martinez, C. R. Hopkins, C. C. Hong and D. M. Bader (2011). "Application of small organic molecules reveals cooperative TGFbeta and BMP regulation of mesothelial cell behaviors." ACS Chem Biol **6**(9): 952-961.

Cui, Y., F. Jean, G. Thomas and J. L. Christian (1998). "BMP-4 is proteolytically activated by furin and/or PC6 during vertebrate embryonic development." EMBO J **17**(16): 4735-4743.

Dahia, P. L. (2014). "Pheochromocytoma and paraganglioma pathogenesis: learning from genetic heterogeneity." Nat Rev Cancer **14**(2): 108-119.

Dahia, P. L., K. N. Ross, M. E. Wright, C. Y. Hayashida, S. Santagata, M. Barontini, A. L. Kung, G. Sanso, J. F. Powers, A. S. Tischler, R. Hodin, S. Heitritter, F. Moore, R. Dluhy, J. A. Sosa, I. T. Ocal, D. E. Benn, D. J. Marsh, B. G. Robinson, K. Schneider, J. Garber, S. M. Arum, M. Korbonits, A. Grossman, P. Pigny, S. P. Toledo, V. Nose, C. Li and C. D. Stiles (2005). "A HIF1alpha regulatory loop links hypoxia and mitochondrial signals in pheochromocytomas." PLoS Genet **1**(1): 72-80.

De Martino, M. C., P. M. van Koetsveld, R. Pivonello and L. J. Hofland (2010). "Role of the mTOR pathway in normal and tumoral adrenal cells." Neuroendocrinology **92 Suppl 1**: 28-34.

Di Liddo, R., C. Grandi, M. Venturini, D. Dalzoppo, A. Negro, M. T. Conconi and P. P. Parnigotto (2010). "Recombinant human TAT-OP1 to enhance NGF neurogenic potential: preliminary studies on PC12 cells." Protein engineering, design & selection : PEDS **23**(11): 889-897.

Dodic, M., E. M. Wintour, J. A. Whitworth and J. P. Coghlan (1999). "Effect of steroid hormones on blood pressure." Clin Exp Pharmacol Physiol **26**(7): 550-552.

Duffy, M. J. (1992). "The role of proteolytic enzymes in cancer invasion and metastasis." Clin Exp Metastasis **10**(3): 145-155.

Dyson, N. (1998). "The regulation of E2F by pRB-family proteins." Genes Dev **12**(15): 2245-2262.

Edstrom Elder, E., A. L. Hjelm Skog, A. Hoog and B. Hamberger (2003). "The management of benign and malignant pheochromocytoma and abdominal paraganglioma." Eur J Surg Oncol **29**(3): 278-283.

Eisenhofer, G., S. R. Bornstein, F. M. Brouwers, N. K. Cheung, P. L. Dahia, R. R. de Krijger, T. J. Giordano, L. A. Greene, D. S. Goldstein, H. Lehnert, W. M. Manger, J. M. Maris, H. P. Neumann, K. Pacak, B. L. Shulkin, D. I. Smith, A. S. Tischler and W. F. Young, Jr. (2004). "Malignant pheochromocytoma: current status and initiatives for future progress." Endocrine-related cancer **11**(3): 423-436.

Eisenhofer, G., T. T. Huynh, K. Pacak, F. M. Brouwers, M. M. Walther, W. M. Linehan, P. J. Munson, M. Mannelli, D. S. Goldstein and A. G. Elkahloun (2004). "Distinct gene expression profiles in norepinephrine- and epinephrine-producing hereditary and sporadic pheochromocytomas: activation of hypoxia-driven angiogenic pathways in von Hippel-Lindau syndrome." Endocr Relat Cancer **11**(4): 897-911.

Ernsberger, U., H. Patzke, J. P. Tissier-Seta, T. Reh, C. Goridis and H. Rohrer (1995). "The expression of tyrosine hydroxylase and the transcription factors cPhox-2 and Cash-1: evidence for distinct inductive steps in the differentiation of chick sympathetic precursor cells." Mech Dev **52**(1): 125-136.

Ernsberger, U., E. Reissmann, I. Mason and H. Rohrer (2000). "The expression of dopamine beta-hydroxylase, tyrosine hydroxylase, and Phox2 transcription factors in sympathetic neurons: evidence for common regulation during noradrenergic induction and diverging regulation later in development." Mech Dev **92**(2): 169-177.

Even, J. L., C. G. Crosby, Y. Song, M. J. McGirt and C. J. Devin (2012). "Effects of epidural steroid injections on blood glucose levels in patients with diabetes mellitus." Spine (Phila Pa 1976) **37**(1): E46-50.

Farias-Eisner, R., L. Vician, A. Silver, S. Reddy, S. A. Rabbani and H. R. Herschman (2000). "The urokinase plasminogen activator receptor (UPAR) is preferentially induced by nerve growth factor in PC12 pheochromocytoma cells and is required for NGF-driven differentiation." J Neurosci **20**(1): 230-239.

Fassnacht, M., D. Weismann, S. Ebert, P. Adam, M. Zink, F. Beuschlein, S. Hahner and B. Allolio (2005). "AKT is highly phosphorylated in pheochromocytomas but not in benign adrenocortical tumors." J Clin Endocrinol Metab **90**(7): 4366-4370.

Favier, J., L. Amar and A. P. Gimenez-Roqueplo (2015). "Paraganglioma and phaeochromocytoma: from genetics to personalized medicine." Nat Rev Endocrinol **11**(2): 101-111.

Fernandez-Calvet, L. and R. V. Garcia-Mayor (1994). "Incidence of pheochromocytoma in South Galicia, Spain." J Intern Med **236**(6): 675-677.

Fero, M. L., E. Randel, K. E. Gurley, J. M. Roberts and C. J. Kemp (1998). "The murine gene p27Kip1 is haplo-insufficient for tumour suppression." Nature **396**(6707): 177-180.

Fong, Y. C., T. M. Li, C. M. Wu, S. F. Hsu, S. T. Kao, R. J. Chen, C. C. Lin, S. C. Liu, C. L. Wu and C. H. Tang (2008). "BMP-2 increases migration of human chondrosarcoma cells via PI3K/Akt pathway." J Cell Physiol **217**(3): 846-855.

Franzen, A. and N. E. Heldin (2001). "BMP-7-induced cell cycle arrest of anaplastic thyroid carcinoma cells via p21(CIP1) and p27(KIP1)." Biochemical and biophysical research communications **285**(3): 773-781.

Fritz, A., A. Walch, K. Piotrowska, M. Rosemann, E. Schaffer, K. Weber, A. Timper, G. Wildner, J. Graw, H. Hofler and M. J. Atkinson (2002). "Recessive transmission of a multiple endocrine neoplasia syndrome in the rat." Cancer research **62**(11): 3048-3051.

Frontelo, P., J. E. Leader, N. Yoo, A. C. Potocki, M. Crawford, M. Kulik and R. J. Lechleider (2004). "Suv39h histone methyltransferases interact with Smads and cooperate in BMP-induced repression." Oncogene **23**(30): 5242-5251.

Ge, G., D. R. Hopkins, W. B. Ho and D. S. Greenspan (2005). "GDF11 forms a bone morphogenetic protein 1-activated latent complex that can modulate nerve growth factor-induced differentiation of PC12 cells." Mol Cell Biol **25**(14): 5846-5858.

Gespach, C., C. Grijelmo, C. Rodrigue, M. Svrcek, E. Bruyneel, A. Hendrix and O. de Wever (2007). "Proinvasive activity of BMP-7 through SMAD4/src-independent and ERK/Rac JNK-dependent signaling pathways in colon cancer cells." Cellular Signalling **19**(8): 1722-1732.

Gimenez-Roqueplo, A. P., P. L. Dahia and M. Robledo (2012). "An update on the genetics of paraganglioma, pheochromocytoma, and associated hereditary syndromes." Horm Metab Res **44**(5): 328-333.

Gimenez-Roqueplo, A. P., J. Favier, P. Rustin, C. Rieubland, M. Crespin, V. Nau, P. Khau Van Kien, P. Corvol, P. F. Plouin, X. Jeunemaitre and C. Network (2003). "Mutations in the SDHB gene are associated with extra-adrenal and/or malignant phaeochromocytomas." Cancer Res **63**(17): 5615-5621.

Goldstein, R. E., J. A. O'Neill, Jr., G. W. Holcomb, 3rd, W. M. Morgan, 3rd, W. W. Neblett, 3rd, J. A. Oates, N. Brown, J. Nadeau, B. Smith, D. L. Page, N. N. Abumrad and H. W. Scott, Jr. (1999). "Clinical experience over 48 years with pheochromocytoma." Ann Surg **229**(6): 755-764; discussion 764-756.

Gombos, E. A., W. H. Hulet, P. Bopp, Goldringw, D. S. Baldwin and H. Chasis (1962). "Reactivity of renal and systemic circulations to vasoconstrictor agents in normotensive and hypertensive subjects." J Clin Invest **41**: 203-217.

Goto, J., F. Otsuka, M. Yamashita, J. Suzuki, H. Otani, H. Takahashi, T. Miyoshi, Y. Mimura, T. Ogura and H. Makino (2009). "Enhancement of aldosterone-induced catecholamine production by bone morphogenetic protein-4 through activating Rho and SAPK/JNK pathway in adrenomedullar cells." Am J Physiol Endocrinol Metab **296**(4): E904-916.

Guan, J. L. (1997). "Role of focal adhesion kinase in integrin signaling." Int J Biochem Cell Biol **29**(8-9): 1085-1096.

Hansford, J. R. and L. M. Mulligan (2000). "Multiple endocrine neoplasia type 2 and RET: from neoplasia to neurogenesis." J Med Genet **37**(11): 817-827.

Hao, H. X., O. Khalimonchuk, M. Schraders, N. Dephoure, J. P. Bayley, H. Kunst, P. Devilee, C. W. Cremers, J. D. Schiffman, B. G. Bentz, S. P. Gygi, D. R. Winge, H. Kremer and J. Rutter (2009). "SDH5, a gene required for flavination of succinate dehydrogenase, is mutated in paraganglioma." Science **325**(5944): 1139-1142.

Hao, J., J. N. Ho, J. A. Lewis, K. A. Karim, R. N. Daniels, P. R. Gentry, C. R. Hopkins, C. W. Lindsley and C. C. Hong (2010). "In vivo structure-activity relationship study of dorsomorphin analogues identifies selective VEGF and BMP inhibitors." ACS Chem Biol **5**(2): 245-253.

Hao, J., R. Lee, A. Chang, J. Fan, C. Labib, C. Parsa, R. Orlando, B. Andresen and Y. Huang (2014). "DMH1, a small molecule inhibitor of BMP type i receptors, suppresses growth and invasion of lung cancer." PLoS One **9**(6): e90748.

Hata, A., J. Seoane, G. Lagna, E. Montalvo, A. Hemmati-Brivanlou and J. Massague (2000). "OAZ uses distinct DNA- and protein-binding zinc fingers in separate BMP-Smad and Olf signaling pathways." Cell **100**(2): 229-240.

Haubold, M., A. Weise, H. Stephan and N. Dunker (2010). "Bone morphogenetic protein 4 (BMP4) signaling in retinoblastoma cells." Int J Biol Sci **6**(7): 700-715.

Haynie, D. T. (2014). "Molecular physiology of the tensin brotherhood of integrin adaptor proteins." Proteins **82**(7): 1113-1127.

He, X. C., J. Zhang, W. G. Tong, O. Tawfik, J. Ross, D. H. Scoville, Q. Tian, X. Zeng, X. He, L. M. Wiedemann, Y. Mishina and L. Li (2004). "BMP signaling inhibits intestinal stem cell self-renewal through suppression of Wnt-beta-catenin signaling." Nat Genet **36**(10): 1117-1121.

Heldin, C. H., K. Miyazono and P. ten Dijke (1997). "TGF-beta signalling from cell membrane to nucleus through SMAD proteins." Nature **390**(6659): 465-471.

Hood, J. D. and D. A. Cheresh (2002). "Role of integrins in cell invasion and migration." Nat Rev Cancer **2**(2): 91-100.

Hosoi, H., M. B. Dilling, L. N. Liu, M. K. Danks, T. Shikata, A. Sekulic, R. T. Abraham, J. C. Lawrence, Jr. and P. J. Houghton (1998). "Studies on the mechanism of resistance to rapamycin in human cancer cells." Mol Pharmacol **54**(5): 815-824.

Howe, J. R., S. Roth, J. C. Ringold, R. W. Summers, H. J. Jarvinen, P. Sistonen, I. P. Tomlinson, R. S. Houlston, S. Bevan, F. A. Mitros, E. M. Stone and L. A. Aaltonen (1998). "Mutations in the SMAD4/DPC4 gene in juvenile polyposis." Science **280**(5366): 1086-1088.

Hsu, M. Y., S. Rovinsky, S. Penmatcha, M. Herlyn and D. Muirhead (2005). "Bone morphogenetic proteins in melanoma: angel or devil?" Cancer Metastasis Rev **24**(2): 251-263.

Huber, K. (2006). "The sympathoadrenal cell lineage: specification, diversification, and new perspectives." Dev Biol **298**(2): 335-343.

Huber, K., A. Franke, B. Bruhl, S. Krispin, U. Ernsberger, A. Schober, O. von Bohlen und Halbach, H. Rohrer, C. Kalcheim and K. Unsicker (2008). "Persistent expression of BMP-4 in embryonic chick adrenal cortical cells and its role in chromaffin cell development." Neural Dev **3**: 28.

Huber, K., A. Franke, B. Bruhl, S. Krispin, U. Ernsberger, A. Schober, O. von Bohlen und Halbach, H. Rohrer, C. Kalcheim and K. Unsicker (2008). "Persistent expression of BMP-4 in embryonic chick adrenal cortical cells and its role in chromaffin cell development." Neural development **3**: 28.

Huttenlocher, A., M. H. Ginsberg and A. F. Horwitz (1996). "Modulation of cell migration by integrin-mediated cytoskeletal linkages and ligand-binding affinity." J Cell Biol **134**(6): 1551-1562.

Hynes, R. O. (1987). "Integrins: a family of cell surface receptors." Cell **48**(4): 549-554.

Hynes, R. O. (2002). "Integrins: bidirectional, allosteric signaling machines." Cell **110**(6): 673-687.

Hynes, R. O., E. E. Marcantonio, M. A. Stepp, L. A. Urry and G. H. Yee (1989). "Integrin heterodimer and receptor complexity in avian and mammalian cells." J Cell Biol **109**(1): 409-420.

Ille, F., S. Atanasoski, S. Falk, L. M. Ittner, D. Marki, S. Buchmann-Moller, H. Wurdak, U. Suter, M. M. Taketo and L. Sommer (2007). "Wnt/BMP signal integration regulates the balance between proliferation and differentiation of neuroepithelial cells in the dorsal spinal cord." Dev Biol **304**(1): 394-408.

Iwasaki, S., A. Hattori, M. Sato, M. Tsujimoto and M. Kohno (1996). "Characterization of the bone morphogenetic protein-2 as a neurotrophic factor - Induction of neuronal differentiation of PC12 cells in the absence of mitogen-activated protein kinase activation." Journal of Biological Chemistry **271**(29): 17360-17365.

Johnsen, I. K. and F. Beuschlein (2010). "Role of bone morphogenetic proteins in adrenal physiology and disease." Journal of molecular endocrinology **44**(4): 203-211.

Ju, L. and C. Zhou (2013). "Association of integrin beta1 and c-MET in mediating EGFR TKI gefitinib resistance in non-small cell lung cancer." Cancer Cell Int **13**(1): 15.

Kallioniemi, A., E. L. Alarmo, J. Rauta, P. Kauraniemi, R. Karhu and T. Kuukasjarvi (2006). "Bone morphogenetic protein 7 is widely overexpressed in primary breast cancer." Genes Chromosomes & Cancer **45**(4): 411-419.

Kano, Y., F. Otsuka, M. Takeda, J. Suzuki, K. Inagaki, T. Miyoshi, M. Miyamoto, H. Otani, T. Ogura and H. Makino (2005). "Regulatory roles of bone morphogenetic proteins and glucocorticoids in catecholamine production by rat pheochromocytoma cells." Endocrinology **146**(12): 5332-5340.

Kantorovich, V. and K. Pacak (2010). "Pheochromocytoma and paraganglioma." Progress in brain research **182**: 343-373.

Karagiannis, A., D. P. Mikhailidis, V. G. Athyros and F. Harsoulis (2007). "Pheochromocytoma: an update on genetics and management." Endocrine-related cancer **14**(4): 935-956.

Keely, P. J., J. K. Westwick, I. P. Whitehead, C. J. Der and L. V. Parise (1997). "Cdc42 and Rac1 induce integrin-mediated cell motility and invasiveness through PI(3)K." Nature **390**(6660): 632-636.

Khwaja, A., P. Rodriguez-Viciana, S. Wennstrom, P. H. Warne and J. Downward (1997). "Matrix adhesion and Ras transformation both activate a phosphoinositide 3-OH kinase and protein kinase B/Akt cellular survival pathway." EMBO J **16**(10): 2783-2793.

Kimura, N., R. Matsuo, H. Shibuya, K. Nakashima and T. Taga (2000). "BMP2-induced apoptosis is mediated by activation of the TAK1-p38 kinase pathway that is negatively regulated by Smad6." J Biol Chem **275**(23): 17647-17652.

Kirshner, N. and M. Goodall (1957). "The formation of adrenaline from noradrenaline." Biochim Biophys Acta **24**(3): 658-659.

Knudsen, K. A., A. F. Horwitz and C. A. Buck (1985). "A monoclonal antibody identifies a glycoprotein complex involved in cell-substratum adhesion." Exp Cell Res **157**(1): 218-226.

Koch, C. A. (2005). "Molecular pathogenesis of MEN2-associated tumors." Familial cancer **4**(1): 3-7.

Korpershoek, E., F. H. Van Nederveen, H. Dannenberg, B. J. Petri, P. Komminoth, A. Perren, J. W. Lenders, A. A. Verhofstad, W. W. De Herder, R. R. De Krijger and W. N. Dinjens (2006). "Genetic analyses of apparently sporadic pheochromocytomas: the Rotterdam experience." Ann N Y Acad Sci **1073**: 138-148.

Kreuz, L. E., R. M. Rose and J. R. Jennings (1972). "Suppression of plasma testosterone levels and psychological stress. A longitudinal study of young men in Officer Candidate School." Arch Gen Psychiatry **26**(5): 479-482.

Kwak, C., Y. H. Park, I. Y. Kim, K. C. Moon and J. H. Ku (2007). "Expression of bone morphogenetic proteins, the subfamily of the transforming growth factor-beta superfamily, in renal cell carcinoma." J Urol **178**(3 Pt 1): 1062-1067.

Lagna, G., A. Hata, A. Hemmati-Brivanlou and J. Massague (1996). "Partnership between DPC4 and SMAD proteins in TGF-beta signalling pathways." Nature **383**(6603): 832-836.

Lai, M., C. D. Hermann, A. Cheng, R. Olivares-Navarrete, R. A. Gittens, M. M. Bird, M. Walker, Y. Cai, K. Cai, K. H. Sandhage, Z. Schwartz and B. D. Boyan (2015). "Role of alpha2beta1 integrins in mediating cell shape on microtextured titanium surfaces." J Biomed Mater Res A **103**(2): 564-573.

Laiho, M., M. B. Weis and J. Massague (1990). "Concomitant loss of transforming growth factor (TGF)-beta receptor types I and II in TGF-beta-resistant cell mutants implicates both receptor types in signal transduction." J Biol Chem **265**(30): 18518-18524.

Lane, K. B., R. D. Machado, M. W. Pauciulo, J. R. Thomson, J. A. Phillips, J. E. Loyd, W. C. Nichols, R. C. Trembath and I. P. Consortium (2000). "Heterozygous germline mutations in BMPR2, encoding a TGF-beta receptor, cause familial primary pulmonary hypertension." Nature Genetics **26**(1): 81-84.

Langenfeld, E. M., S. E. Calvano, F. Abou-Nukta, S. F. Lowry, P. Amenta and J. Langenfeld (2003). "The mature bone morphogenetic protein-2 is aberrantly expressed in non-small cell lung carcinomas and stimulates tumor growth of A549 cells." Carcinogenesis **24**(9): 1445-1454.

Lee, M., I. Marinoni, M. Irmler, T. Psaras, J. B. Honegger, R. Beschorner, N. Anastasov, J. Beckers, M. Theodoropoulou, F. Roncaroli and N. S. Pellegata (2013). "Transcriptome analysis of MENX-associated rat pituitary adenomas identifies novel molecular mechanisms involved in the pathogenesis of human pituitary gonadotroph adenomas." Acta Neuropathol **126**(1): 137-150.

Lee, M. and N. S. Pellegata (2013). "Multiple endocrine neoplasia syndromes associated with mutation of p27." J Endocrinol Invest **36**(9): 781-787.

Lee, M., B. Waser, J. C. Reubi and N. S. Pellegata (2012). "Secretin receptor promotes the proliferation of endocrine tumor cells via the PI3K/AKT pathway." Mol Endocrinol **26**(8): 1394-1405.

Lehnert, H. (1998). "Regulation of catecholamine synthesizing enzyme gene expression in human pheochromocytoma." Eur J Endocrinol **138**(4): 363-367.

Lim, M., C. M. Chuong and P. Roy-Burman (2011). "PI3K, Erk signaling in BMP7-induced epithelial-mesenchymal transition (EMT) of PC-3 prostate cancer cells in 2- and 3-dimensional cultures." Horm Cancer **2**(5): 298-309.

Liu, A. and L. A. Niswander (2005). "Bone morphogenetic protein signalling and vertebrate nervous system development." Nat Rev Neurosci **6**(12): 945-954.

Liu, F., F. Ventura, J. Doody and J. Massague (1995). "Human type II receptor for bone morphogenic proteins (BMPs): extension of the two-kinase receptor model to the BMPs." Mol Cell Biol **15**(7): 3479-3486.

Liu, Y., J. Chen, Y. Yang, L. Zhang and W. G. Jiang (2012). "Muolecular impact of bone morphogenetic protein 7, on lung cancer cells and its clinical significance." Int J Mol Med **29**(6): 1016-1024.

Lopez-Jimenez, E., G. Gomez-Lopez, L. J. Leandro-Garcia, I. Munoz, F. Schiavi, C. Montero-Conde, A. A. de Cubas, R. Ramires, I. Landa, S. Leskela, A. Maliszewska, L. Inglada-Perez, L. de la Vega, C. Rodriguez-Antona, R. Leton, C. Bernal, J. M. de Campos, C. Diez-Tascon, M. F. Fraga, C. Boullosa, D. G. Pisano, G. Opocher, M. Robledo and A. Cascon (2010). "Research resource: Transcriptional profiling reveals different pseudohypoxic signatures in SDHB and VHL-related pheochromocytomas." Mol Endocrinol **24**(12): 2382-2391.

Machens, A., M. Brauckhoff, H. J. Holzhausen, P. N. Thanh, H. Lehnert and H. Dralle (2005). "Codon-specific development of pheochromocytoma in multiple endocrine neoplasia type 2." J Clin Endocrinol Metab **90**(7): 3999-4003.

Maira, S. M., F. Stauffer, J. Brueggen, P. Furet, C. Schnell, C. Fritsch, S. Brachmann, P. Chene, A. De Pover, K. Schoemaker, D. Fabbro, D. Gabriel, M. Simonen, L. Murphy, P. Finan, W. Sellers and C. Garcia-Echeverria (2008). "Identification and characterization of NVP-BEZ235, a new orally available dual phosphatidylinositol 3-kinase/mammalian target of rapamycin inhibitor with potent in vivo antitumor activity." Mol Cancer Ther **7**(7): 1851-1863.

Manger, W. M. (2006). "Diagnosis and management of pheochromocytoma - recent advances and current concepts." Kidney International **70**: S30-S35.

Marinoni, I. and N. S. Pellegata (2011). "p27kip1: a new multiple endocrine neoplasia gene?" Neuroendocrinology **93**(1): 19-28.

Martinez, V. G., L. Hidalgo, J. Valencia, C. Hernandez-Lopez, A. Entrena, B. G. del Amo, A. G. Zapata, A. Vicente, R. Sacedon and A. Varas (2014). "Autocrine activation of canonical BMP signaling regulates PD-L1 and PD-L2 expression in human dendritic cells." Eur J Immunol **44**(4): 1031-1038.

Marumo, T., K. Hishikawa, M. Yoshikawa and T. Fujita (2008). "Epigenetic regulation of BMP7 in the regenerative response to ischemia." J Am Soc Nephrol **19**(7): 1311-1320.

Massague, J. (1992). "Receptors for the TGF-beta family." Cell **69**(7): 1067-1070.

Masumoto, A., S. Arao and M. Otsuki (1999). "Role of beta1 integrins in adhesion and invasion of hepatocellular carcinoma cells." Hepatology **29**(1): 68-74.

Mierke, C. T., B. Frey, M. Fellner, M. Herrmann and B. Fabry (2011). "Integrin alpha5beta1 facilitates cancer cell invasion through enhanced contractile forces." J Cell Sci **124**(Pt 3): 369-383.

Mise, N., M. Drosten, T. Racek, A. Tannapfel and B. M. Putzer (2006). "Evaluation of potential mechanisms underlying genotype-phenotype correlations in multiple endocrine neoplasia type 2." Oncogene **25**(50): 6637-6647.

Missan, D. S., S. V. Chittur and C. M. DiPersio (2014). "Regulation of fibulin-2 gene expression by integrin alpha3beta1 contributes to the invasive phenotype of transformed keratinocytes." J Invest Dermatol **134**(9): 2418-2427.

Mitu, G. and R. Hirschberg (2008). "Bone morphogenetic protein-7 (BMP7) in chronic kidney disease." Frontiers in bioscience : a journal and virtual library **13**: 4726-4739.

Molatore, S., E. Kiermaier, C. B. Jung, M. Lee, E. Pulz, H. Hofler, M. J. Atkinson and N. S. Pellegata (2010). "Characterization of a naturally-occurring p27 mutation predisposing to multiple endocrine tumors." Mol Cancer **9**: 116.

Molatore, S., S. Liyanarachchi, M. Irmler, A. Perren, M. Mannelli, T. Ercolino, F. Beuschlein, B. Jarzab, J. Wloch, J. Ziaja, S. Zoubaa, F. Neff, J. Beckers, H. Hofler, M. J. Atkinson and N. S. Pellegata (2010). "Pheochromocytoma in rats with multiple endocrine neoplasia (MENX) shares gene expression patterns with human pheochromocytoma." Proceedings of the National Academy of Sciences of the United States of America **107**(43): 18493-18498.

Montero, J. A., B. Kilian, J. Chan, P. E. Bayliss and C. P. Heisenberg (2003). "Phosphoinositide 3-kinase is required for process outgrowth and cell polarization of gastrulating mesendodermal cells." Curr Biol **13**(15): 1279-1289.

Moriguchi, T., N. Kuroyanagi, K. Yamaguchi, Y. Gotoh, K. Irie, T. Kano, K. Shirakabe, Y. Muro, H. Shibuya, K. Matsumoto, E. Nishida and M. Hagiwara (1996). "A novel kinase cascade mediated by mitogen-activated protein kinase kinase 6 and MKK3." J Biol Chem **271**(23): 13675-13679.

Morrissey, C., L. G. Brown, T. E. Pitts, R. L. Vessella and E. Corey (2010). "Bone morphogenetic protein 7 is expressed in prostate cancer metastases and its effects on prostate tumor cells depend on cell phenotype and the tumor microenvironment." Neoplasia **12**(2): 192-205.

Motoyama, K., F. Tanaka, Y. Kosaka, K. Mimori, H. Uetake, H. Inoue, K. Sugihara and M. Mori (2008). "Clinical significance of BMP7 in human colorectal cancer." Ann Surg Oncol **15**(5): 1530-1537.

Mulligan, L. M., J. B. Kwok, C. S. Healey, M. J. Elsdon, C. Eng, E. Gardner, D. R. Love, S. E. Mole, J. K. Moore, L. Papi and et al. (1993). "Germ-line mutations of the RET proto-oncogene in multiple endocrine neoplasia type 2A." Nature **363**(6428): 458-460.

Muscarella, P., M. Bloomston, A. R. Brewer, A. Mahajan, W. L. Frankel, E. C. Ellison, W. B. Farrar, C. M. Weghorst and J. Li (2008). "Expression of the p16INK4A/Cdkn2a gene is prevalently downregulated in human pheochromocytoma tumor specimens." Gene Expr **14**(4): 207-216.

Na, Y. R., S. H. Seok, D. J. Kim, J. H. Han, T. H. Kim, H. Jung, B. H. Lee and J. H. Park (2009). "Bone morphogenetic protein 7 induces mesenchymal-to-epithelial transition in melanoma cells, leading to inhibition of metastasis." Cancer science **100**(11): 2218-2225.

Neganova, I. and M. Lako (2008). "G1 to S phase cell cycle transition in somatic and embryonic stem cells." J Anat **213**(1): 30-44.

Neumann, H. P., B. Bausch, S. R. McWhinney, B. U. Bender, O. Gimm, G. Franke, J. Schipper, J. Klisch, C. Altehoefer, K. Zerres, A. Januszewicz, C. Eng, W. M. Smith, R. Munk, T. Manz, S. Glaesker, T. W. Apel, M. Treier, M. Reineke, M. K. Walz, C. Hoang-Vu, M. Brauckhoff, A. Klein-Franke, P. Klose, H. Schmidt, M. Maier-Woelfle, M. Peczkowska, C. Szmigielski, C. Eng and G. Freiburg-Warsaw-Columbus Pheochromocytoma Study (2002). "Germ-line mutations in nonsyndromic pheochromocytoma." N Engl J Med **346**(19): 1459-1466.

Niemann, S. and U. Muller (2000). "Mutations in SDHC cause autosomal dominant paraganglioma, type 3." Nat Genet **26**(3): 268-270.

Nistico, P., F. Di Modugno, S. Spada and M. J. Bissell (2014). "beta1 and beta4 integrins: from breast development to clinical practice." Breast Cancer Res **16**(5): 459.

Nohe, A., S. Hassel, M. Ehrlich, F. Neubauer, W. Sebald, Y. I. Henis and P. Knaus (2002). "The mode of bone morphogenetic protein (BMP) receptor oligomerization determines different BMP-2 signaling pathways." J Biol Chem **277**(7): 5330-5338.

Nolting, S., E. Garcia, G. Alusi, A. Giubellino, K. Pacak, M. Korbonits and A. B. Grossman (2012). "Combined blockade of signalling pathways shows marked anti-tumour potential in phaeochromocytoma cell lines." J Mol Endocrinol **49**(2): 79-96.

Nomura, K., H. Kimura, S. Shimizu, H. Kodama, T. Okamoto, T. Obara and K. Takano (2009). "Survival of Patients with Metastatic Malignant Pheochromocytoma and Efficacy of Combined Cyclophosphamide, Vincristine, and Dacarbazine Chemotherapy." Journal of Clinical Endocrinology & Metabolism **94**(8): 2850-2856.

Nussey, S. and S. Whitehead (2001). Endocrinology: An Integrated Approach. Oxford.

Owens, P., H. Polikowsky, M. W. Pickup, A. E. Gorska, B. Jovanovic, A. K. Shaw, S. V. Novitskiy, C. C. Hong and H. L. Moses (2013). "Bone Morphogenetic Proteins stimulate mammary fibroblasts to promote mammary carcinoma cell invasion." PLoS One **8**(6): e67533.

Oxburgh, L. (2009). "Control of the bone morphogenetic protein 7 gene in developmental and adult life." Current genomics **10**(4): 223-230.

Pajni-Underwood, S., C. P. Wilson, C. Elder, Y. Mishina and M. Lewandoski (2007). "BMP signals control limb bud interdigital programmed cell death by regulating FGF signaling." Development **134**(12): 2359-2368.

Park, J., C. Song, M. Park, S. Yoo, S. J. Park, S. Hong, B. Hong, C. S. Kim and H. Ahn (2011). "Predictive characteristics of malignant pheochromocytoma." Korean J Urol **52**(4): 241-246.

Pellegata, N. S., L. Quintanilla-Martinez, G. Keller, S. Liyanarachchi, H. Hofler, M. J. Atkinson and F. Fend (2007). "Human pheochromocytomas show reduced p27Kip1 expression that is not associated with somatic gene mutations and rarely with deletions." Virchows Arch **451**(1): 37-46.

Pellegata, N. S., L. Quintanilla-Martinez, H. Siggelkow, E. Samson, K. Bink, H. Hofler, F. Fend, J. Graw and M. J. Atkinson (2006). "Germ-line mutations in p27Kip1 cause a multiple endocrine neoplasia syndrome in rats and humans." Proceedings of the National Academy of Sciences of the United States of America **103**(42): 15558-15563.

Perlman, R. L. and M. Chalfie (1977). "Catecholamine release from the adrenal medulla." Clin Endocrinol Metab **6**(3): 551-576.

Perron, J. C. and J. Dodd (2009). "ActRIIA and BMPRII Type II BMP receptor subunits selectively required for Smad4-independent BMP7-evoked chemotaxis." PLoS One **4**(12): e8198.

Philipp-Staheli, J., S. R. Payne and C. J. Kemp (2001). "p27(Kip1): regulation and function of a haploinsufficient tumor suppressor and its misregulation in cancer." Exp Cell Res **264**(1): 148-168.

Postigo, A. A. (2003). "Opposing functions of ZEB proteins in the regulation of the TGFbeta/BMP signaling pathway." EMBO J **22**(10): 2443-2452.

Pouponnot, C., L. Jayaraman and J. Massague (1998). "Physical and functional interaction of SMADs and p300/CBP." J Biol Chem **273**(36): 22865-22868.

Qian, Y., X. Zhong, D. C. Flynn, J. Z. Zheng, M. Qiao, C. Wu, S. Dedhar, X. Shi and B. H. Jiang (2005). "ILK mediates actin filament rearrangements and cell migration and invasion through PI3K/Akt/Rac1 signaling." Oncogene **24**(19): 3154-3165.

Qin, Y., L. Yao, E. E. King, K. Buddavarapu, R. E. Lenci, E. S. Chocron, J. D. Lechleiter, M. Sass, N. Aronin, F. Schiavi, F. Boaretto, G. Opocher, R. A. Toledo, S. P. Toledo, C. Stiles, R. C. Aguiar and P. L. Dahia (2010). "Germline mutations in TMEM127 confer susceptibility to pheochromocytoma." Nat Genet **42**(3): 229-233.

Ramel, M. C. and C. S. Hill (2013). "The ventral to dorsal BMP activity gradient in the early zebrafish embryo is determined by graded expression of BMP ligands." Dev Biol **378**(2): 170-182.

Reddi, A. H. and N. S. Cunningham (1993). "Initiation and promotion of bone differentiation by bone morphogenetic proteins." J Bone Miner Res **8 Suppl 2**: S499-502.

Rhodes, N., D. A. Heerding, D. R. Duckett, D. J. Eberwein, V. B. Knick, T. J. Lansing, R. T. McConnell, T. M. Gilmer, S. Y. Zhang, K. Robell, J. A. Kahana, R. S. Geske, E. V. Kleymenova, A. E. Choudhry, Z. Lai, J. D. Leber, E. A. Minthorn, S. L. Strum, E. R. Wood, P. S. Huang, R. A. Copeland and R. Kumar (2008). "Characterization of an Akt kinase inhibitor with potent pharmacodynamic and antitumor activity." Cancer Res **68**(7): 2366-2374.

Roca-Cusachs, P., A. del Rio, E. Puklin-Faucher, N. C. Gauthier, N. Biais and M. P. Sheetz (2013). "Integrin-dependent force transmission to the extracellular matrix by alpha-actinin triggers adhesion maturation." Proc Natl Acad Sci U S A **110**(15): E1361-1370.

Rosenzweig, B. L., T. Imamura, T. Okadome, G. N. Cox, H. Yamashita, P. ten Dijke, C. H. Heldin and K. Miyazono (1995). "Cloning and characterization of a human type II receptor for bone morphogenetic proteins." Proc Natl Acad Sci U S A **92**(17): 7632-7636.

Rothhammer, T., I. Poser, F. Soncin, F. Bataille, M. Moser and A. K. Bosserhoff (2005). "Bone morphogenic proteins are overexpressed in malignant melanoma and promote cell invasion and migration." Cancer Res **65**(2): 448-456.

Rothhammer, T., I. Poser, F. Soncin, F. Bataille, M. Moser and A. K. Bosserhoff (2005). "Bone morphogenic proteins are overexpressed in malignant melanoma and promote cell invasion and migration." Cancer research **65**(2): 448-456.

Sakai, H., M. Furihata, C. Matsuda, M. Takahashi, H. Miyazaki, T. Konakahara, T. Imamura and T. Okada (2012). "Augmented autocrine bone morphogenic protein (BMP) 7 signaling increases the metastatic potential of mouse breast cancer cells." Clin Exp Metastasis **29**(4): 327-338.

Sastry, S. K. and K. Burridge (2000). "Focal adhesions: a nexus for intracellular signaling and cytoskeletal dynamics." Exp Cell Res **261**(1): 25-36.

Schneider, C., H. Wicht, J. Enderich, M. Wegner and H. Rohrer (1999). "Bone morphogenetic proteins are required in vivo for the generation of sympathetic neurons." Neuron **24**(4): 861-870.

Shaw, A., J. Gipp and W. Bushman (2010). "Exploration of Shh and BMP paracrine signaling in a prostate cancer xenograft." Differentiation **79**(1): 41-47.

Shaw, L. M., I. Rabinovitz, H. H. Wang, A. Toker and A. M. Mercurio (1997). "Activation of phosphoinositide 3-OH kinase by the alpha6beta4 integrin promotes carcinoma invasion." Cell **91**(7): 949-960.

Sheaff, R. J., M. Groudine, M. Gordon, J. M. Roberts and B. E. Clurman (1997). "Cyclin E-CDK2 is a regulator of p27Kip1." Genes Dev **11**(11): 1464-1478.

Sherr, C. J. and J. M. Roberts (1999). "CDK inhibitors: positive and negative regulators of G1-phase progression." Genes Dev **13**(12): 1501-1512.

Sherwin, R. S. and L. Sacca (1984). "Effect of epinephrine on glucose metabolism in humans: contribution of the liver." Am J Physiol **247**(2 Pt 1): E157-165.

Shimizu, T., T. Kayamori, C. Murayama and A. Miyamoto (2012). "Bone morphogenetic protein (BMP)-4 and BMP-7 suppress granulosa cell apoptosis via different pathways: BMP-4 via PI3K/PDK-1/Akt and BMP-7 via PI3K/PDK-1/PKC." Biochem Biophys Res Commun **417**(2): 869-873.

Slingerland, J. and M. Pagano (2000). "Regulation of the cdk inhibitor p27 and its deregulation in cancer." J Cell Physiol **183**(1): 10-17.

Solloway, M. J. and E. J. Robertson (1999). "Early embryonic lethality in Bmp5;Bmp7 double mutant mice suggests functional redundancy within the 60A subgroup." Development **126**(8): 1753-1768.

Spector, S., A. Sjoerdsma and S. Udenfriend (1965). "Blockade of Endogenous Norepinephrine Synthesis by Alpha-Methyl-Tyrosine, an Inhibitor of Tyrosine Hydroxylase." J Pharmacol Exp Ther **147**: 86-95.

Stamenkovic, I. (2000). "Matrix metalloproteinases in tumor invasion and metastasis." Semin Cancer Biol **10**(6): 415-433.

Stupack, D. G. and D. A. Cheresh (2002). "Get a ligand, get a life: integrins, signaling and cell survival." J Cell Sci **115**(Pt 19): 3729-3738.

Sulzbacher, I., P. Birner, K. Trieb, S. Lang and A. Chott (2002). "Expression of osteopontin and vascular endothelial growth factor in benign and malignant bone tumors." Virchows Arch **441**(4): 345-349.

Tan, J. and Q. Yu (2013). "Molecular mechanisms of tumor resistance to PI3K-mTOR-targeted therapy." Chin J Cancer **32**(7): 376-379.

Tang, L. and X. Han (2013). "The urokinase plasminogen activator system in breast cancer invasion and metastasis." Biomed Pharmacother **67**(2): 179-182.

Thompson, L. (2006). "World Health Organization classification of tumours: pathology and genetics of head and neck tumours." Ear Nose Throat J **85**(2): 74.

Thosani, S., M. Ayala-Ramirez, L. Palmer, M. I. Hu, T. Rich, R. F. Gagel, G. Cote, S. G. Waguespack, M. A. Habra and C. Jimenez (2013). "The characterization of pheochromocytoma and its impact on overall survival in multiple endocrine neoplasia type 2." J Clin Endocrinol Metab **98**(11): E1813-1819.

Tsaur, I., J. Makarevic, E. Juengel, M. Gasser, A. M. Waaga-Gasser, M. Kurosch, M. Reiter, S. Wedel, G. Bartsch, A. Haferkamp, C. Wiesner and R. A. Blaheta (2012). "Resistance to the mTOR-inhibitor RAD001 elevates integrin alpha2- and beta1-triggered motility, migration and invasion of prostate cancer cells." Br J Cancer **107**(5): 847-855.

Tsiridis, E., E. F. Morgan, J. M. Bancroft, M. Song, M. Kain, L. Gerstenfeld, T. A. Einhorn, M. L. Bouxsein and P. Tornetta, 3rd (2007). "Effects of OP-1 and PTH in a new experimental model for the study of metaphyseal bone healing." J Orthop Res **25**(9): 1193-1203.

Unsicker, K. (1993). "The chromaffin cell: paradigm in cell, developmental and growth factor biology." Journal of anatomy **183 (Pt 2)**: 207-221.

Vainio, S., I. Karavanova, A. Jowett and I. Thesleff (1993). "Identification of BMP-4 as a signal mediating secondary induction between epithelial and mesenchymal tissues during early tooth development." Cell **75**(1): 45-58.

van der Flier, A. and A. Sonnenberg (2001). "Function and interactions of integrins." Cell Tissue Res **305**(3): 285-298.

van Duinen, N., D. Steenvoorden, I. P. Kema, J. C. Jansen, A. H. Vriends, J. P. Bayley, J. W. Smit, J. A. Romijn and E. P. Corssmit (2010). "Increased urinary excretion of 3-methoxytyramine in patients with head and neck paragangliomas." J Clin Endocrinol Metab **95**(1): 209-214.

van Wijk, B., A. F. Moorman and M. J. van den Hoff (2007). "Role of bone morphogenetic proteins in cardiac differentiation." Cardiovasc Res **74**(2): 244-255.

Vasko, V., M. Saji, E. Hardy, M. Kruhlak, A. Larin, V. Savchenko, M. Miyakawa, O. Isozaki, H. Murakami, T. Tsushima, K. D. Burman, C. De Micco and M. D. Ringel (2004). "Akt activation and localisation correlate with tumour invasion and oncogene expression in thyroid cancer." J Med Genet **41**(3): 161-170.

Vicha, A., Z. Musil and K. Pacak (2013). "Genetics of pheochromocytoma and paraganglioma syndromes: new advances and future treatment options." Curr Opin Endocrinol Diabetes Obes **20**(3): 186-191.

von Bubnoff, A. and K. W. Cho (2001). "Intracellular BMP signaling regulation in vertebrates: pathway or network?" Developmental biology **239**(1): 1-14.

Wallace, M. R., D. A. Marchuk, L. B. Andersen, R. Letcher, H. M. Odeh, A. M. Saulino, J. W. Fountain, A. Brereton, J. Nicholson, A. L. Mitchell and et al. (1990). "Type 1 neurofibromatosis gene: identification of a large transcript disrupted in three NF1 patients." Science **249**(4965): 181-186.

Wander, S. A., B. T. Hennessy and J. M. Slingerland (2011). "Next-generation mTOR inhibitors in clinical oncology: how pathway complexity informs therapeutic strategy." J Clin Invest **121**(4): 1231-1241.

Woodgett, J. R. (2005). "Recent advances in the protein kinase B signaling pathway." Curr Opin Cell Biol **17**(2): 150-157.

Wozney, J. M., V. Rosen, A. J. Celeste, L. M. Mitsock, M. J. Whitters, R. W. Kriz, R. M. Hewick and E. A. Wang (1988). "Novel regulators of bone formation: molecular clones and activities." Science **242**(4885): 1528-1534.

Xu, H., Y. Qi, S. Dun, Y. Gao and X. Qiu (2010). "[BMP7 signaling via BMPR1A, BMPR1B inhibits the proliferation of lung large carcinoma NCI-H460 cell]." Zhongguo Fei Ai Za Zhi **13**(7): 659-664.

Xue, G. and B. A. Hemmings (2013). "PKB/Akt-dependent regulation of cell motility." J Natl Cancer Inst **105**(6): 393-404.

Yan, W. and X. Chen (2007). "Targeted repression of bone morphogenetic protein 7, a novel target of the p53 family, triggers proliferative defect in p53-deficient breast cancer cells." Cancer research **67**(19): 9117-9124.

Yang, S., M. Lim, L. K. Pham, S. E. Kendall, A. H. Reddi, D. C. Altieri and P. Roy-Burman (2006). "Bone morphogenetic protein 7 protects prostate cancer cells from stress-induced apoptosis via both Smad and c-Jun NH2-terminal kinase pathways." Cancer research **66**(8): 4285-4290.

Yao, J. C., A. T. Phan, D. Z. Chang, R. A. Wolff, K. Hess, S. Gupta, C. Jacobs, J. E. Mares, A. N. Landgraf, A. Rashid and F. Meric-Bernstam (2008). "Efficacy of RAD001 (everolimus) and octreotide LAR in advanced low- to intermediate-grade neuroendocrine tumors: results of a phase II study." J Clin Oncol **26**(26): 4311-4318.

Yeh, I. T., R. E. Lenci, Y. Qin, K. Buddavarapu, A. H. Ligon, E. Leteurtre, C. Do Cao, C. Cardot-Bauters, P. Pigny and P. L. Dahia (2008). "A germline mutation of the KIF1B beta gene on 1p36 in a family with neural and nonneural tumors." Hum Genet **124**(3): 279-285.

Yuan, S., Q. Pan, C. J. Fu and Z. Bi (2013). "Effect of growth factors (BMP-4/7 & bFGF) on proliferation & osteogenic differentiation of bone marrow stromal cells." Indian J Med Res **138**: 104-110.

Zarnegar, R., L. Brunaud and O. H. Clark (2002). "Multiple endocrine neoplasia type I." Curr Treat Options Oncol **3**(4): 335-348.

Zbar, B., T. Kishida, F. Chen, L. Schmidt, E. R. Maher, F. M. Richards, P. A. Crossey, A. R. Webster, N. A. Affara, M. A. Ferguson-Smith, H. Brauch, D. Glavac, H. P. Neumann, S. Tisherman, J. J. Mulvihill, D. J.

Gross, T. Shuin, J. Whaley, B. Seizinger, N. Kley, S. Olschwang, C. Boisson, S. Richard, C. H. Lips, M. Lerman and et al. (1996). "Germline mutations in the Von Hippel-Lindau disease (VHL) gene in families from North America, Europe, and Japan." Hum Mutat **8**(4): 348-357.

Zhang, Y., X. Chen, M. Qiao, B. Q. Zhang, N. Wang, Z. Zhang, Z. Liao, L. Zeng, Y. Deng, F. Deng, J. Zhang, L. Yin, W. Liu, Q. Zhang, Z. Ya, J. Ye, Z. Wang, L. Zhou, H. H. Luu, R. C. Haydon, T. C. He and H. Zhang (2014). "Bone morphogenetic protein 2 inhibits the proliferation and growth of human colorectal cancer cells." Oncol Rep **32**(3): 1013-1020.

Zhao, M., S. E. Harris, D. Horn, Z. Geng, R. Nishimura, G. R. Mundy and D. Chen (2002). "Bone morphogenetic protein receptor signaling is necessary for normal murine postnatal bone formation." J Cell Biol **157**(6): 1049-1060.

Zhu, Z., J. Kleeff, H. Kayed, L. Wang, M. Korc, M. W. Buchler and H. Friess (2002). "Nerve growth factor and enhancement of proliferation, invasion, and tumorigenicity of pancreatic cancer cells." Mol Carcinog **35**(3): 138-147.

Ziegler, W. H., A. R. Gingras, D. R. Critchley and J. Emsley (2008). "Integrin connections to the cytoskeleton through talin and vinculin." Biochem Soc Trans **36**(Pt 2): 235-239.

Zuber, S. M., V. Kantorovich and K. Pacak (2011). "Hypertension in pheochromocytoma: characteristics and treatment." Endocrinol Metab Clin North Am **40**(2): 295-311, vii.

8. ACKNOWLEDGEMENTS

First of all I would like to thank PD Natalia Pellegata, for giving me the opportunity to carry out my doctoral dissertation under her guidance and supervision, for her support, for giving scientific advice, for helping me to grow as a scientist and for believing in me.

I would also like to express my gratitude to my “Doktorvater”, Prof. Atkinson, for all his ideas and continuous support during the last three years and for critical evaluation of this manuscript and the publication as well as to Prof. Multhoff, for her support within the thesis meetings.

I also say “Thank you” to Dr. Misu Lee. She supported me and taught me many things in the lab. We had great, interesting and helpful discussions and a wonderful cooperation going on for the *in vivo* studies. Especially I want to thank her for the chats, the laughs and for her friendship along the time. It was a great pleasure to have met you and to work with you during this time. 감사합니다 / 고맙습니다

To Andrea Richter for her help and cooperation with the DMH1 experiments and for being great friends! We had a wonderful time and working with you was always a pleasure! Thank you!

To Elke Pulz and Elenore Samson, who gave me great support in the lab. Thank you for all your efforts and your help!

To Natasa Anastasov and Ines Höfig, for the cooperation regarding the cloning, developing a lentiviral system and for the infection of my cells!

To my friends Ewi, Nina, Ela and Laura, we had great lunch times, nice chats and lots of fun along the time!

Ganz besonderer Dank gilt meiner Familie und meinen Freunden. Meinem Mann, Steffen Leinhäuser, der mich während dieser manchmal auch sehr schweren Zeit mit Gesprächen, mit aufmunternden Worten und mit seiner Liebe unterstütz hat. Danke mein Schatz ohne dich hätte ich das nicht geschafft. Außerdem möchte ich meinen lieben Eltern danken, die mich, wo es nur ging, unterstütz haben. Meinen Freunden, die es verstanden haben, wenn ich weniger Zeit hatte und dennoch meine Freunde geblieben sind! ☺